Distribution Agreement

In presenting this thesis or dissertation as a partial fulfillment of the requirements for an advanced degree from Emory University, I hereby grant to Emory University and its agents the non-exclusive license to archive, make accessible, and display my thesis or dissertation in whole or in part in all forms of media, now or hereafter known, including display on the world wide web. I understand that I may select some access restrictions as part of the online submission of this thesis or dissertation. I retain all ownership rights to the copyright of the thesis or dissertation. I also retain the right to use in future works (such as articles or books) all or part of this thesis or dissertation.

Signature:

_____ _____

Alexander N. Wein Date

The roles of IL-36γ and CXCR6 in the immune response to respiratory viral infection

By

Alexander Norwood Wein
Doctor of Philosophy

Graduate Division of Biological and Biomedical Science
Immunology and Molecular Pathogenesis

_____

Jacob E. Kohlmeier, Ph.D.
Advisor

_____

Lawrence H. Boise, Ph.D.
Committee Member

_____

Mehul Suthar, Ph.D.
Committee Member

_____

Rabindra Tirouvanziam, Ph.D.
Committee Member

_____

Edmund K. Waller, M.D., Ph.D.
Committee Member

Accepted:

_____

Lisa A. Tedesco, Ph.D.
Dean of the James T. Laney School of Graduate Studies

_____

Date

The roles of IL-36γ and CXCR6 in the immune response to respiratory viral infection

By

Alexander Norwood Wein

B.S., *summa cum laude*, Emory College of Arts and Sciences, 2010
A.A., *cum laude*, Oxford College of Emory University, 2008

Advisor: Jacob E. Kohlmeier, Ph.D.

An abstract of
A dissertation submitted to the Faculty of the
James T. Laney School of Graduate Studies of Emory University
in partial fulfillment of the requirements for the degree of

Doctor of Philosophy

in Graduate Division of Biological and Biomedical Sciences
Immunology and Molecular Pathogenesis

2018

Abstract

The roles of IL-36γ and CXCR6 in the immune response to respiratory viral infection
By Alexander Norwood Wein

The immune response to infection requires coordination between many cell types for effective pathogen clearance. Cytokines and chemokines serve as secreted proteins that recruit, activate, and regulate immune cells and have been described as the language of the immune system. Just as the study of language can give insight into the human experience and interactions, the study of cytokines and chemokines allows for a better understanding of the immune system.

Influenza virus causes seasonal epidemics that kill 50,000 people in the US each year and occasional pandemics that have killed as many as 100 million people. Many complicated cases of influenza result from dysregulation of cytokine production leading to an inappropriate and deleterious immune response. Defining the roles of individual cytokines is key to understanding the sequelae of influenza infection.

IL-36γ is an important cytokine in the immune response to influenza. It served to promote survival of alveolar macrophages during influenza infection by skewing the macrophages towards an M1 phenotype. The rapid loss of alveolar macrophages in *Il36g*$^{-/-}$ mice led to increased viral titers, pathology, morbidity, and mortality and transfer of WT alveolar macrophages rescued the *Il36g*$^{-/-}$ mice. Thus, IL-36γ acts on alveolar macrophages to enable their survival during respiratory viral infection, decreasing viral replication and pathology.

Preexisitng immunity to influenza can prevent infection, lead to asymptomatic infection, or decrease the severity of symptoms. Unlike neutralizing antibodies, resident memory T cells (T_{RM}) in the lung provide protection across strains of influenza and were found to decrease disease severity during the 2009 H1N1 pandemic. While the factors that lead to the generation of lung T_{RM} cells remain unknown, the chemokine receptor CXCR6 serves to recruit antigen-specific T cells to the airways following respiratory viral infection. CXCR6 is expressed by T cells in the lung and its ligand, CXCL16, is expressed by the airway epithelium in mice and humans. Mice lacking CXCR6 or CXCL16 have decreased airway T_{RM} cells after influenza infection and *Cxcr6*$^{-/-}$ mice have greater morbidity following secondary infection. The data show the importance of CXCR6 for trafficking of T cells to the airways.

The roles of IL-36γ and CXCR6 in the immune response to respiratory viral infection

By

Alexander Norwood Wein

B.S., *summa cum laude*, Emory College of Arts and Sciences, 2010
A.A., *cum laude*, Oxford College of Emory University, 2008

Advisor: Jacob E. Kohlmeier, Ph.D.

A dissertation submitted to the Faculty of the
James T. Laney School of Graduate Studies of Emory University
in partial fulfillment of the requirements for the degree of

Doctor of Philosophy

in Graduate Division of Biological and Biomedical Sciences
Immunology and Molecular Pathogenesis

2018

Acknowledgements

I would like to begin by thanking all current and former members of the Kohlmeier lab including Sean McMaster, Paul Dunbar, Sarah Hayward, Tiger Li, Emily Cartwright, Nivedha Kumar, Ida Uddback, and Laurel Lawrence. Paul Dunbar deserves special recognition as my partner in crime from my first day and Laurel has been invaluable in handling our animal colony so I could concentrate on my research.

I would like to thank my family for their support throughout my endless education. My parents, Andrew and Sherry, and grandparents, Eddie, Marie, Pat, and Amnon, were constant source of encouragement as a child and supported my love of science. My soon-to-be wife, Shenan, was key in my perseverance through the past 5 years and will continue to be a source of support in medical school and beyond.

I must thank the families and organ donors who provided lungs for research in our lab. Their gift was key to my work. I thank Dr. Tamas Nagy, DVM, PhD for pathological examination of mouse lungs and Aaron Rae for sorting of cells and assistance with flow cytometry.

The work in this dissertation was supported by NIH grants HL122559, HL138508, and Centers of Excellence in Influenza Research and Surveillance contract HHSN272201400004C. This work utilized shared resources or received reagents from the Winship Research Pathology Core Lab, Children's Healthcare of Atlanta and Emory University Pediatric Flow Cytometry Core, and the NIH Tetramer Core Facility (contract HHSN272201300006C).

Finally, I want to thank my advisor and mentor, Jacob Kohlmeier. He is an example of mentorship at its finest. He had high expectations, but was always patient, kind, and understanding.

Table of Contents

Chapter 1. Cytokines, Chemokines, and Influenza

Cytokines and Chemokines

The immune system consists of many different cell types that must be able to communicate with each other to effectively initiate, regulate, and discontinue immune responses to a variety of pathogens in any tissue of the body. Failure of any aspect of the immune response can result in uncontrolled pathogen replication, local pathology, systemic immune hyperactivation, or auto-immunity. All of these outcomes can lead to death of the host. Cytokines are small, usually soluble proteins that signal in an autocrine, paracrine, or endocrine fashion between cells of the immune system, but can also act on non-hematopoietic cells (Haynes et al., 2015). Cytokines signal via binding to a cell surface receptor that initiates an intracellular signaling cascade to regulate gene expression via activation of transcription factors and modify protein function post-transcriptionally via activation of kinases and phosphatases (Turner et al., 2014). These signals can initiate intrinsic anti-pathogen defenses, recruit effector cells to areas of inflammation, instruct effector cells in the type of pathogen to eradicate, promote survival of activated cells, inhibit activated cells, and localize cells within the microenvironment. Cytokines play such a dominant role in the immune response that T-cell mediated immunity is divided into Th1, Th2, and Th17 responses based on the types of cytokines produced. Cytokines are both pleiotropic and redundant, making study of cytokine pathways difficult since knockout or inhibition of a single cytokine may have multiple effects on several cell types or not show a phenotype at all. In all, the network of cytokines and their respective receptors is a complicated web that remains an active area of investigation.

Cytokines are an ancient part of the immune system: analogs of mammalian cytokines have been reported in jawless vertebrates (Guo et al., 2009). Cytokines can be divided into three main families based on structure: hematopoietin family, the TNF/IL-1/PDGF/TGF family, and the chemokine family (Haynes et al., 2015). Others divide cytokines based on structure and function, resulting in many more divisions, but this dissertation will focus on the IL-1 family and chemokines. The IL-1 family consists of at least 11 members and serves a mainly pro-inflammatory role (Turner et al., 2014). Chemokines (**chemo**tactic cyto**kines**) are functionally and structurally distinct cytokines that signal via G-protein coupled receptors and direct the movement of cells up a gradient of the chemokine towards the site of production (Griffith et al., 2014). The IL-1 family and specifically, IL-36, will be introduced first, followed by an introduction to chemokines in general and the chemokine receptor CXCR6 in detail.

IL-1 family

The IL-1 family is large and consists of several functionally distinct members with unique receptors (Turner et al., 2014). Many members serve to agonize the receptor and activate its intracellular TIR domains, but a few IL-1 family members antagonize the receptor and inhibit signaling. The evolutionary pressure driving the selection for both activating and inhibitory proteins is clear given the need to quickly start and stop immune responses based on the state of an infection.

IL-1 family members are produced by cells following activation of pattern recognition receptors by endogenous or exogenous factors. Following translation, the proteins are secreted from cells via one of several pathways and bind to their respective receptors on the surface of target cells. However, many members of the family require proteolytic cleavage of the protein for full biological activity (Turner et al., 2014). The

agonist/receptor complex then recruits a co-receptor, often IL-1RAcP, and there is transphosphorylation of the intracellular TIR domains of the receptor and co-receptor. This recruits MyD88 to the intracellular portion of the receptor via interaction of its TIR domain with the TIR domain of the receptor. The IL-1R/MyD88 complex binds one of several IRAK proteins that drive polyubiquitination of TRAF6, which then interacts with TAK1, TAB1, and TAB2. This leads to signaling via MKK3/6 to activate JNK and p38 as well as activation of IKK that phosphorylates IκBα, releasing the p65 and p50 subunits of NF-κB to enter the nucleus and act as a transcription factor (Turner et al., 2014). The JNK, p38, and NF-κB pathways are canonical immune activation pathways that are key for initiation of a successful immune response. In the presence of an antagonist, the agonist is unable to bind the receptor and signaling is prevented. One group of recently discovered and relatively understudied IL-1 family members are the IL-36 cytokines.

IL-36 Discovery and Characterization

The IL-36 family is a recently-described group of cytokines that share many aspects of the IL-1 family, which is not surprising since they share a locus (in humans 2q14-21) and are thought to have arisen from gene duplications of a common ancestral IL-1 precursor. There are three IL-36 agonist proteins designated IL-36α, IL-36β, and IL-36γ, which bind to a common and unique receptor, aptly named IL-36R. The agonist–bound receptor then recruits IL-1RAcP, which is also the coreceptor for IL-1R. As with other IL-1 family members, the heterodimeric receptor complex cross phosphorylates its intracellular TIR domains to activate the NF-κB and MAPK signaling cascades. Binding of IL-36 receptor antagonist (IL-36Ra) to IL-36R blocks this interaction.

Several members of the IL-36 family were first described in 2000, based on a

genome-wide search for IL-1 family members, which contain the consensus sequence

F(X_{10-12})F*X*S(AVS)*XX*(PE)*XX*(FY)(LI)(CAS)(TC) (Smith et al., 2000).

The three genes identified were originally named *FIL1δ* (*IL36RN*, the gene for IL-36Ra), *FIL1ε* (*IL36A*, the gene for IL-36α), and *FIL1η* (*IL36B*, the gene for IL-36β)[1]. The paper performed sequence analysis of the genes, which showed that IL-36Ra was most similar to IL-1Ra, while the other two proteins were most similar to themselves. This paper also measured expression levels of the proteins in hematopoietic cells by qPCR of isolated RNA. *IL36RN* was expressed by monocytes, dendritic cells, and B cells, but not T cells. *IL36A* was expressed by T cells, monocytes, and B cells, but not dendritic cells. *IL36B* was found to be expressed in monocytes and B cells. The paper also characterized the expression patterns in whole tissues by analysis of published EST databases or qPCR. *IL36RN* was expressed in immune tissues as well as other tissues such as the brain, placenta, lung, prostate, and testis. The expression of *IL36A* and *IL36B* were much more restricted to immune tissues such as the lymph node, spleen, tonsil and thymus. However, expression of *IL36B* was noted in the placenta, lung, and testis. The paper attempted to identify the receptor for the new proteins, but was unsuccessful.

Another report was published at the same time which identified *IL36G* (the gene for IL-36γ) as Il-1H1, *IL36B* as Il-1H2, and *IL36RN* as IL-1H3 (Kumar et al., 2000). This paper showed that IL-36γ protein production is induced by treatment of primary human keratinocytes or A431 epithelial cells with TNF or IFNγ, but the protein is present only within the cells and not within conditioned media. IL-36γ was not induced in mouse ears during UVB- or oxazolone-induced acute inflammation; however, chronic

[1] For the review of the discovery of IL-36 family members, the name used in the paper will be used once, and then the modern name will appear for the rest of the description.

oxazolone administration induced *Il36g*[2] mRNA in keratinocytes. Interestingly, acute oxazolone treatment drives a Th1 response while chronic treatment causes a Th2-type inflammation. The authors concluded that IL-36γ is important in a Th2 response, but not a Th1 response, which is the opposite of modern thinking on the role of the cytokine family. The paper also evaluated production of IL-36γ during infection with HSV-1. IL-36γ protein was first detected by western blot on day 1 postinfection, before even the detection of viral glycoproteins, and continued to rise until day 7 of infection. IHC revealed that the major source of the protein was keratinocytes

A third report identified family members *IL1RP2* (*IL36G*) and *IL1RP3* (*IL36RN*) (Busfield et al., 2000). *IL36RN* was expressed in the placenta and uterus by Northern blot and *IL36G* was expressed in esophagus squamous epithelium, but only in deeper layers. *IL36RN* was constitutively expressed by primary human keratinocytes and *IL36G* was rapidly induced following treatment with TNF, PMA, or cyclohexamide. This paper also attempted to identify the receptor, but was unsuccessful.

One other short report characterized *IL1L1* (*IL36RN*) (Barton et al., 2000). This paper also found that the mRNA was expressed in the placenta, and identified expression of the protein in the trophoblast cell line JEG-3. Northern blot showed the mRNA in stimulated monocytes and BMDMs, but not lymphocytes, NK cells, or BMDCs.

The first report of the IL-36 receptor was in a *Journal of Immunology* article from 2001 (Debets et al., 2001). This paper described *IL1δ* (IL-36Ra) and IL-1ε (IL-36γ) serving to antagonize and agonize, respectively, a previously orphaned receptor IL-1Rrp2 (IL-36R). This paper identified and characterized IL-36γ and IL-36Ra in much

[2] The homologs of *IL36A, IL36B,* and *IL36G* in mice are officially named *Il1f6, Il1f8,* and *Il1f9*, respectively. However, for ease of understanding, the alternate names *Il36a, Il36b,* and *Il36g* will be used throughout this dissertation.

the same way as the other reports. However, this report tested the activity of IL-36γ and IL-36Ra to signal through orphaned relatives of IL-1 receptor in combination with orphaned relatives of the IL-1 co-receptor, IL-1AcP. The various combinations of receptors were transfected into Jurkat cells and it was found that IL-1R6 (IL-36R) was the only protein that conferred responsiveness to IL-36γ over mock control, but no protein provided responsiveness to IL-36Ra. IL-36Ra was then tested for its ability to antagonize various IL-1 family receptors. IL-36Ra antagonized IL-1R at 1000-fold molar excess to IL-1α while it could antagonize IL-36R at equimolar or lower concentrations of IL-36γ. This paper went on to report that *IL36G*, *IL36RN*, and *IL36R* mRNA are upregulated in psoriatic skin as compared to skin from healthy controls.

IL-36 Protein Regulation, Structure, and Signaling

The IL-1 superfamily of immune receptors is located on human chromosome 2. *IL36* family members lie within a 300-kb locus flanked by *IL1R* and *IL1RN*, suggesting that the genes arose from duplication of a common ancestor. *IL36* family members share 20-35 % sequence similarity to each other, which is approximately the same degree of similarity between all IL-1 family members. Despite only moderate sequence similarity, the IL-36R ligands are all expected to adopt the common 12-stranded, β-trefoil motif found in IL-1α and IL-1β (Smith et al., 2000).

This was recently confirmed in human IL-36γ by X-ray crystallography (Gunther and Sundberg, 2014). Binding of one of the three IL-36 agonist proteins to the receptor leads to recruitment of IL-1RAcP to form a signaling heterodimer. The crystal structures of human IL-36γ and IL-1RAcP as well as a IL-36R homology structure based on IL-1R was used to model this interaction *in silico*. The β4/5 and β11/12 loops of IL-36γ are likely to interact with IL-1RAcP, allowing for recruitment of the co-receptor.

The greatest difference between IL-36γ and IL-36Ra was in these two loops. IL-36Ra has a longer β11/12, which is predicted to sterically hinder IL-1RAcP recruitment, and a shorter β4/5 loop, which prevents interaction between IL-36Ra and Il-1RAcP. Construction of an IL-36γ construct containing the β11/12 loop from IL-36Ra reduced receptor affinity by 14-fold and biological activity by >1000 fold. A loop swapping technique was used to examine which portions of IL-36γ and IL-36Ra endow them with agonist and antagonist activity. The β4/5 loop contributes only slightly to IL-1RAcP recruitment, but may be important in IL-36R interaction. In addition, loop β8/9 is expected to interact with IL-1RAcP. IL-36γ has much smaller residues in this chain than IL-36Ra and mutation of two sites within the β8/9 chain of IL-36Ra lead to increased affinity for the receptor/co-receptor complex. Several differences in the structure of IL-1 vs. IL-36 family members indicate that these two families bind their receptor and recruit their co-receptor by different strategies. It is likely that IL-36 agonists also differ slightly from each other as a polar residue that is thought to be important for recruitment of IL-1RAcP to the IL-36R/IL-36 complex is absent from IL-36γ, but present in IL-36Ra.

IL-36α, β, and γ all signal exclusively through IL-36R and not any other IL-1 family receptors. In addition, IL-1RAcP is the only IL-1 family co-receptor that is able to allow signaling through IL-36R (Towne et al., 2004). When the two receptors form the active heterodimer, their intracellular TIR domains interact to allow recruitment of MyD88, IRAK4, TRAF6, and other signaling proteins. A recent report characterized IL-36R signaling, endocytosis, and recycling in depth; however, its conclusions are difficult to independently critique since many claims are backed by data not shown (Saha et al., 2015). The authors found that knockdown of *Myd88* or *Tollip* reduced IL-6 production

by cells stimulated with IL-36α, IL-36β, or IL-36γ. Tollip co-localized with IL-36R at baseline, but this increased 2-fold upon treatment with IL-36γ. Co-precipitation of MyD88 or Tollip found that Tollip, but not MyD88 directly interacted with IL-36R. They also found that treatment of cells with IL-36 agonists led to internalization of the receptor complex, most likely into endosomes. Addition of the caveolae-mediated endocytosis inhibitor methyl-β-cyclodextrin to cells incubated with IL-36 agonists did not affect IL-6 production; however, chlorpromazine, an inhibitor of clathrin-mediated endocytosis, specifically inhibited IL-6 production in response to IL-36. Clathrin and IL-36R were found to colocalize within 10 minutes following IL-36γ treatment. Acidification of the endosome is not required for signaling as treatment of cells with bafilomycin A1, ammonium chloride, or chloroquine did not affect IL-6 production in response to IL-36γ. IL-36R cycles through endosomes in the absence of agonists; however, in the presence of agonists, IL-36R began to be trafficked to lysosomes within 5 minutes of treatment. Upon agonist treatment of cells knockdowned for *Tollip*, IL-36R had reduced trafficking to lysosomes and increased presence in endosomes. The half-life of IL-36R and IL-1RAcP were both approximately 8 hours regardless of the presence of agonist, suggesting that trafficking of IL-36R to the lysosome does not lead degradation of the protein.

Regulation of the expression of *IL36* agonists is complex and not well characterized; however, one recent paper found that *Il36a* expression is controlled by C/EBPβ (Nerlich et al., 2015). Knockdown of *Cebpb* led to decreased expression of *Il36a* and rescue of *Cebpb* expression restored *Il36a* expression. Characterization of the *Il36a* mRNA found that there are two different splice variants that differ in the inclusion of exon 4, both of which were found to be produced by RAW264.7 and J774A.1

macrophages upon stimulation with LPS. The two splice variants also have different expression levels in unstimulated cells, indicating differences in regulation at baseline. Analysis of the ~1200 bp upstream of the TSS found that there are 5 CEBP binding sites, 2 NF-κB binding sites, and one half-CRE site. Sequential deletion of the 5 CEBP sites led to a gradual, but moderate decrease in expression. Deletion of the proximal NF-κB site led to considerable decrease in expression of *Il36a* upon stimulation, and deletion of the distal NF-κB and half-CRE sites totally abolished expression of *Il36a*. Using a luciferase reporter, single mutation of CEBP sites did not significantly affect promoter activity upon stimulation and deletion of all CEBP sites decreased activity by 32-34 %. Deletion of the half-CRE or NF-κB sites singly or together led to marked decrease of luciferase activity. *In vitro* supershift experiments found that C/EBPβ and C/EBPδ, but not C/EBPα, CREB-1, or ATF4 interacted with the half-CRE site in the *Il36a* promoter. Occupancy of the half-CRE site was 6.5-fold and 4-fold higher in LPS-treated RAW264.7 and primary BMDM cells, respectively.

The three agonist proteins have similar dose response curves to each other and activate NF-κB, ERK, and JNK at similar concentrations. Originally, it was reported that the EC_{50} values of IL-36 family members were 1000-fold higher than IL-1; however, it was later reported that processing of the full-length proteins increased activity 1000-fold. Recently, it was determined that IL-36α is cleaved by cathepsin G or elastase, cathepsin G is able to activate IL-36β, and IL-36γ is processed by elastase and proteinase 3 (Henry et al., 2016). IL-36 agonists lack leader sequences and are expected to accumulate in the cytoplasm of cells prior to release. This was confirmed using BMDMs transduced with a retrovirus that expressed *Il36a* constitutively (Martin et al., 2009). IL-36α was readily detected within cell lysates, but not in conditioned media.

Stimulation with LPS or ATP individually did not cause externalization of IL-36α, but sequential stimulation with LPS followed by ATP lead to release of the cytokine into the media. The kinetics of the release of IL-36α were similar to the release of the non-cytokine GFP expressed by the same vector. IL-36 proteins lack obvious caspase cleavage sequences and inhibition of caspases by Ac-YVAD-CMK does not affect release of the protein following LPS/ATP treatment. However, pharmacological inhibition of the $P2X_7$ receptor, as well as culture in potassium-rich medium, prevented the release of IL-36α.

Effects of IL-36 by Cell Type

Synovial Fibroblasts and Articular Chondrocytes. Treatment of human synovial fibroblasts with IL-1β and/or TNF lead to increased *IL36B* mRNA expression by RT-PCR, but IL-36β protein was not detected in conditioned media by ELISA following 48 or 72 hours of stimulation by IL-1β. Expression of *IL36A* is constitutive and does not impact expression levels of *IL36R*. IL-36α and IL-36β are able to induce *IL6* and *IL8* expression in human articular chondrocytes and synovial fibroblasts (Frey et al., 2013; Magne et al., 2006). Expression of the receptor occurs at baseline in human articular chondrocytes and synovial fibroblasts and is not induced by treatment with IL-1β, IL-36α, and/or TNF (Franzke et al., 2012; Magne et al., 2006).

Primary Human Bronchial epithelial cells. *IL36G*, but not *IL36A* or *IL36B* is one of the 50 most upregulated genes following *ex vivo* exposure of primary human bronchial epithelial cells to *P. aeruginosa* (Vos et al., 2005).

Jurkat cells. Treatment of Jurkat cells expressing IL-36R with IL-36α, IL-36β, or IL-36γ led to activation of JNK within 5 minutes of stimulation and reached a maximum by 15 minutes (Towne et al., 2004). Signaling decreased from 30 to 60 minutes post-

treatment, reaching baseline levels at one hour. This was a faster peak than IL-1, which did not peak until 30 minutes after stimulation, but also decreased to baseline by one hour after treatment. Also, IL-36 caused strong phosphorylation of p46 JNK but lower levels of phosphorylation of the p52 isoform, whereas IL-1 activates the two isoforms equally, which raised the possibility of differential regulation of the IL-1R1 and IL-36R TIR regions. Activation of ERK followed similar kinetics with IL-36 leading to an earlier peak than IL-1 and both returning to baseline by 1 hour after treatment.

Adipocytes. In human adipocytes differentiated from cells isolated from a neonate with Simpson-Golabi-Behmel Syndrome and treated with TNF, *IL36RN* was down regulated by both microarray and real time qPCR.

Neuronal Cells. Neurons do not express *Il36r* by qPCR, but astrocytes and microglia were found to express high levels of *Il36r* mRNA while immature oligodendrocytes were found to express the receptor at low levels (Berglöf et al., 2003). Treatment of mixed glial cell cultures with LPS led to a time-dependent increase in *Il36r* over 1-6 hours post-treatment, which returned to baseline by 24 hours after exposure. However, addition of IL-36γ to mixed glial cell culture failed to induce IL-6 production or activate ERK, JNK, p38, or NF-κB. Injection of IL-36γ into the spinal columns of mice did not result in elevated temperature or decreased appetite, which was seen with injection of IL-1β. Another study found *Il36b* is expressed in mixed glia, neurons, mature oligodendrocytes, and microglia with lower expression in astrocytes, and treatment of glial cells with IL-36β in culture caused a modest, but not statistically significant increase in *Il36b* (Wang et al., 2005). Treatment of mixed or pure glial cultures with IL-36β did not cause MAPK activation, NF-κB activation, or IL-6/PGE2 expression, in accordance with the previous study.

Normal Human Keratinocytes. Treatment of NHK cultures *in vitro* with IL-36α, IL-36β, or IL-36γ led to significant increase in macrophage (CCL2/3/4/5/17/22), T cell (CCL2/5/17/20/22), and neutrophil (CXCL1/8, CCL20) chemoattractants (Foster et al., 2014). Administration of TNF, IL-1α, and IL-17A, but not IL-22, led to expression of *IL36* family members in normal human keratinocytes (Johnston et al., 2011). IL-22 was able to potentiate the ability of IL-17A to induce *IL36* expression. None of these treatments led to the secretion of IL-36 into the medium unless the cells were incubated with ATP. IL-36β treatment of reconstituted human epithelium led to increased expression of several antimicrobial peptides including defensin-β4, HBD-3, lipocalin-2, serpinB1 and elafin. IL-36β and IL-36γ were able to induce expression of matrix metalloproteases 1/19 and 10/19, respectively, in RHE samples. Stimulation of primary human keratinocytes with IL-36γ, but not IL-12, IL-17C, or IL-23 led to increased expression of mRNA for *IL1b*, *IL8*, *CCL20*, *DEFB4A*, *S100A3*, and *S100A9* (Friedrich et al., 2014). IL-36γ also caused increased expression and release of IL-17C and IL-36γ as measured by mRNA and ELISA of conditioned media. IL-36γ was also able to induce *TNF* mRNA.

Mouse keratinocytes. Treatment of mouse keratinocytes with IL-36α led to a dose-dependent increase in *CXCL1* mRNA and protein levels (Milora et al., 2015). Culture of keratinocytes with IL-1α or IL-1β induced *Il36a* expression.

Osteoclasts. Treatment of human osteoclast precursors with either IL-36α, IL-36Ra, or soluble IL-36R did not affect differentiation *in vitro* and IL-36R blockade does not affect bone density during development in mice (Derer et al., 2014). Mature osteoclasts may not express *IL36R*.

Microglia. Treatment of BV2 microglial cells with IL-36γ induced the expression

of *Csf1*, *Il1b*, *IL1a*, *Irak3, Nos2, Tnf, Fas*, and *Cxcl2* (Bozoyan et al., 2015a).

PBMCs. An initial examination of the expression of *Il36r* on blood leukocytes from mice revealed that monocytes and monocyte-derived DCs (mDCs), but not T cells or neutrophils expressed *Il36r* by qPCR (Foster et al., 2014). Positive results by qPCR were confirmed with flow cytometric staining of isolated blood cells. Culture of mDCs with PGE_2, IL-6, and IL-1 or IL-36 revealed a greater increase in CD86 expression over cells cultured with PGE_2 and IL-6. Two more recent studies found that mouse $CD4^+$ T cells, $CD8^+$ T cells, γδ T cells, and NK cells express *Il36r* message, contradicting this work (Tsurutani et al., 2015; Wang et al., 2015). $CD8^+$ T cells stimulated with αCD3/CD28 increased in diameter in a dose-dependent manner to IL-36γ. This effect was greater in magnitude than TCR activation in the presence of IL-2 and was additive to either IL-2 or IL-12. *Ex vivo* stimulation of OT-I cells with IL-12 followed by gene ChIP analysis showed increased *Il36r* expression over controls (Tsurutani et al., 2015). Adoptive transfer of OT-I cells followed by immunization with the cognate antigen led to increased expression of *Il36r*, but not *I1r1*, *Il18r1*, or *Il1rap*. Culture for 24 hours with TCR activation and IL-36γ induced IL-2 and IFNγ expression dose-dependently and at higher levels than TCR activation alone. IL-36γ also made stimulated T cells proliferate more as measured by CFSE dilution and increased the percentage of live cells after 72 hours of culture. These effects were mediated in part by IL-2 and MyD88. IL-36γ was able to increase the production of IFNγ by $CD8^+$ T cells upon secondary stimulation. Culture of effector T cells with IL-36γ alone did not lead to production of IFNγ, and IL-12 caused only limited production; however, IL-36γ was able to potentiate the IFNγ response to IL-12 stimulation (Tsurutani et al., 2015; Wang et al., 2015). IL-36γ/IL-2 treatment of T cells caused high levels of IFNγ protein production as well as gene

transcription at 4 hours following stimulation. Intracellular staining for IFNγ demonstrated that T cells were the source of the cytokine. This effect could also be observed when effector OT-I cells were generated with WSN-Ova influenza. The effects seen in $CD8^+$ T cells also extend to γδ T cells. TCR stimulation in the presence of IL-36γ greatly increased the number of live cells and IFNγ production at 72 hours. IL-36γ alone did not increase NK cell survival or stimulate IFNγ release, but did have an additive effect on both measures in the presence of IL-2. The order of exposure to the cytokines may be important as IL-2 induces IFNγ when given before or with IL-36β, but not when given after IL-36β. IL-2 was shown to induce expression of IL-36R mRNA within 90 minutes in a STAT5-dependent manner, possibly conferring increased sensitivity to IL-36β and allowing for the cytokine to have maximum effect. Culture of human T cells with TCR activation and IL-36γ led to significantly greater IFNγ production than TCR activation alone, demonstrating a role for IL-36γ in the activation of human, as well as murine, T cells.

Culture of monocytes with IL-36α, IL-36β, or IL-36γ led to significant upregulation of *Il1a*, *Il1b*, and *Il6* message and greater release of IL-1β and IL-6 protein into conditioned medium (Foster et al., 2014). Stimulation of mDCs increased the proportion of $CD83^+$, $CD86^+$, and $HLA\text{-}DR^+$ cells and caused release of IL-1β and IL-6 into the supernatant. DCs that were stimulated with IL-36α prior to co-culture with T cells led to more CFSE dilution and super-diploid T cells than DCs that were matured with IL-6 and PGE_2 alone. Another work found culture of MDDCs with only IL-36α decreased CD1a expression while increasing the levels of cell surface CD83 and HLA-DR (Higgins et al., 2015). Incubation of IL-36α with immature MDDCs led to increased cell surface CD40, but no changes in CD80/86 expression compared to isotype and no

treatment controls. IL-36α treatment of MDDCs also increased the release of IL-12p70 and IL-18 into culture supernatant, albeit at a lower level than treatment with IL-1β or IL-36β. This paper also found that culture of MDDCs in the presence of IL-36α increased their ability to induce proliferation and IFNγ in $CD3^+$ T cells, but once again, the effect was not as great as MDDCs cultured in the presence of IL-36β or IL-1β. Incubation of MDDCs with IL-36α, IL-36β, or IFNγ singly was able to induce a $CD14^{Hi}/CD11c^{Lo}$ phenotype in MDDC, which was synergistically increased when IFNγ was combined with either IL-36α or IL-36β. Culture with IFNγ and IL-36α was able to significantly increase phagocytosis of bacteria by MDDCs. Analysis of the phenotype of cells cultured with IFNγ and/or IL-36α showed that there was no difference in CD1a or CD83 expression between the groups, but IL-36α induced less HLA-DR expression than either IFNγ alone or IFNγ and IL-36α.

Treatment of PBMCs with heat-inactivated (HI) conidia from *Aspergillus fumigatus* did not lead to expression of *Il36* cytokines while *Il36a* was only induced by HI *Aspergillus* hyphae (Gresnigt et al., 2013). Expression of *Il36g* required treatment with live conidia or HI hyphae while all forms of *Aspergillus* induced expression of *Il36rn* at 15- to 120-fold above baseline. Treatment of cells with IL-36Ra prior to treatment with *Aspergillus* inhibited IL-17 and IFNγ production, but did not alter IL-13 production or proliferation of $FoxP3^+$ T_{reg} cells. Inhibition of IL-36Ra led to significantly higher production of IL-17 and IFNγ by cells following *Aspergillus* stimulation as compared to non-treated controls. The effect of *Aspergillus* on the transcription of *Il36g* was dependent on both Dectin-1 and Syk, as inhibition of these proteins caused reduced response upon treatment, while CR3 and TLR2 caused increased *Il36g*

transcription. Treatment of $CD4^+$ T cells with IL-36α or IL-36β did not lead to IFNγ or IL-17 production, even when combined with IL-12 or IL-23.

IL-36 in Disease

Psoriasis. The disease in which IL-36 has been best characterized is psoriasis. An early report found that *IL36G* and *IL36RN* were both overexpressed in psoriasis lesions compared to control skin by microarray analysis (Zhou et al., 2003). A follow-up study showed *IL36R* was expressed in the lesional, but not the normal skin of 9/10 psoriasis patients (Blumberg et al., 2007). *IL36G* was also strongly expressed in plaques of psoriasis patients, but not in normal skin. *IL36RN* was detectable in all skin samples analyzed. However, *IL36G* levels are higher than *IL36RN* within lesion skin (Johnston et al., 2011). A whole genome approach to defining molecular signatures of healthy, psoriatic, or eczematous skin found that expression of *IL36A* and *IL36G* were higher in skin from psoriatic lesions than other groups. Along with 8 other genes, *IL36A* and *IL36G* were included in a machine-learning algorithm to diagnose skin lesions by qPCR of patient samples. The algorithm was predictive of psoriasis versus eczema with a 97 % accuracy rate (Quaranta et al., 2014). *Il36a*, *Il36b,* and *Il36g* are also overexpressed in transgenic and chemically-induced mouse models of psoriasis. Treatment of patients with etanercept (a decoy TNF receptor) led to significantly decreased expression of *IL36A*, *IL36B*, and *IL36G* mRNA in skin biopsies. Another study found that a gene cluster running from the end of the *IL1B* gene, through *IL37* and *IL36B*, and into *IL1F10* is associated with a higher risk of psoriatic arthritis in humans (Rahman et al., 2006). *IL36A*, *IL36B*, and *IL36G* mRNA and protein were all expressed at significantly higher levels in psoriasis vulgaris skin samples as compared to normal skin (He et al., 2013). Histological analysis of the skin revealed differential expression of *IL36* family members

in various layers of skin. IL-36α is expressed in the cytoplasm of cells in all skin layers while IL-36β and IL-36γ were most expressed in the granular and middle/upper spinous layers. Injection of 5 μg of IL-36α into healthy mouse skin every other day for 10 days did not cause gross changes in skin appearance, but histological examination revealed increased collagen as well as a pronounced leukocyte infiltrate that was granulocytic in character with few lymphocytes (Foster et al., 2014). This was associated with increased expression of *Ccl3*, *Ccl4*, *Cxcl12*, *Il1b*, and *Hbegf*.

IL36 was also found to be expressed in the apical layers of lesional skin from patients with Crohn's Disease who developed anti-TNF-induced psoriasis but not from healthy controls (Friedrich et al., 2014). This expression correlated with expression of IL-17C and IFNα.

One study overexpressed *Il36a* under the control of the human K14 promoter and found the transgenic mice had severe skin abnormalities (Blumberg et al., 2007). The phenotype was so extreme that the founder mouse with highest *Il36a* expression had to be euthanized and the next four highest expressers were used to found the line. These mice all had *Il36a* mRNA at least 70-fold above endogenous levels. The mice developed flaky skin and ringtail beginning at day 5 of life and resolving by day 21; however, skin lesions, predominately on the face, reoccurred at 6 months of age. This correlated with *Il36a* expression, which decreased over the first 21 days if life. Microscopic analysis of the skin of transgenic mice revealed acanthosis, hyperkeratosis, and a neutrophil, macrophage, and lymphocyte infiltrate. The skin infiltrate was decreased by treatment with a TNF-neutralizing antibody or when the mice were crossed to *Tnf*$^{-/-}$ or Tnfsfr1a$^{-/-}$ mice. Depletion of neutrophils with Gr-1 antibody was incomplete, but led to a decreased skin inflammation score while skin thickness was unchanged.

Crossing of the *Il36a*-overexpressing mice to a RAG2-KO mouse line did not change gross skin appearance and only a small difference in microscopic analysis was noted, indicating that neutrophils, but not lymphocytes, were critical for IL-36α-driven skin pathology. This pathology was exacerbated by deletion of *Il36rn*, which only 1 of an expected 109 pups from a K14-*Il36a*$^{+}$*Il36rn*$^{+/-}$ x *IL36rn*$^{-/-}$ cross survived to adulthood. 13 runted, dead pups were found to have intracorneal and intraepithelial pustules, hyperkeratosis, dilated dermal vasculature, and dermal infiltrate. Treatment of these K14-*Il36a* mice with 12-O-tetradecanoylphorbol-13-acetate (TPA) when the skin is phenotypically normal lead to much worse lesions than TPA treatment of non-transgenic mice (Blumberg et al., 2010). This phenomenon was shown to be dependent of expression of the transgene by treatment with an IL-36R-blocking antibody. These lesions resembled human psoriatic lesions macro- and microscopically, except that the mouse model did not require CD3^{+} lymphocytes, which are thought to be essential for human psoriasis. Expression of several pro-inflammatory cytokines, including IL-23p19, IL-12p40, IL-17A, IL-22, IL-20, IL-1β, IL-19, IL-24, S100A8, S100A9, and β-defensin 4, was higher in treated, transgenic skin as compared to either treated WT skin or untreated transgenic skin. Injection of IL-36α into WT FVB mice led to increased expression of *Il17a*, *Il23*, *Ccl2*, *Ccl20*, *S100a8*, *Tnf*, and *Ifng*, as well as its own mRNA. Injection of TNF, IL-17A, IL-23, and IFNγ was able to induce *Il36a* as well as *Il36b* and *Il36g*, indicating the presence of a positive-feedback loop. Therapeutic blockage of the TNF, IL-12, or IL-23 pathways in the context of TPA-treated K14-*Il36a* mice led to micro- and macroscopic improvements in skin lesions, indicating that therapies used in human psoriasis were also effective in this model.

The importance of IL-36α in psoriasis was explored in another recent study using the imiquimod model of psoriasis (Milora et al., 2015). Imiquimod treatment of skin strongly induced *Il36a*, *Il36b*, and *Il36g* expression, but only IL-36α was released into conditioned medium upon *ex vivo* culture of treated keratinocytes. Interestingly, the IL-36α was detected as the unprocessed protein, which has a 3-fold reduction in EC_{50} values. Production of IL-36α was not altered in *Casp1*$^{-/-}$*Casp4*$^{-/-}$ mice but was dependent on IL-1R1. Using mice lacking *Il36a*, *Il36b*, or *Il36g*, the authors found that only knockout of IL-36α affected the disease phenotype. Treated skin from *Il36a*$^{-/-}$ animals had reduced disease upon gross and microscopic examination with fewer microabcesses and reduced neutrophil infiltrates. *Il36a* deficiency also led to decreased IL-1α and IL-18, but not IL-1β, production. This suggests a feedback loop where IL-1R1 stimulation causes IL-36α release, which then increases IL-1R1 stimulation via IL-1α release. Imiquimod treatment of *Il36a*$^{-/-}$*Il1r1*$^{-/-}$ mice found that disease severity and *Cxcl1* expression was significantly decreased compared to either single KO.

Another study found that deletion of *Adam17* in keratinocytes using a K14-Cre mouse crossed to Adam17$^{fl/fl}$ mice led to prominent expression of *Il36a* at day 10 of life, while no elevation was detected at days 2 and 6 of life. This correlated with a neutrophil infiltrate at day 21 of life (Franzke et al., 2012). Transplant of human psoriatic skin lesions onto SCID mice followed by blockade of human IL-36R led to improved pathology compared to untreated mice with diseased skin grafts. The dependence on local IL-36 agonists and IL-36R is confirmed by the lack of cross reactivity between mouse and human IL-36 members.

The most convincing evidence of the role of IL-36 in psoriasis is generalized pustular psoriasis. GPP is an inherited disorder that presents in early life with a diffuse

pustular erythematous rash accompanied by fever and weakness. Blood work will show elevated C-reactive protein as well as increased neutrophils. Death from sepsis is possible. A recent NEJM report characterized the genetic cause of this disorder (Marrakchi et al., 2011). Nine families with at least one member developing GPP were genotyped and a region of homozygosity was found in the *IL1* locus. The disease was linked to a L27P substitution in IL-36Ra, which was present in all affected persons. The L27P allele was detected in 3/287 unaffected persons of Tunisian descent, but in none of 500 unaffected Europeans. This region is highly conserved across all species and L27 is absolutely conserved in mammals. The L27P mutation is predicted to affect protein stability as well as receptor affinity. Transfection of the mutant *IL36RN* into HEK293T or HaCat cells led to very little protein expression as compared to WT, L27A, or L27R IL-36Ra proteins. The purified mutant protein is less able to inhibit IL-36R signaling than the WT protein and is more sensitive to heat denaturation. The c.115+6C>T mutation leads to aberrant splicing of the *IL36RN* mRNA causing a premature stop codon (Farooq et al., 2013). L21P is predicted to negatively affect IL-36Ra protein stability (Ellingford et al., 2015). T123 lies within a hydrophobic area of IL-36Ra. Substitution of this residue with arginine disrupts hydrophobic interactions in the core of IL-36Ra and is predicted to decrease protein stability. When an overexpression vector containing the T123R substitution was transfected in HEK293T or HeLa cells, protein expression was much lower than the same vector containing WT IL-36Ra and the T123R protein is unable to antagonize IL-36R. Patients with the T123R protein expressed much higher levels of *IL8*, *IL36A* and *IL36G* in their skin, but this was also observed in GPP patients without known *IL36RN* mutation. The R10X substitution is frequently seen in patients of Japanese descent. A heterozygous mutation in R10X has

also been linked to acute generalized exanthematous pustulosis following administration of dihydrocodeine phosphate (Nakai et al., 2015). Inhibition of TNF by infliximab, adalimumab, or etanercept has been shown to be an effective therapy for GPP with low side effects when properly managed (Sugiura et al., 2015).

When keratinocytes from GPP patients were treated with IL-36α, IL-36β, IL-36γ, IL-1β and poly I:C, they produced much higher levels of IL-8 than similarly treated cells from healthy controls. The cells also overproduced IL-36γ following stimulation with IL-1β or poly I:C. This overexpression was not found in patients with other inflammatory skin diseases such as lichen planus or erythema multiforme.

Arthritis. *IL36A*, *IL36B*, *IL36R*, and *IL36RN* are all expressed in normal and inflamed joints of psoriatic and rheumatoid arthritis patients, but expression levels do not correlate with disease activity (Frey et al., 2013; Lamacchia et al., 2013). Expression of *IL36R* is mainly on infiltrating leukocytes and the synovial lining. IL-36β is found in the synovial fluid of inflamed joints and serum of patients with osteoarthritis, rheumatoid arthritis, or sepsis at similar levels to healthy joints or patients and was not changed in RA patients following anti-TNF treatment (Magne et al., 2006). IL-36 expression was higher in joint with signs of inflammation, coming mainly from $CD138^{+}$ plasma cells (Frey et al., 2013). Use of a blocking IL-36R antibody had no impact on incidence or severity of collagen-induced arthritis in mice (Lamacchia et al., 2013). The same antibody had no effect on the development of antigen-induced arthritis as measured by ^{99}Tc uptake and histological examination of joints. In support of the dispensability of IL-36 in these disease models, there were no differences in disease severity between WT and *Il36r*$^{-/-}$ mice in the antigen-induced or K/BxN serum transfer models of arthritis.

Another paper examined the role of IL-36 in a transgenic mouse model of arthritis driven by the overexpression of human TNF (Derer et al., 2014). Examination of the joints of WT and hTNFtg found that *Il36a* mRNA was expressed in the joints of transgenic mice but was nearly undetectable in WT joints. The levels of *Il36r* were comparable between the two groups. Therapeutic blockade of the IL-36 pathway with an antagonistic antibody did not alter grip strength or joint swelling, indicating that the treatment did not alter the disease course. Histological examination of the two groups revealed no differences in area of inflammation, number of osteoclasts, or depth of bone or cartilage erosion.

Sjörgen's Syndrome. *IL36A*, but not *IL36R* mRNA, was significantly upregulated in salivary gland tissue of patients with primary Sjörgen's syndrome (pSS) and this increase correlated with expression of IL-17, IL-22, and IL-23p19. *IL36RN* mRNA was downregulated compared to healthy controls while *IL1F10* mRNA was upregulated. Serum levels of IL-36α were higher in pSS patients than healthy donors. When patients were stratified by IL-36α levels (high vs. low), patients with a high serum IL-36α were found to have more severe disease activity. IHC for IL-36α in healthy and pSS salivary glands revealed little expression in healthy tissue while expression of IL-36α was mainly confined to the lymphoid, dendritic, and plasma cell infiltrate. FACS and immunofluorescent analysis of leukocytes isolated from salivary glands confirmed that macrophages and TCRαβ$^+$ T cells were the main sources of IL-36α. Very few plasma cells produced IL-36α. In addition, TCRγδ$^+$ T cells were found to express IL-36α at a higher frequency than in healthy controls.

Systemic lupus erythematous. While IL-36α, IL-36β, and IL-36γ were present in the serum of healthy controls as well as SLE patients, patients with active disease had

higher levels of IL-36α and IL-36γ than normal controls (Chu et al., 2015). Levels of IL-36α and IL-36γ positively correlated with disease score and serum IL-10. Patients with active SLE also had a higher percentage of IL-36R^{+} B cells compared to healthy controls and this percentage negatively correlated with the frequency of regulatory B cells.

Acute Liver Injury. *Il36g* mRNA was found to be upregulated at 24 hours following induction of liver injury with acetaminophen and therapeutic administration of IL-22 decreased *Il36g* expression (Scheiermann et al., 2015). Stimulation of primary murine hepatocytes or Huh7 hepatocellular carcinoma cells with a combination of IL-1β, TNF, and IFNγ led to induction of *Il36g* mRNA and incubation with IL-36γ led to expression of CCL20. *Il36r* mRNA levels were upregulated at 6 hours following liver injury and had returned to baseline by 24 hours after injury. *Il36r* is virtually undetectable in healthy murine livers. Expression of *Ccl20* was delayed compared to *Il36g*, peaking days after liver injury and IL-22 treatment decreased hepatic *Ccl20* levels in similar fashion to IL-36γ. Treatment of mice with IL-36Ra along with acetaminophen decreased liver *Ccl20* levels in a specific manner, but led to greater increases in serum ALT compared to mice treated with acetaminophen alone. This correlated with increased area of necrosis upon serial section and analysis of livers, as well as decreased numbers of Ki67^{+} hepatocytes at 48 hours after treatment, suggesting a potential healing role for IL-36 signaling in acute liver injury. In addition, endotoxemia led to hepatic expression of *Il36g* and *Ccl20* mRNA.

Irritable Bowel Disease. Microarray analysis of colonic lamina propria from DSS-treated mice found that *Il36g* was the most increased cytokine in diseased mice. This was validated by qPCR which also found that *Il36a* and *Il36b* were not expressed in the inflamed colon. This effect was found in other models of colitis including CD45RB^{Hi}

transfer and *H. hepaticus* infection, as well as samples from the colons of human patients with IBD. The main sources of *Il36g* were macrophages and intestinal epithelial cells and the production was dependent on gut microbiota. Expression of *Il36g* peaked at day three while *Il22* expression began on day 4 and peaked at day 5 of DSS treatment, suggesting a role for *Il36g* in the induction of *Il22*. *Il22* expression was absent in *Il36r*$^{-/-}$ mice following DSS treatment, confirming that *Il36g* expression is required for *Il22* production in the model. When DSS colitis was induced in *Il36r*$^{-/-}$ mice, the *Il36r*$^{-/-}$ mice were slightly protected during the insult phase of the model, but never recovered body weight. Examination of the colon revealed greatly increased inflammation and tissue damage in *Il36r*$^{-/-}$ mice when compared to WT mice. This is likely due to a defect in IL-22 production in *Il36r*$^{-/-}$ neutrophils which prevents induction of wound healing. In fact, DSS-treated *Il36r*$^{-/-}$ mice showed decreased morbidity and no mortality when FICZ was used to induce *Il22* expression.

Chronic Kidney Disease. Using the CGN model of chronic kidney disease, *Il36a* was found to be expressed in the diseased kidney at 186-fold above WT levels, much higher than any other IL-1 family member (Ichii et al., 2010). Early in life, CGN mice did not show IL-36α expression within the kidney, but aged CGN mice showed high expression of IL-36α within renal tubules and the number of IL-36α^{+} tubules correlated with histopathologic disease score. Female mice developed more severe disease than male mice and also expressed more IL-36α. This expression increased with the age of the mouse. IL-36α was expressed in the distal convoluted tubule and the cortical collecting duct and monocyte infiltration was found in some IL-36α^{+} tubules. This phenomenon was also found in several other models of kidney disease including steptozocin-treated DBA2 mice, male BXSB mice, female NZB/W F1 mice, and female

MRL/*lpr* mice. To extend these results, the kidney epithelial cell line M-1 was studied for *Il36a* expression following stimulation with serum, urine, and splenocytes. Only splenocytes were able to stimulate *Il36a* production by the kidney epithelial cells.

As a cancer therapy. Analysis of publicly available gene expression data from melanoma samples found that melanoma tumors expressed less *IL36G* than melanoma precursor lesions and that metastatic cancers had lower *IL36G* expression than primary tumors (Wang et al., 2015). In addition, qPCR analysis of lung cancer samples found that advanced tumors (stage III) expressed less *IL36G* than early-stage tumors (stage I and II).

Intratumoral injection of an adenovirus expressing *Il36b* into mice bearing MCA205 tumors led to a significant reduction in tumor burden after a single administration and was curative in a majority of mice following four doses of virus (Gao et al., 2003). Challenge of cured mice led to rejection of the tumor in all animals tested. The effect was abrogated in nude SCID mice lacking B and T cells, *Il12b*$^{-/-}$, *Fasl*$^{-/-}$, and *Ifng*$^{-/-}$ animals. However, lack of NKT cells did not prevent tumor reduction by the adenovirus. Since FasL is required for IL-18-mediated antitumor immunity, the authors reasoned that IL-36β has an antitumor effect that is a mix of IL-12 and IL-18-like mechanisms. The authors did not investigate this effect further, although a more recent paper used a similar system to evaluate the role of IL-36γ in anti-tumor immunity (Wang et al., 2015).

B16 melanoma cells transfected with an *Il36g* overexpression vector grew tumors in C57BL/6 mice at a significantly slower rate than B16 cells with an empty vector. A similar growth phenotype was seen with 4T1 tumors in BALB/c mice, despite the predisposition of this mouse strain to a Th2 response. The 4T1 tumors expressing *Il36g*

also seeded fewer metastatic lesions than control tumors. *Il36g*-expressing B16 tumors had a higher number of $CD45^+$ tumor-infiltrating leukocytes and more $CD8^+$ T cells than control tumors, but the percentage of lymphocytes was unchanged. Percentages of $FoxP3^+$ $CD4^+$ T cells, γδ T cells and NK cells were increased, and myeloid derived suppressor cells and B-cells, which may enhance tumor growth, were decreased in B16-*Il36g* tumors compared to control lesions. The MDSCs that remained showed higher expression of HLA-DR, indicating a more inflammatory and less regulatory phenotype. IFNγ and IL-12 were strongly induced and IL-17, IL-23, IL-1β, IL-10, TNF and GzmB were elevated in *Il36g*-expressing tumors when compared to controls. This suggests a complex regulation and effect of IL-36γ within the tumor microenvironment. No difference in tumor growth or intratumoral leukocytes was noted between the two tumor types when implanted in *Il36r*$^{-/-}$ mice, demonstrating the necessity of IL-36R on the host immune cells. Specifically, $CD8^+$ T cells and NK cells were required for this effect as antibody depletion of either cell type caused a partial reversal of the IL-36γ-mediated rejection and use of *Rag2*$^{-/-}$*Il2rg*$^{-/-}$ double KO mice completely abrogated the phenotype of IL-36γ expressing tumors. When tumors were implanted in *Ifng*$^{-/-}$ or *Prf1*$^{-/-}$ mice, there was a significant difference between WT and *Ifng*$^{-/-}$ mice, but only a slight difference between *Prf1*$^{-/-}$ and WT mice, indicating that the main mediator of IL-36γ mediated rejection of tumors is via induction of IFNγ.

Experimental Autoimmune Encephalitis. *Il36g* and *Il36r* mRNA were found to be upregulated in the brains and spinal cords of sick mice versus controls using three different models of EAE (MOG/CFA, adoptive transfer of MOG-specific cells, and pertussis toxin treatment of 2D2 mice) (Bozoyan et al., 2015a). Active induction of EAE led to a later peak of *Il36g* mRNA (day 12) as compared to passive transfer of pathogenic

cells (day 9). Active, but not passive induction also led to an increase of *Il36g* mRNA in the blood of animals. This systemic increase was found to be dependent on adjuvant while the expression in the nervous system was dependent on MOG. Isolation of various cell types from the spleen and spinal cord of EAE mice found that $Ly6G^+$ neutrophils were the primary producers of *Il36g* message and expression was confirmed at the protein level by western blotting and in situ hybridization. *Il36r* was found to be expressed by microglia and macrophages, though other cell types could not be excluded. Induction of EAE in $Il36g^{-/-}$ and $Il36r^{-/-}$ found no difference in disease severity or spinal cord infiltrate when compared to WT control mice, indicating that these pathways are dispensable for EAE induction.

Chemokines

Chemokines are cytokines that serve to regulate cellular trafficking and localization as opposed to activation. They are the largest family of cytokines, having approximately 50 endogenous ligands in mammals that can bind to about 20 receptors (Griffith et al., 2014; Rot and Andrian, 2004). Some viral genomes also contain chemokine-like molecules, which are presumably important for their pathogenesis (Rot and Andrian, 2004). The majority of chemokine receptors are cell-surface GPCRs that signal by activating G_i-type G proteins; however, some members have no known signaling function and are thought to act as a sink to dampen responses or fine-tune gradients of chemokines in the microenvironment. Chemokines are defined and classified based on the location of four cysteine residues, of which the first two are either next to each other (CC chemokines) or separated by a single residue (CXC chemokines). Other closely-related proteins with similar functions are also considered to be chemokines (Rot and Andrian, 2004).

When released from a cell, chemokines diffuse away to form a gradient which target cells will use to migrate toward the source. This diffusion is limited by binding of chemokines to glycosaminoglycans in the extracellular matrix, which may retain the chemokines in the area from which they originated. This is key for the translocation of intravascular leukocytes into tissues as chemokines bound to the extracellular matrix on endothelial cells are sensed by leukocytes and trigger tethering and rolling of leukocytes (Rot and Andrian, 2004).

When a cell is stimulated by a chemokine, the activated receptors bind G-proteins, which exchange GDP for GTP and dissociate into active forms and activate PI3K. PI3K produces PIP_3 that activates Rac at the location of chemokine binding. The cell polarizes and begins to move towards the source of the chemokine via Rac-mediated actin polarization at the leading edge of the cell. Signaling via GCPRs is transient and cell motility depends on a continued source of the chemokine (Rot and Andrian, 2004). One chemokine/receptor pair is CXCL16 and CXCR6, which will be explored in greater detail below.

CXCR6 Discovery and Characterization

CXCR6 was first identified as a coreceptor for HIV in three separate papers and given the names Bonzo, STRL33, and TYMSTR, as was often the case in the late 1990's and early 2000's (Deng et al., 1997; Liao et al., 1997; Loetscher et al., 1997). In one report, additional co-receptors for HIV were theorized based on the ability of $CXCR4^-$ $CCR5^-$ cell lines to be infected with SIV (Deng et al., 1997). A human cDNA library was transfected into $CXCR4^-CCR5^-$ cells and a HIV virus encoding puromycin resistance along with puromycin selection of treated cells was used to identify infected clones. Two

cDNAs were detected and one of these was *BONZO/CXCR6*[3]. CXCR6 was found to have homology with chemokine receptors and African green money and pigtail macaque homologs were identified.

The second report identified STRL33/CXCR6 using real time qPCR on the tumor infiltrating lymphocyte (TIL) cell line F9 (Liao et al., 1997). *CXCR6* was found to be expressed in $CD4^+$ and $CD8^+$ TILs as well as a variety of human tissues at two different molecular weights. Expression was highest in the spleen, lymph node, thymus and placenta. Based on previous reports showing chemokine receptors serving as HIV co-receptors, cells transfected with *CXCR6* were tested for fusion with TCL-tropic and M-tropic HIV viruses. CXCR6 was able to promote fusion of both types of HIV viruses as well as productive infection with HIV-1.

TYMSTR/CXCR6 was identified using degenerate oligonucleotide primers to known motifs of chemokine receptors (Loetscher et al., 1997). An amplified DNA fragment from this reaction was used to identify *CXCR6* from a $CD4^+$ T cell cDNA library. CXCR6 was most closely related to CCR1 and CXCR2, indicating it was a chemokine receptor, but transfection with *CXCR6* did not endow cells with responsiveness to any known chemokines. *CXCR6* was found to co-localize with CC-type chemokines on chromosome 3. Transfection of NIH3T3 with *CD4* and *CXCR6* allowed HIV to fuse with the cells, and murine 300-19 cells expressing *CD4* and *CXCR6* produced proviral DNA, indicating CXCR6's role as an HIV coreceptor.

Rat CXCR6 is structurally similar to human and mouse CXCR6 (Latta et al., 2007). CXCR6 is expressed on< 10 % of T cells in the blood, spleen or LN of a healthy

[3] As with the review of the discovery of IL-36 proteins, originally published names will be used once, followed by CXCR6.

rat, but upon vaccinia virus infection, the percentages were increased 2-fold. *In vitro* reactivation of T cells from animals with EAE or *M. butryicum* arthritis with cognate antigen caused 40-50 % of T cells to express CXCR6. Intraperitoneal injections of vaccinia virus caused a massive lymphocyte influx and 40-50 % of T cells and 75 % of NK cells were $CXCR6^+$. In this case, CXCL16-mediated *ex vivo* chemotaxis was poor and the cells preferentially migrated on a CXCL10 gradient.

It was subsequently determined that use of CXCR6 by HIV is rare and inefficient (Pöhlmann et al., 1999; Sharron et al., 2000). CXCR6 expression in the blood was mainly limited to B cells, $CD16^{-/Lo}$ NK cells and $CD45RA^+CCR7^+$ naïve $CD4^+$ T cells, which implies that experiments using PBMCs should be able to show infection of $CD4^+$ T cells (Sharron et al., 2000). However, Ficoll purification of cells showed downregulation of CXCR6 compared to whole blood. Using CCR5Δ32 homozygous human T cells in the presence or absence of a potent CXCR4 inhibitor, approximately 15 % of cells became infected. These cells were predominately $CXCR6^+$, suggesting a role for CXCR6 in the infection of these cells. In addition, human CXCR6 is more efficient than rhesus CXCR6 as an HIV coreceptor.

A follow-up paper from Dan Littman's group found that CXCR6 expression was restricted to memory T cells and was upregulated following stimulation with IL-2, IL-7 or IL-15 (Unutmaz et al., 2000). There was weak upregulation on culture with IL-4. This work found that in human PBMCs, CXCR6 is most expressed on $CD45RO^+$ memory T cells, with weak expression on γδ T cells and $CD16^+$ NK cells, and no expression on $CD14^+$ monocytes, $CD19^+$ B cells, or HLA-DR^+ dendritic cells. These findings were independently confirmed (Tabata et al., 2005). CXCR6 expression was always higher in $CD8^+$ T cells compared to $CD4^+$ T cells and most $CCR5^+$ cells were $CXCR6^+$, but CXCR6

expression was not affected in a CCR5Δ32 homozygous individual (Unutmaz et al., 2000). CXCR6 expression also correlated well with CCR6 but was inversely correlated with CXCR4. In contrast with previous mRNA expression results, this paper found that CXCR6 protein was expressed in less than 1 % of lymphocytes in thymus and SLOs.

This paper also generated mice with GFP knocked in at the *Cxcr6* locus. These are the mice utilized in Chapter 3 of this dissertation. No histological evidence of GFP expression was detected in non-lymphoid tissues while strong CXCR6(GFP) signal was found in LNs and the spleen. In the spleen, CXCR6(GFP)-expressing cells were in the periarteriolar lymphoid sheath of the white pulp, a known T cell area. There was very limited expression of CXCR6(GFP) in the thymus. In agreement with the human data, CXCR6(GFP) expression in the mouse was limited to $CD44^{Hi}CD45RB^{Lo}$ memory T cells and IL-2 upregulated GFP expression.

Separately from the antibody staining and GFP expression above, expression of CXCR6 on immune cell types was determined by flow cytometric analysis using a chimeric CXCL16-Ig fusion protein (Matloubian et al., 2000). Expression of the receptor was noted on $CD8^+$ T cells and $CD4^+$ T cells, but not B cells, neutrophils, macrophages. It was expressed on $CD8^+$ and $CD4^-CD8^-$ cells within the thymus. Expression of CXCR6 was very high on intestinal epithelial lymphocytes. In mice, $CD4^+CD8^-$ and $CD4^-CD8^-$ NKT cells express high levels of CXCR6 in the thymus and these cells migrate to CXCL16 *ex vivo* (Germanov et al., 2008). CXCR6 expression occurred concomitantly with CD44 upregulation and before expression of NK1.1, but is not required for thymic NKT cell development. In the periphery, CXCR6 is preferentially expressed by $CD4^-CD8^-$ and $CD4^-CD8^+$ NKT cells (Kim et al., 2002; Thomas et al., 2003).

Stimulation of freshly isolated human PBMCs with PMA/Ionomycin followed by staining for cell surface CXCR6 found that $CXCR6^+$ cells consisted mainly of Th1/Tc1 and Th0 cells, with very few Th2/Tc2 cells (Kim et al., 2001). The majority of $CXCR6^+$ cells were $GzmA^+$ and vice-versa. In addition, $CD56^+$ $CD8^+$ T cells had higher expression of CXCR6 than $CD56^-$ $CD8^+$ T cells. CXCR6 expression was correlated with CLA and $\alpha_4\beta_7$ and inversely correlated with CCR7 and CD62L expression, suggesting a role in homing to extra-lymphoid tissues. Indeed, $CXCR6^+$ T cells were enriched in synovial fluid from arthritic joints and inflamed livers. However, another work found that stimulation of $CD8^+$ T cells with either PMA/Ionomycin or anti-CD3/CD28 reduced expression of CXCR6 via a calcineurin-dependent mechanism (Koprak et al., 2003). Culture of T cells with CHO cells expressing CXCL16 increased IFNγ production (Yamauchi et al., 2004).

CXCR6 lacks the common DRY motif found in most GPCRs and instead has a DRF motif (Koenen et al., 2017). While the DRY is important for stabilization of a GPCR in its active form, the DRF motif of CXCR6 is conserved across mammals, indicating some key function for this change. Change of the native DRF motif to DRY did not affect expression, ligand binding, receptor internalization, receptor recycling, or Akt activation. However, cells expressing the non-native DRY motif had 5-fold higher calcium flux upon CXCL16 exposure and greater chemotactic potential.

Discovery and characterization of CXCL16

CXCL16 is the only transmembrane C-X-C chemokine and has a unique structure shared with CX_3CL1. It has an N-terminal chemokine domain, a mucin-like stalk that is highly glycosylated, a transmembrane α-helix, and a cytoplasmic tail that contains a putative tyrosine phosphorylation and SH2-binding YXPR domain (Matloubian et al.,

2000). Interestingly, binding of CXCR6 to CXCL16 was recently shown to induce phosphorylation of ERK1/2 via CXCL16's cytoplasmic tail (Adamski et al., 2017).

In the original report of *CXCL16*, mRNA for the gene was detected by Northern blot in spleen, lymph nodes, Peyer's patches, thymus, lungs, small intestine, kidney and heart (Matloubian et al., 2000). It was not detected in purified or B cells, bone marrow, or the brain. CXCL16 is expressed on the surface of $CD11c^+$ dendritic cells from lymph nodes and the spleen. Intraperitoneal injection of LPS, anti-CD40, or poly I:C increased surface CXCL16. CXCL16 expression was identified in T cell areas of spleens and lymph nodes by IHC. CXCL16 is chemotactic to cells and its function is sensitive to pertussis toxin. The other report of CXCL16 found expression of the mRNA for *CXCL16* is the liver and placenta in addition to the tissues examined by Matloubian et. al. The second report also found expression of CXCL16 on B cells and monocytes in the PBMCs (Wilbanks et al., 2001). Use of conditioned media from macrophage culture caused chemotaxis in L1.2 cells expressing CXCR6 and addition of either LPS of TNF to the macrophages increased the chemotactic potential of conditioned medium. Wilbanks also found that primary human $CD4^+$ T cells from tonsils migrated to CXCL16 and that an anti-CXCR6 antibody blocked the effect. CXCL16 expression has also been reported in human T and B cells (Nakayama et al., 2003; Shashkin et al., 2003). Myeloma cells lines as well as primary plasma and myeloma cells consistently express CXCR6, and CXCL16 was able to induce migration of these cells (Nakayama et al., 2003). By flow cytometry, CXCL16 is constitutively expressed on human monocytes, MoDCs, and mDCs, and expression of CXCL16 can be increased by maturation (Tabata et al., 2005). In this report, pDCs expressed very low to no cell surface CXLC16, but produced a soluble variant; another work found that 25-40 % of pDCs express surface CXCL16

(Gursel et al., 2006). Murine BMDCs expressed CXCL16 in parallel with CD11c and CD80, with expression peaking 9 days after isolation (van der Voort et al., 2010).

Structure and non-canonical functions of CXCL16

CXCL16 is found in cells as three species that are 48, 30, and 16 kDa and exists as a 32-kDa fragment in conditioned media (Abel et al., 2004). A separate paper found similar fragments of 14, 28, and 50 kDa (Tohyama et al., 2007). To determine the mechanism of CXCL16 release, cells were treated with batimastat and the levels of CXCL16 in the media were decreased while cellular levels were increased (Abel et al., 2004). Use of either GI254023X or GW280264X blocked release of both human and murine CXCL16 into the supernatant. Both of these block ADAM10 while only GI254023X blocks ADAM17, indicating that blockade of ADAM17 is not necessary for blockage of CXCL16 release and that CXCL16 is released by ADAM10. CXCL16 expression is increased in human monocytic THP-1 cells and human bronchial BEAS 2B cells by treatment with IFNγ (Day et al., 2009b; Wuttge et al., 2004).

Using a tagged CXCL16 protein, C-terminal fragments of 24 and 20 kDa were identified in conditioned media of HEK293 and COS7 cells (Schulte et al., 2007). This was traced to ADAM10-mediated cleavage of CXCL16. The C-terminal fragments are degraded by γ-secretases.

CXCL16 can also be released as a soluble splice variant with chemotactic ability (van der Voort et al., 2010). This was first detected as two species of mRNA during qPCR for *CXCL16*, and a third unique mRNA sequence was later identified. These variants included 2 novel exons after the third exon of previously published *CXCL16*, the first novel exon contained a stop codon that prevented translation of the mucin-like stalk, transmembrane domain, and intracellular tail. Soluble CXCL16 had a N-terminal

signal sequence that is cleaved as well as a unique C terminus. This isoform of *CXCL16* was expressed at high levels by mature DCs and is found in many tissues including the spleen, lymph nodes, lungs, kidney, colon, skin, heart, and brain.

Residue E3 of CXCL16 is important for protein expression, but the E3Q mutant of CXCL16 was still active in migration assays (Petit et al., 2008). Sulfation, O-linked glycosylation, or sialylation of CXCL16 is not important for expression or chemotaxis, but N-linked glycosylation was important for expression only. Extension of the N-terminus of CXCL16 by 24 amino acids reduced, but did not eliminate chemotaxis. Residues E94 and N176 of CXCR6 were critical for binding soluble CXCL16, but CXCR6-E94Q still bound membrane-bound CXCL16, suggesting conformational differences between soluble and membrane-bound CXCL16. Binding of CXCL16 to CXCR6 induced receptor internalization *ex vivo* (Latta et al., 2007).

CXCL16 was found to be identical to SR-PSOX (scavenger receptor that binds phosphatidylserine and oxidized lipoprotein) which had been previously described to bind and endocytose oxidized lipoprotein and phosphatidylserine (Shimaoka et al., 2003). Transfection of cells with *CXCL16* allowed them to take up FITC-labeled *E. coli* and *S. aureus*. Uptake of the bacteria was sensitive to cytochalasin D treatment, but not serum in the media, indicating that actin remodeling was necessary. Bacterial uptake could be blocked by using a $F(ab')_2$ specific to CXCL16, oxidized LDL, or dextran sulfate, but not native LDL or chondroitin sulfate. Bacterial binding required the chemokine domain and the mucin domain was necessary for full phagocytosis. The ability to bind to bacteria was eventually shown to be true of chemokines generally (Shimaoka et al., 2004b). CXCL16 was also able to bind D-type CpG analogues (Gursel et al., 2006). The chemokine domain of CXCL16 had antibacterial activity against *E. coli* and *S. aureus*

and its activity against *S. aureus* approached that of beta-defensin (Tohyama et al., 2007).

CXCL16 also served as an adhesion molecule via CXCR6 independent of its chemotactic function (Shimaoka et al., 2004a). Immobilized CXCL16 was able to trap cells expressing CXCR6, but not cells expressing CX_3CR1 and this trapping was reduced by the presence of soluble CXCL16. Adhesion of the cells was not sensitive to pertussis toxin, wortmannin, PD098059, or EGTA; therefore, G proteins, PI3K, MAPKK proteins, and calcium-dependent integrin activation are not necessary for the adhesion. Domain shuffling showed that the binding of CX_3CR1/CX_3CL1 and CXCR6/CXCL16 is specific for the chemokine domain on the ligand. Inhibition of metalloproteases by GM6001 inhibited release of CXCL16 and this led to increased binding of CXCR6-expressing cells to CXCL16. Additionally, primary human plasma cells can adhere to CXCL16-coated tissue culture dishes and this adherence was dependent on CXCR6 but not G-protein signaling (Nakayama et al., 2003).

Function of CXCR6/CXCL16 in various tissues

Bone Marrow and SLOs. CXCL16 expression has been reported in the bone marrow and may contribute to recruitment of plasma cells to the marrow (Nakayama et al., 2003). There was also a unique population of $CXCR6^+CD69^+$ NK cells in the bone marrow, spleen, and lymph nodes of humans (Lugthart et al., 2016). This population was distinct from the $CD56^{Bright}$ and $CD56^{Dim}$ populations commonly found in the circulation. These cells made up 30 % of NK cells in the marrow and 45-55 % of cells in the spleen and LNs. $CD69^+CXCR6^+$ cells expressed NKp46, ICAM-1, 50 % expressed CD27, but they did not express c-kit, CX_3CR1, or CD127. They were intermediate for CD56 and about 20 % of these cells expressed CD16.

Liver. Compared to 50 % of thymic and 80 % of splenic NKT cells, 99 % of NKT cells in the liver expressed GFP under control of the CXCR6 promoter in the liver (Geissmann et al., 2005). NK cells and T cells in the liver also had increased expression of CXCR6(GFP) compared to other tissues. CXCL16 was expressed by endothelial cells lining the liver sinusoid in human and mouse specimens. This was independently confirmed when another group found CXCL16 on expression on hepatocytes, cholangiocytes, and sinusoidal endothelial cells. They also observed $CXCR6^+$ cells could adhere to $CXCL16^+$ primary human cholangiocytes. This was shown to occur by CXCL16 triggering conformational changes in VCAM-1 and VLA-4 (Heydtmann et al., 2005). $CXCR6(GFP)^+$ NKT cells were found in the hepatic sinusoids but not portal tracts (Geissmann et al., 2005). In humans, $CXCR6^+$ NK cells were much more common in the liver than $CD49a^+$ NK cells and a small proportion of NK cells were $CXCR6^+CD49a^+$ (Hydes et al., 2018). The $CXCR6^+CD49a^+$ cells behaved like $CD49a^+$ cells. $CXCR6^+$ and $CD49a^+$ NK cells were phenotypically distinct with the prior expressing CD69 but not CD16 or CD57 while $CD49a^+$ cells were KIR^+ and $NKG2C^+$. Culture of liver NK cells with IL-2, IL12, IL-15 or IL-18 induced increased expression of CD49a, but not CXCR6. However, culture of peripheral NK cells with IL-2, IL-12 or IL-15 increased expression of CXCR6(GFP). Two-photon intravital microscopy showed that $CXCR6(GFP)^+$ cells were attached to the wall of the sinusoids and migrated along the wall in random directions at very slow speed (Geissmann et al., 2005). Cells passed each other in different directions and reversed direction. The livers, but not thymus, blood, spleen, bone marrow, or lung, of *Cxcr6*$^{-/-}$ mice showed decreased numbers of CD1d-reactive T cells, most likely due to a survival defect.

Another work found that NKT cells continued to express CXCR6(GFP) following egress from the thymus and this directed them to the liver and lung (Germanov et al., 2008). In the absence of CXCR6, numbers of NKT cells were decreased in the lung and liver, but increased in the bone marrow, suggestive of altered distribution of NKT cells in the absence of CXCR6. Treatment with anti-CXCL16 decreased the numbers of recently emigrated $NK1.1^+$ NKT cells in the liver, but not $NK1.1^-$ NKT cells or $NK1.1^+$ NKT cells that were already mature in the liver. Production of IFNγ, IL-2 and IL-4 was decreased in NKT cells from the livers of *Cxcr6*$^{-/-}$ mice following administration of α-GalCer. Stimulation with PMA/Ionomycin showed similar levels of IFNγ production in WT and *Cxcr6*$^{-/-}$ NK T cells, but decreased production of IL-4 in the *Cxcr6*$^{-/-}$ cells, indicating an intrinsic defect in these cells.

Knockout of CXCR6 also affected the ability of liver-derived NKT cells to induce contact hypersensitivity in an adoptive transfer model. Sorting of $CXCR6^+$ and $CXCR6^-$ hepatic NKT cells on GFP expression followed by adoptive transfer showed that only $CXCR6(GFP)^+$ cells could induce contact hypersensitivity. Treatment of mice with anti-CXCR6 reduced responses to cutaneous DNFB application and abolished NK cell-mediated protection against influenza or VSV. In an *ex vivo* killing assay, *in vivo*, but not *in vitro*, blockade of CXCR6 or CXCL16 increased NK-cell mediated killing of haptenated cells. Additionally, CXCR6 was required for the maintenance of the $CXCR6(GFP)^+$ population in the liver, but not the spleen.

Similar to *Cxcr6*$^{-/-}$ animals, genetic knockout of *Cxcl16* diminished the serum levels of IFNγ and IL-4 upon injection of α-GalCer and the anti-cancer effects of α-GalCer, which is NK-cells dependent, were lost in the knockout mice (Shimaoka et al., 2007). Knockout mice had decreased numbers of NKT cells in their livers, but normal

numbers of NK cells and T cells. There was no difference in apoptosis between WT and *Cxcl16*$^{-/-}$ NKT cells. CXCL16 was expressed by CD1d^{+}CD11c^{+} DCs in the liver and knockout of the molecule does not change the number of these cells or their expression of CD80 or CD86. Incubation of whole liver mononuclear cells from WT and *Cxcl16*$^{-/-}$ mice with α-GalCer showed decreased production by *Cxcl16*$^{-/-}$ cells. Co-culture experiments showed that WT and *Cxcl16*$^{-/-}$ NKT cells mixed with WT CD1c^{+} DCs produced IFNγ and IL-4 upon α-GalCer stimulation, but this effect was diminished when *Cxcl16*$^{-/-}$ CD1c^{+} DCs were used.

Skin. CXCL16 was expressed on the surface of keratinocytes in the skin of mice and humans (Scholz et al., 2007; Tohyama et al., 2007). Cultured keratinocytes released CXCL16 into the media constitutively and the release was upregulated upon stimulation with TLR 2 or 3 ligands, TNF, IL-1α, or IFNγ (Tohyama et al., 2007). In mice, CXCL16 was released into the fluid around wounds, peaking at days 3-4 post-injury. Release of CXCL16 by keratinocytes was mediated by ADAM10 and was upregulated upon stimulation with PMA or UV radiation. This work also found CXCR6^{+} T cells in the skin at sites of disease, but not in healthy skin.

CXCR6 was required for formation of resident memory T cells (T_{RM}) in the skin following HSV infection. Transfer of WT and *Cxcr6*$^{-/-}$ OT-I T cells followed by HSV infection of the skin led to decreased numbers of *Cxcr6*$^{-/-}$ OT-I T cells acutely and at memory. To determine if the defect was in recruitment of retention of cells, WT and Cxcr6$^{-/-}$ OT-I T cells were injected directly into the mouse dermis prior to HSV infection. Direct injection of T cells did not rescue the defect in *Cxcr6*$^{-/-}$ OT-I T cells, demonstrating that CXCR6 is important for retention of T cells in the skin. (Zaid et al., 2017).

CXCR6/CXCL16 in Disease

Experimental Endotoxemia. *CXCL16* mRNA and protein was upregulated in the blood of human patients following experimental endotoxemia (Lehrke et al., 2007). *In vitro*, aspirin, a COX2 inhibitor; rosiglitazone, a PPARγ inhibitor; and SN50, a IKK inhibitor, all blocked *CXCL16* upregulation following LPS treatment.

Multiple Sclerosis. An early report found that myelin basic protein-specific T cells lines had high expression of CXCR6 and this was the best predictor of conversion to T_{EM} (Calabresi et al., 2002).

Cancer. *CXCL16* expression has been found to correlated with increased survival in colorectal cancer, but poor prognosis in prostate cancer (Darash-Yahana et al., 2009; Hojo et al., 2007). In colon cancer, out of 9 chemokines examined, *CXCL16* mRNA was uniquely upregulated in tumor tissue compared to normal mucosa from the same patient. The gene was also expressed in four colon cancer lines. IHC on patient samples showed expression only in tumor cells and not in surrounding normal mucosa as well as variable expression from patient to patient. Strong vs weak expression of CXCL16 correlated with $CD4^+$ and $CD8^+$ tumor infiltrating lymphocytes.

In prostate cancer, CXCL16 expression was found on PC3, DU145, and 22Rv1 prostate cell lines and IHC showed increased staining for CXCL16 and CXCR6 on tumor cells in prostate cancer tissue compared to healthy tissue (Darash-Yahana et al., 2009). The IHC staining for CXCR6 and CXCL16 correlated to both stage and grade of tumor. CXCR6 and CXCL16 are induced in cancer cells by TNF and IFNγ and have the most intense staining in areas with reactive stroma. TILs were found to express both CXCR6 and CXCL16.

CXCR6 expression occurred in melanoma with *de novo* expression gained as

lesions metastasize to lymph nodes or visceral organs (Seidl et al., 2007). Sorting of human melanoma cells on CXCR6 showed that only CXCR6$^+$ tumor cells were able to form tumors when implanted in NOD-SCID mice (Taghizadeh et al., 2010). Microarray analysis of cells cultured in a model of asymmetric division showed that *CXCR6* was upregulated on stem cells in asymmetric division compared to a model of symmetric division.

In nasopharyngeal carcinoma, CXCR6 expression was increased on TILs compared to blood from the same donor but no expression of CXCR6 was observed on the tumor cells (Parsonage et al., 2012). CXCL16 was expressed by the tumor cells as well as intratumoral mononuclear cells. CXCL16 was also expressed and secreted by the nasopharyngeal cancer cell line c666.1.

AIDS. In addition to its role as a co-receptor for HIV, a *CXCR6* allele was found to affect the time from PCP diagnosis to death (Duggal et al., 2003). The SNP 1469G->A encodes an E3K mutation in the N terminal of CXCR6. This was found to be prevalent in African Americans but rare in European Americans. Humans with the CXCR6-E3K mutation had lower median survival following PCP diagnosis and HAART had no effect on this difference.

Serum levels of CXCL16 were elevated in patients with HIV compared to healthy controls and levels of CXCL16 inversely correlated with CD4$^+$ and CD8$^+$ T cell numbers (Landrø et al., 2009). Patients with opportunistic *M. avium Complex* infections had higher levels of CXCL16 than AIDS patients without that infection. Non-progressors had stable levels of CXCL16 expression while progressors showed an increase in CXCL16 over time. There was no change in CXCL16 levels in patients following 24 months of HAART. The rs2234358-T SNP in the 3'-UTR of human *CXCR6* was more common in

uninfected controls than long-term non-progressors (Limou et al., 2010). This mutation could affect mRNA stability or translation, but was in linkage disequilibrium with SNPs in putative transcription factor binding regions in the gene's promoter, complicating identification of a mechanism.

Allograft Rejection. Allogeneic transplant of mouse hearts showed increased expression of CXCL16 and CXCR6 compared to syngeneic transplant (Jiang et al., 2010). Analysis of the systemic $CD8^+$ T cells showed increased expression of CXCR6 on $CD8^+$ T cells in mice with an allograft. Neutralization of CXCL16 with an antibody did not extend graph survival or affect $CD8^+$ T cell killing.

Psoriasis. The numbers of $CD8^+$ T cells in lesions from patients with psoriasis was significantly increased compared to skin from atopic dermatitis lesions or healthy controls. qPCR of $CD8^+$ T cells from the lesions and blood of psoriasis patients showed an increase in *CXCR6* mRNA in skin-resident cells and this was confirmed by flow cytometry. $CXCR6^+$ $CD8^+$ T cells from psoriatic skin had a calcium flux upon CXCL16 exposure, indicating activation of CXCR6. The SCID-hu skin mouse model showed that administration of CXCL16, but not PBS, into xenographs was sufficient to induce T cell infiltration. CXCL16 is expressed by keratinocytes, $CD11c^+$ dendritic cells, and $CD163^+$ macrophages in the dermis and treatment of patients with etanercept decreased CXCL16 expression as well as infiltration of $CXCR6^+$ $CD8^+$ T cells.

Vitiligo. CXCL16 was increased in the serum of patients with vitiligo compared to healthy controls and correlated with levels of hydrogen peroxide in the skin (ROS are a driver of vitiligo) (Li et al., 2017). In addition, *CXCL16* mRNA was upregulated in perilesions from patients with vitiligo. CXCL16 serum levels decreased upon treatment for vitiligo and culture of primary human keratinocytes in the presence of hydrogen

peroxide increased CXCL16 in a time- and dose-dependent manner. CXCL16 expression increased in parallel with phosphorylation of PERK, IRE1α, and eIF2α and knockdown of either of *EIF2AK3* or *ERN1* attenuated the CXCL16 production in response to hydrogen peroxide. The promoter of *CXCL16* was found to have 6 NF-κB binding sites and NF-κB p65 was phosphorylated following treatment with hydrogen peroxide. Knockdown of *RELA* also attenuated *CXCL16* expression. ChIP showed that the *CXCL16* promoter fragment at -149 to -338 bound NF-κB following hydrogen peroxide treatment. Immunofluorescence microscopy of perilesional and nonlesional skin from vitiligo patients as well as healthy controls showed that perilesional skin had increased numbers and altered localization of $CXCR6^{+}CD8^{+}$ T cells compared to the nonlesional or healthy skin. The numbers of $CXCR6^{+}CD8^{+}$ T cells inversely correlated with the number of $MelanA^{+}$ cells. Transwell assays with $CD8^{+}$ T cells from vitiligo patients showed migration towards primary keratinocytes exposed to hydrogen peroxide in a CXCL16-dependent manner.

Atherosclerosis and Endocarditis. *CXCL16* expression was detected in the endothelial cells covering endocardial cushions of the embryonic mouse heart at early as day e11.5 (Yamauchi et al., 2004). Analysis of human cardiac values from patients undergoing valve replacement due to mitral prolapse and infective endocarditis showed expression of CXCL16 in the macrophages and vascular endothelium only in the presence of infection. CXCL16 expression in these lesions correlated with $CD8^{+}$ T cell infiltration and culture of T cells with CXCL16 induced adherence to VCAM-1, but not ICAM-1, in a VLA-4-dependent manner. Expression of CXCL16 was increased in human plaques obtained during endarterectomy compared to normal human aorta (Minami et

al., 2001). Another study confirmed these findings in humans and *Apoe*$^{-/-}$ mice (Wuttge et al., 2004). CXCL16 was expressed by CD68^{+} macrophages in the intima of atherosclerotic plaques by IHC (Minami et al., 2001). Yet another study found that CXCL16 colocalized with CD41 and CD68, indicating clusters of platelets and monocytes/macrophages (Linke et al., 2017). Treatment of *Apoe*$^{-/-}$ mice with IFNγ increased CXC16 expression and *in vitro* culture of THP-1 cells with IFNγ increased uptake of ox-LDL (Wuttge et al., 2004). CXCR6 was expressed by human aortic smooth muscle cells and treatment of these cells with CXCL16 increased NF-κB activity (Minami et al., 2001). CXCR6 increased aortic smooth muscle cell proliferation, cell-cell adhesion, and Bad phosphorylation (Chandrasekar et al., 2004). In humans, a SNP encoding CXCL16-A181V, located near the ADAM10 cleavage site, showed increased severity, but not frequency, of coronary stenosis (Lundberg et al., 2005). Soluble CXCL16 was correlated with CRP, soluble ICAM-1, resistin, triglycerides, and inversely correlated with HDL (Lehrke et al., 2007). Soluble CXCL16 levels were higher in patients with chronic coronary artery disease than healthy controls. This paper also found that females, African Americans, the aged, and smokers had higher levels of soluble CXCL16.

Listeria monocytogenes infection. Infection with *L. monocytogenes* induced expression of CXCR6 on CD8^{+} T cells in the spleens and livers of infected mice but *Cxcr6*$^{-/-}$ mice did not show an increase in bacteria load and actually showed decreased *Listeria* CFU and increased CD4^{+}IFNγ^{+} cells in the liver and spleen (Heesch et al., 2014). Transfer of WT and *Cxcr6*$^{-/-}$ OT-I cells showed decreased homing to the liver in *Cxcr6*$^{-/-}$ cells upon infection with a *L. monocytogenes* strain that expressed Ova. The ratio of WT to *Cxcr6*$^{-/-}$ cells in the lung and liver increased over time despite equivalent

cytokine production. Memory *Cxcr6*$^{-/-}$ OT-I cells had decreased proliferation by Ki67 staining, but also decreased apoptosis by FLICA staining. CXCL16 treatment was unable to induce proliferation of memory OT-I cells but could induce survival *ex vivo*. No difference was noted in bacterial load upon secondary infection.

Malaria. Upon infection with two different malaria strains, liver-resident, antigen-specific T cells had increased expression of CXCR6 compared to splenic cells (Tse et al., 2013; 2014). Immunization of WT, *Ccr5*$^{-/-}$, *Cxcr3*$^{-/-}$, and *Cxcr6*$^{-/-}$ mice with SIINFEKL-expressing malaria showed that only *Cxcr6*$^{-/-}$ mice had a defect in the number of OVA-specific T cells in the liver (Tse et al., 2014). Adoptive transfer of WT and *Cxcr6*$^{-/-}$ OT-I cells showed decreased numbers of *Cxcr6*$^{-/-}$ T cells in the livers at memory, but no difference was observed in the skin-draining LN, liver, lung, or spleen at 3 or 9 days post-immunization. *Cxcr6*$^{-/-}$ and WT cells had no difference in BrdU uptake at memory. No difference was noted in the chemokine production by WT and *Cxcr6*$^{-/-}$ OT-I T cells, but *Cxcr6*$^{-/-}$ cells had decreased expression of CXCR3 and increased KLRG1 expression. This skewing towards a short-lived effector phenotype may have been the cause of decreased cell numbers at memory. Vaccination with a vaccinia virus expressing SIINFEKL protected mice that received WT and *Cxcr6*$^{-/-}$ OT-I cells from challenge with malaria similarly after 7 days. However, when mice were challenged three weeks after vaccination, mice that received *Cxcr6*$^{-/-}$ OT-I cells showed no protection to malaria challenge.

Hepatitis. Expression of *CXCL16* and *CXCR6* was found to be induced in chronically diseased human livers, and while expression increased with greater disease severity, there was no difference in expression between etiologies (Wehr et al., 2013). This expression was also seen in experimental models of acute and chronic liver injury.

In addition to reports of *CXCL16* expression by epithelium and endothelium, *CXCL16* mRNA was also detected in Kupffer cells. CXCR6 was expressed by $CD56^{+}$ T cells in the livers of patients with alcoholic cirrhosis or HCV and $CD56^{Bright}$ NK cells in healthy tissues resected around hepatocellular carcinoma (Hudspeth et al., 2016; Kim et al., 2001). The $CD56^{Bright}$ NK cells expressed the tissue residency marker CD69, but lacked CD57 or HLA-DR, markers of maturity, activation, and antigen experience (Hydes et al., 2018; Stegmann et al., 2016). These cells were $Tbet^{Lo}Eomes^{Hi}$, a unique phenotype compared to circulating NK cells. A study of explanted livers in patients with chronic hepatitis due to either hepatitis C virus or other causes investigated this further and found that CXCR6 expression was higher on $CD69^{+}$ T cells, NK cells, and NKT cells (Boisvert et al., 2003). Liver infiltrating lymphocytes from patients with end-stage HCV had an increase in percentage of $CXCR6^{+}$ cells as well as CXCR6 MFI compared to matched PBMCs (Heydtmann et al., 2005).

CXCR6 and CXCL16 were upregulated in the livers of mice in a GvHD model and infiltrating T cells showed increased levels of CXCR6 expression compared to syngeneic transfers (Sato et al., 2005). Transfer of allogenic *Cxcr6*$^{-/-}$ T cells showed no difference in total liver-infiltrating lymphocytes, but decreased numbers of transferred cells in the liver, but not the spleen of mice. This defect was due to recruitment, not proliferation, of transferred T cells. In a model of acute liver injury, imaging of *Cxcr6*$^{+/gfp}$ mice showed that $CXCR6(GFP)^{+}$ cells increased their crawling within 6 hours of injury and became stationary within 24 hours (Wehr et al., 2013). Some cells migrated into the liver parenchyma. $CXCR6^{-/-}$ mice had decreased numbers of $CXCR6(GFP)^{+}$ lymphocytes in the livers and those lymphocytes that were present moved faster compared to WT controls. *Cxcr6*$^{-/-}$ mice had attenuated pathology and decreased serum alanine

aminotransferase. This correlated with decreased accumulation of NKT cells in the livers of *Cxcr6*$^{-/-}$ animals. *Cxcr6*$^{-/-}$ animals were also protected from chronic liver injury.

Influenza virus

Influenza virus is a spherical pleomorphic virus that is ~100 nM in diameter and contains a single-stranded negative sense RNA genome with 8 segments (Carroll et al., 2015). The surface of the virion is a lipid bilayer with hemagglutinin (HA) and neuraminidase (NA) proteins projecting from the virus. These are important in binding to a target cell and release of nascent virions, respectively. To infect a cell, influenza binds to terminal sialic acids on glycosylated cell-surface proteins via the HA protein and is endocytosed. Acidification of the endosome causes fusion of the virus's membrane with the membrane of the endosome, causing release of the viral RNA into the cytoplasm of the cell. Replication and transcription of the influenza virus genome takes place in the nucleus of the cell using a virally encoded polymerase that is packaged in the virus bound to the 5' and 3' ends of the genome segments (Velthuis and Fodor, 2016). For replication, influenza uses its polymerase to create a complementary RNA molecule that is then copied into vRNA for integration into daughter virions. For transcription, influenza "snatches" the 5' caps of cellular mRNA to use as primers for transcripts and produces cRNA with the host's 5' cap and a poly(A) tail. These mRNA are exported from the nucleus and translated using cellular machinery. The three polymerase subunits and NP are imported into the nucleus and associate with the vRNA. The viral ribonucleoproteins are then exported to the cell surface for integration into progeny virions. These virions bud from the cell membrane and are released by the action of the viral NA protein. The process occurs quickly with host protein translation shut down within 3 hours of infection and release of virions beginning after 8-10 hours.

Influenza virus belongs to the Orthomyxoviriade family and consists of three separate genera (A, B, and C) based on the internal antigens in the NP and matrix (M) proteins (Cohen and Dolin, 2015). Influenza A is further divided based on the surface proteins HA and NA. There are 18 HA and 11 NA subtypes known, but only a few of these (H1, H2, H3, N1, N2) have been shown to cause epidemics in human. Aquatic birds are the natural hosts for influenza virus, but chickens, pigs, horses, bats, and seals can be infected by influenza and have their own circulating strains (Carroll et al., 2015). In the past two decades avian subtypes such as H5N1 and H7N9 have shown the ability to cross from chickens to human in southeast Asia, prompting concern that these new subtypes may emerge as a global pandemic (Hui et al., 2017).

Influenza and human health

Influenza viral illness kills 51,000 people annually in the United States and 400,000 people globally (Iuliano et al., 2018). The majority of cases occur during yearly epidemics that start in the fall and run through winter, infecting as much as 20 % of the population (Dolin, 2012). Influenza virus's high mutation rate allows it to evade the host's immunological memory by changing cell-surface epitopes (Chen and Holmes, 2006). Therefore, the virus is able to infect a host without being neutralized by antibodies from previous infections. This ability, together with the fact that several strains of influenza circulate at the same time, complicates efforts to control the illness by vaccination. Influenza vaccines must be updated each spring to protect against the strains expected to cause disease in the coming fall, and each vaccine must carry antigen from several different strains in order to induce a broadly-protective antibody response. Even with these measures, vaccination is still only 50-80% effective in preventing disease (Dolin, 2012).

Another consequence of the high mutation rate is the ability of avian strains of influenza to acquire the capability to infect human cells. Mutations that allow for a virus to infect both avian and human cells have been documented for avian influenza types H5N1 and H7N9 (Short et al., 2014). These zoonotic viruses preferentially replicate in the lower respiratory tract in humans, leading to an increased incidence of pneumonia and fatality rates as high as 60 % (Dolin, 2012; Taubenberger and Morens, 2008; Tscherne and García-Sastre, 2011). Many of the destructive properties of the anti-viral immune response described below create a fertile environment for colonization of bacteria. When combined with a reduced phagocytic ability of neutrophils and macrophages to combat bacterial invasion following influenza infection, a vigorous anti-viral response can lead to a mixed bacterial/viral or secondary bacterial pneumonia (Braciale et al., 2012; McNamee and Harmsen, 2006; Neil, 2010). These complications are common, and in the 1957 H2N2 pandemic were found in 2/3 of fatal cases. Zoonotic viruses can also gain human infectious potential by antigenic shift. When a single host is infected by two strains of influenza simultaneously, random combinations of genome segments will mix in co-infected cells. The resulting virions contain genomic material from both parent viruses, potentially giving it new virulence in humans. This was the case for 2009 H1N1 influenza, which resulted from the reassortment of four influenza strains from three different species over a period of 10 years (Tscherne and García-Sastre, 2011). The many mechanisms by which novel strains of influenza can arise make it a very difficult pathogen to control.

Immune response to influenza

Understanding the host response to influenza infection is key in preventing pathologic immune responses and secondary bacterial infection in the lung. An

aggressive response by the innate immune system has been found to correlate with poor outcomes in models of 1918 H1N1 and contemporary H5N1 infection (Teijaro, 2014).

When a naïve human is infected with influenza, the virus binds to epithelial cells in the nasopharynx and begins to reproduce (Carroll et al., 2015; Chen et al., 2018). As the viral replication progresses, virus spreads down the respiratory tract and may begin to infect the trachea and lungs. Cells of the immune system, including DCs and alveolar macrophages, may also be infected by some strains of the virus (Chen et al., 2018). During the latent phase of infection, which can last 18-72 hours, depending on inoculum, several viral proteins are at work to suppress the host's immune response. One protein is polymerase basic 1-F2 (PB1-F2), which is transcribed from an alternate reading frame of *PB1*. This protein is able to inhibit RIG-I signaling by direct interaction with MAVS, preventing the induction of type I and III interferons, and induces apoptosis in APCs by disrupting the mitochondrial membrane (Hsu, 2018). The PB1-F2 protein of Spanish flu has been found to be particularly effective and mutagenesis of PR8 to express the 1918 PB1-F2 led to increased morbidity and mortality (McAuley et al., 2007). Influenza's other immune evasion protein, non-structural 1 (NS1), is polyfunctional and shuts down host mRNA translation and antagonizes interferon signaling by inhibiting the polyubiquitination of RIG-I, binding to PKR and inhibiting signaling, and by binding to vRNA and preventing its recognition by OAS or PKR (Hsu, 2018). Eventually, the viral PAMPs overwhelm the ability of PB1-F2 and NS1 to block host antiviral responses and infected cells begin to produce IFNα and IL-6 (Teijaro, 2014). This coincides with symptom onset in humans and the levels of pro-inflammatory cytokines correlate with symptom severity.

The production and release of IFNα, IL-6, IL-1, and other pro-inflammatory cytokines sets up an antiviral state in adjacent cells and helps to control spread of the virus (Teijaro, 2014). TNF, IL-1, IL-6 and IL-8 can also act systemically on the hypothalamus to induce fever and the liver to begin synthesis of acute phase proteins. These cytokines, along with CCL2, CCL5, and CXCL10 recruit cells of the innate immune system to the site of infection (Pulendran and Maddur, 2014). Neutrophils, NK cells, and alveolar macrophages have been shown to be important for early control of viral replication and various types of DCs take up antigen and travel to the draining lymph nodes to initiate the adaptive immune response (Pulendran and Maddur, 2014).

Neutrophils are among the first cells to arrive to sites of infection. Neutrophils phagocytose virus as well as apoptotic infected cells, but are not permissive for infection. In mice, neutrophils are important for control of influenza virus infection and depletion of neutrophils caused increased viral titers in the lung (Pulendran and Maddur, 2014). NK cells are also important for control of virus as their depletion also leads to delayed viral clearance and worsened disease in mouse models (Pulendran and Maddur, 2014). This correlates with decreased numbers of NK cells in the lung infiltrates of fatal cases of influenza infection. In humans, NK cells can recognize viral HA on the surface of infected cells via the NKp46 and NKG2D proteins, leading to lysis of infected cells. NK cells can be infected by influenza virus and this inhibits their function. However, both neutrophils and NK cells have been shown to contribute to influenza pathogenesis in some models and their arrival in the lung takes 4-5 days, limiting their activity in early control of viral replication (Lim et al., 2015; Pulendran and Maddur, 2014; Schultz-Cherry, 2015).

Alveolar macrophages during influenza infection

Unlike other innate cell populations important for the control of influenza infection, alveolar macrophages are already present within the alveoli of the lung and do not need to be recruited from the circulation. These cells were originally shown to reduce T cell responses to respiratory viral infeciton by removing antigen and downregulating LN priming of T cells without an effect on viral clearance, but they have since been found to be critical for control of influenza infection in mice, ferrets, and pigs (Cardani et al., 2017; Kim et al., 2013; 2008; Schneider et al., 2014; Wijburg et al., 1997). Depletion of alveolar macrophages by liposomes, transgenic expression of the diphtheria toxin receptor (DTR), or knockout of key developmental proteins was found to increase viral titers, pathology, and mortality and restoration of alveolar macrophages rescued the effects of depletion or knockout (Cardani et al., 2017; Purnama et al., 2014; Schneider et al., 2014; Tumpey et al., 2005). Additionally, administration or transgenic expression in the lung of GM-CSF, a key cytokine for alveolar macrophage development, improved survival of mice in several lethal infection models and knockout of *Csf2* decreased survival (Huang et al., 2011; 2010; Sever-Chroneos et al., 2011; Subramaniam et al., 2015). Using mice that express DTR under the control of CD11c, the protective effect of alveolar macrophages was found to be during the first 48 hours of infection (Cardani et al., 2017). Notably, depletion of alveolar macrophages using a CD169-DTR mouse did not affect adaptive immune responses, contradicting the early work on alveolar macrophages in influenza (Purnama et al., 2014). However, alveolar macrophages are necessary for mediating protection by broadly neutralizing and non-neutralizing antibodies (He et al., 2017). There are two possible mechanisms by which alveolar macrophages improve host outcome during influenza infection. Macrophages,

as well as neutrophils are able to phagocytose influenza virus-infected cells and inhibition of this process using Annexin V increased mortality in a mouse model of lethal influenza (Hashimoto et al., 2007; Watanabe et al., 2005). In addition, alveolar macrophages express higher levels of viral sensing genes and are the major producers of IFNα and IL-1β during influenza infection (Helft et al., 2012; Peiró et al., 2018).

In humans, alveolar macrophages are resistant to infection by circulating seasonal strains, but H5N1 avian influenza can productively infect alveolar macrophages (Ettensohn et al., 2016; van Riel et al., 2011). The resistance of alveolar macrophages to infection leads to decreased cytokine production compared to recruited monocytes (IFNα notwithstanding), but this may be protective since H5N1 infection leads to much greater cytokine production which correlates with increased mortality. However, there is contradicting evidence in this area. In mice, alveolar macrophages can be infected by some, but not all influenza viruses. For example, the reassortment viruses PR8 and BJx109 have the same internal proteins but differ in their HA and NA proteins. BJx109 can infect alveolar macrophages and had a mild disease course while PR8 cannot infect alveolar macrophages and had a severe disease course (Tate et al., 2010). Depletion of alveolar macrophages increased the severity of BJx109 but not PR8, suggesting that infection of alveolar macrophages was key for host survival. A different work found that alveolar macrophages could be infected by PR8 and that injection of alveolar macrophages from infected animals into eggs resulted in growth of influenza (Helft et al., 2012). This work reasoned that infection of alveolar macrophages was important for viral sensing and initiation of innate immune responses. Murine alveolar macrophages could also be infected by a pandemic 2009 H1N1 influenza virus expressing the Venus fluorescent protein (DiPiazza et al., 2017). Staining of cell surface HA along with Venus

to distinguish infected cells versus cells carrying antigen found that 43 % of alveolar macrophages carrying Venus were productively infected, the highest of any cell type examined.

There is conflicting evidence on the sources of alveolar macrophages in adult lungs. The first alveolar macrophages were seeded from the yolk sac on day e8 in mice and require different transcription factors for their development compared to other hematopoietic cells (Bertrand et al., 2005; Schulz et al., 2012). However, neonatal monocytes also have the ability to seed the lungs and develop into alveolar macrophages (Guilliams et al., 2013). Using fate mapping, bone marrow chimeras, and parabiosis, another work showed that alveolar macrophages are able to proliferate in a M-CSF- and GM-CSF-dependent fashion following depletion and these macrophages were functional and able to prevent alveolar proteinosis in irradiated mice that received *Csf1r*$^{-/-}$ or *Csf2ra*$^{-/-}$ bone marrow (Hashimoto et al., 2013).

Alveolar macrophages decrease during influenza infection, though this was not seen in all viral or mouse strains (Ghoneim et al., 2013; Janssen et al., 2011). One mechanism by which this may have occurred is PB1-F2-mediated induction of apoptosis in alveolar macrophages by disruption of the mitochondrial membrane (Chen et al., 2001). Alternatively, IFNα drove apoptosis of alveolar macrophages (Coulombe et al., 2014). In one model, alveolar macrophages survived the infection while recruited macrophages underwent Fas-mediated apoptosis during resolution of the infection (Janssen et al., 2011). Another work found that alveolar macrophages were lost in BALB/cAnNCrl, but not C57BL/6NCrl mice and claimed to resolve inconsistencies in the field, but that claim is without substance since only 2 viruses and one supplier of mice were used for initial characterization of AM loss (Califano et al., 2018). We

observed that in C57BL/6J mice, alveolar macrophages were decreased during the course of influenza infection (see chapter 3).

Lung-resident memory T cells

In the absence of neutralizing antibodies, influenza-specific memory T cells resident in the airways can decrease the severity of infection. In a heterosubtypic influenza infection model, naïve mice had infectious virus in the nose to day 10 postinfection and in the lungs to day 7 postinfection. However, when a heterosubtypic virus was used to challenge mice with influenza-specific T cells, the virus was largely cleared from the nose by day 6 and the lung by day 4 (Liang et al., 1994). This protection was found to wane over time and be dependent on shared T cell epitopes between the viruses. Protection in the nose was mediated by $CD4^+$ and $CD8^+$ T cells and depletion of both subsets virtually eliminated protection. In the lung, CD4 depletion did not affect protection while CD8 depletion showed a partial decrease in protection. The protection was not dependent on NK cells and was mediated by resident $CD8^+$ T cells (Wu et al., 2014). In humans, numbers of pre-existing T cells to conserved epitopes in 2009 H1N1 inversely correlated with symptom score, but this was done with PBMCs (Sridhar et al., 2013). A more recent work used experimental infection of human volunteers with RSV and found that preexisting RSV-specific cells in the airways inversely correlated with disease severity (Jozwik et al., 2015).

Antigen-specific T cells persist in the lungs and airways of mice for greater than 1 year after infection with either influenza or Sendai viruses (Hogan et al., 2001). These cells expressed CD69, CD25, and CD43, markers of activation and cytolytic activity, and upon stimulation, divided and were cytolytic.

Airway-resident T cells must be continually repopulated from cells in the lung (Ely et al., 2006). These cells were transcriptionally unique as represented by decreased expression of CD11a within 48 hours after entry into the airways. Transfer of cells from the airways to the peritoneal cavity of mice restored CD11a expression. Airway cells were also poorly cytolytic, instead mediating protection by production of IFNγ within 2 hours of antigen exposure (McMaster et al., 2015). Chemokine receptors are known to be important for trafficking of T_{RM} to tissues, so it is likely that the airway has a unique (set of) chemokine(s) that recruit cells (Mackay et al., 2013; Slütter et al., 2013).

Cytokine storm

The anti-viral response is highly regulated, as infected and uninfected cells are equally susceptible to killing from neutrophils. However, in cases of highly pathogenic influenza virus infection, the anti-viral immune response spirals out of control as activated immune cells secrete chemokines that recruit more chemokine- and cytokine-secreting cells in a feed-forward fashion. The loop eventually surpasses the ability of regulatory cells, such as alveolar macrophages, to control inflammation and tissue damage. As this process occurs in the lungs, blood levels of IL-1β, TNF-α, and other proinflammatory markers spike, earning the moniker cytokine storm (Teijaro, 2014).

Cytokine storm due to highly pathogenic influenza virus infection, and the accompanying burst of innate immune cell activity, causes widespread desquamation of the respiratory epithelium and submucosal edema and congestion. Alveolar necrosis, capillary thrombosis, hyaline membranes, and thickening of alveolar septa lead to impeded gas exchange and ventilation-perfusion mismatch (Short et al., 2014; Taubenberger and Morens, 2008). The end state of these symptoms is acute respiratory distress syndrome (ARDS), where the epithelial-endothelial barrier breaks down,

allowing fluid to accumulate in the lungs. ARDS is driven in part by IL-1β and has a fatality rate of up to 60 % (Tisoncik et al., 2012).

Disease modifying agents in influenza

The role of pro-inflammatory cytokines in morbidity and mortality of pandemic influenza virus infection is well documented; however, there are no disease-modifying agents that target the host cytokine response to respiratory pathogens. One cytokine that has not been explored in influenza-induced morbidity and mortality is IL-36.

IL-36 in the lung

Chronic Obstructive Pulmonary Disease. Patients with acute exacerbation of COPD had significantly lower levels of IL-36α and IL-36Ra than patient with stable COPD or healthy controls (Chen et al., 2012). There was also an inverse correlation between IL-36α protein levels and the digital evaluation score system, an established method of evaluating COPD disease status.

Pulmonary Bacterial Infection. Intratracheal administration of LPS into the lungs of mice induced the expression of *Il36g* mRNA, but not *Il36a*, *Il36b*, or *Il36g* (Segueni et al., 2015). Infection of mice with *M. bovis* BCG led to a transient increase in *Il36g* mRNA and IL-36γ protein was observed in granulomas by FISH. WT and *Il36r*$^{-/-}$ were infected with BCG and there were no differences in survival or body weight to 6 months post infection. Flow cytometry of lung cells found no differences in numbers of $CD4^+$ T cells, $CD8^+$ T cells, $CD11b^+$ cells, or $B220^+$ cells, or in bacterial burden or histopathologic appearance at 6 months post-infection. Of more than 10 cytokines whose transcript levels were analyzed, the only differences between WT and *Il36r*$^{-/-}$ mice were decreased levels of *Il6*, *Cxcl1*, and *Cxcl2* in *Il36r*$^{-/-}$ mice.

Infection of WT mice with *M. tuberculosis* led to no changes in expression levels of *Il36g* or *Il36r* over the first 27 days of infection. Comparison of the pathogenicity of

M. tuberculosis in WT and *Il36r*$^{-/-}$ mice found no differences in body weight or mortality out to 4 months. In addition, there were no differences in bacterial load, lung weight, histopathologic findings, or *Cxcl1* expression between the two strains at either 1 or 4 months post-infection and no differences in T cells at 1 month post-infection. Overall, this evidence suggests that IL-36 plays no role in the control of pulmonary mycobacterium infection.

Il36g was induced in the lung during infection with *Klebsiella pneumoniae* and *Streptococcus pneumonaie* and IL-36γ was released by epithelial cells into the alveolar space (Kovach et al., 2017). Infection of mice with *Pseudomonas aeruginosa* led to release of IL-36α and IL-36γ by epithelial cells and macrophages (Aoyagi et al., 2017b). Knockout of IL-36γ impaired bacterial clearance, increased bacterial dissemination, and increased mortality in *S. pneumoniae* infection, but increased survival during *Pseudomonas* infection. The mortality defect in *S. pneumoniae* was attributed to decreased M1 macrophage activation and transfer of IL-36γ-containing microparticles rescued the death of *Il36g*$^{-/-}$ mice. In *Pseudomonas* infection, IL-36γ induced COX-2 expression and the resultant PGE_2 impaired the bacterial clearance. In human ARDS, IL-36γ can be found in the airways and serum of patients and, surprisingly, the serum levels were 10-fold higher.

Asthma. In mice, the *Il36* family lies within the *Abhr1* locus that determines the asthma responsiveness of two strains of mice: A/J (hyper-responsive) and C3H/HeJ (hypo-responsive) (Ramadas et al., 2006). In an OVA mouse model of bronchial hyper-responsiveness, *Il36g* mRNA was upregulated in the hyper-responsive A/J strain treated with OVA compared to both the PBS control group and the Ova-treated

C3H/HeJ strain. mRNA levels in whole lung tissue lysate increased within 6 hours of intratracheal OVA administration and returned to baseline by 72 hours post-administration. *Il36a*, *Il36b*, and *Il36rn* mRNA was not detected in the time period measured. In the house dust mite model of asthma, IL-36γ protein was detectible in the lungs of both HDM- and PBS-treated mice at 1, 6, 24, and 48 hours following the last dose suggesting a basal, constitutive level of expression (Ramadas et al., 2012). However, at 24 hours post-dosing, HDM-treated mice showed increased expression of IL-36γ compared to PBS-treated control. Using IFM to analyze sections of lungs from HDM-treated mice, it was found that epithelial cells are the source of IL-36γ protein during basal expression, but the authors did not determine the source of HDM-induced IL-36γ protein expression. Intratracheal administration of 10 μg IL-36γ twice a day for 2 days led to increased mucus production at 24 hours following the last dose and led to airway and airspace infiltrates at 6 and 24 hours postdosage. qPCR analysis of whole lung at these time points showed that IL-36γ administration led to increased expression of neutrophil chemoattractants *Cxcl1* and *Cxcl2*, monocyte chemokines *Ccl2*, *Ccl7*, and *Ccl12*, and lymphocyte-homing proteins *Cxcl9*, *Cxcl10*, and *Cxcl11*, but not eosinophil chemokines *Ccl11* and *Ccl24*. IL-36γ also induced production of *Il1a*, but not *Il1b*. A single administration of IL-36γ was sufficient to increase airway hypersensitivity compared to PBS-treated control mice. Analysis of BAL fluid harvested from mice 24 hours after a single dose of IL-36γ showed increased neutrophils but no eosinophils. The same analysis after multiple doses of IL-36γ showed the airway infiltrate to be of similar composition except with increased lymphocytes and increased cell numbers. Finally, challenge with HDM followed by IL-36γ caused a purely neutrophil influx without eosinophils or lymphocytes. This was not due to endotoxin contamination as

C3H/HeJ mice, which lack TLR4, showed a similar response. IL-36γ administration led to increased NF-κB binding activity on a DNA probe assay 2 hours after administration, which returned to baseline by 6 hours after the last dose. Several other transcription factors had reduced binding activity at 2 hours postdose, including the androgen receptor, HIF, MEF2, NF1, and NKx2.5. At 6 hours postdosage, there was decreased activity of GATA and ISRE. Treatment of RAW264.7 mouse macrophages with IL-36γ led to dose-dependent expression of an NF-κB reporter construct and treatment of alveolar macrophage line MH-S led to transiently increased *Cxcl1* and *Cxcl2* expression, confirming *in vivo* results.

In humans, IL-36γ mRNA was upregulated during *ex vivo* culture of human bronchial epithelial cells from asthma patients and was one of only two genes further induced when cells from asthma patients were infected with rhinovirus (Bochkov et al., 2010).

IL-36 in influenza

Il36a and *Il36g* were expressed in the lung following influenza infection and IL-36α was released in microparticles from alveolar epithelial cells in a caspase-1- and caspase-3/7- dependent manner. Knockout of *Il36r* protected mice from lung injury and mortality during influenza infection by reducing early cytokine and chemokine expression and subsequent leukocyte influx and activation. This study used *Il36g*$^{-/-}$ mice but only as a control in challenge experiments where WT mice had 100 % mortality.

CXCR6/CXCL16 in the lung

Healthy Lung. CXCL16 expression by alveolar macrophages in the lungs of healthy and diseased patients has been reported (Morgan et al., 2005). Alveolar macrophages released CXCL16 constitutively regardless of disease state and CXCL16

release was increased by treatment with LPS, but not TNF or IFNγ. Soluble CXCL16 was present in the BAL fluid of humans and does not correlate with disease state. Cultured human bronchial epithelial cells expressed CXCL16 at ng/mL concentrations at baseline and expression was upregulated upon stimulation with IFNγ (Day et al., 2009b).

CXCR6 was found to be differentially expressed on human $CD103^+$ and $CD69^-$ $CD8^+$ T cells isolated from lung explants, with $CD103^+$ cells having a much greater percentage of $CXCR6^+$ cells than the $CD69^-$ population (Morgan et al., 2008). $CD8^+$ T cells from the human lung expressed 40-fold more *CXCR6* mRNA than $CD8^+$ T cells from the blood (Day et al., 2009a).

Sarcoidosis. In one report, approximately half of T cells recovered from the BAL of patients with active sarcoidosis were $CXCR6^+$ compared with 20 % in patients with inactive sarcoidosis and 6 % in healthy controls (Agostini et al., 2005). Another work found that 85 % of BAL T cells in sarcoidosis expressed CXCR6 compared to 7 % of blood T cells and that only 50 % of BAL T cells expressed CXCR6 in healthy controls (Morgan et al., 2005). This was also observed in non-sarcoid interstitial lung disease and patients with sarcoidosis had greater expression of CXCR6 than patients with asthma. Increased CXCR6 protein correlated with increased mRNA levels, cells expressing CXCR6 also expressed CXCR3, and these cells migrated toward CXCL16 and CXCL10 (Agostini et al., 2005). IHC showed that T cell infiltrates in the lung of patients with active sarcoidosis were $CXCR6^+$ and that the T cells surrounding the central core of the granuloma were also $CXCR6^+$. CXCL16 was expressed by monocytes, macrophages, multinucleated giant cells, and epithelioid cells within the granuloma. Explants from

pulmonary fibrosis patients who underwent lung transplant showed staining for CXCL16 limited to the alveolar wall.

Asthma. In an allergen challenge model of asthma in Brown Norway rats, CXCR6 was expressed on 30-40 % of lymphocytes isolated from the lungs and 10-20 % of lymphocytes in the BAL fluid (Latta et al., 2007). CXCL16 expression was not increased in bronchial epithelial cell cultures from asthmatic donors compared to healthy controls (Day et al., 2009b).

COPD. While <1 % of CD8 T cells expressed CXCR6, the level of CXCR6 expression correlated with disease severity. CXCL16 was constitutively expressed and did not correlate with disease severity.

M. tuberculosis. Intranasal, but not intradermal vaccination with an adenovirus expressing the 85A antigen of *M. tuberculosis*, induced increased expression of CXCR6 on lung-resident $CD8^+$ T cells (Lee et al., 2011). Increased numbers of $CXCR6^+$ $CD8^+$ T cells were found in the lungs and BAL fluid of mice 3 weeks after vaccination and many of these were antigen-specific. $CXCR6^+$ cells were $CD27^{Lo}$, produced IFNγ and TNF, and depletion of the cells decreased the efficacy of vaccination. Following vaccination, serum levels of CXCL16 increased and returned to baseline in one week. Intranasal dosage of rec85A, but not CXCL16, increased the number of T cells in the BAL, and administration of both proteins synergized.

IL-36 and CXCR6 play important roles in the immune system in the healthy and diseased lung. My research concentrated on the role of IL-36γ during acute influenza infection and how CXCR6 homes antigen-specific memory T cells to the airways. While seemingly disparate topics, they both involve cytokine signaling in the context of respiratory virus infection.

Chapter 2. IL-36γ protects against severe influenza infection by promoting lung alveolar macrophage survival and limiting viral replication

Despite the broad availability of licensed vaccines, influenza viral illness remains a major threat to public health, particularly among children and the elderly (Dolin, 2012; Thompson et al., 2003). In severe cases, influenza infection can cause primary viral pneumonia or sensitize the host to secondary bacterial infection, and can also exacerbate underlying health problems including congestive heart failure, chronic obstructive pulmonary disease, and asthma. One reason for the continued public health burden of influenza is the imperfect antigenic match between the vaccine and circulating influenza strains that results in only 50-80 % protection in the best of years (Dolin, 2012). In the absence of effective cellular or humoral memory responses, the innate defenses of the respiratory tract serve as the only mechanisms to control the spread of virus in the early phases of infection.

Influenza infection of the respiratory epithelium leads to the activation of antiviral responses via the extracellular and endosomal TLR receptors or the intracellular receptors RIG-I and NLRP3, causing cells to release interferons as well as pro-inflammatory and chemotactic factors (Ichinohe, 2010; Iwasaki and Pillai, 2014; Loo et al., 2008; Pulendran and Maddur, 2014). Interferons serve to limit protein translation within infected cells and decrease the permissibility of uninfected cells to the virus during the mobilization and recruitment of immune cells from the bone marrow and circulation, which can take 4-5 days (Lim et al., 2015; Schultz-Cherry, 2015; Weiss et al., 2010). Several innate cell types have been shown to be key to controlling influenza infection. NK cells can recognize infected cells via NKp46 binding to surface hemagglutinin, leading to lysis of cells that are displaying viral proteins (Schultz-Cherry,

2015). Neutrophils can also serve to promote viral clearance in severe cases of influenza, but neutrophils, along with monocytes, and have been shown to contribute to immune pathology during some models of influenza infection (Camp and Jonsson, 2017; Lin et al., 2008). In contrast, among the earliest responders to influenza infection in the lung are tissue-resident alveolar macrophages. In mice, these cells have been shown to decrease the infection of type I alveolar epithelial cells during the initial 48 hours of infection, before other innate cell types arrive in the lung (Cardani et al., 2017). Depletion of alveolar macrophages by either genetic knockout or liposomal clondronate treatment increases morbidity, mortality, and viral load during influenza infection (Cardani et al., 2017; Schneider et al., 2014). Therefore, lung alveolar macrophages play a critical role as one of the few lung-resident innate immune cell types capable of responding to influenza infection during the initial stages of infection, prior to immune recognition that leads to the initial inflammatory burst alerting the systemic immune system to a lung infection.

Severe influenza infections are characterized by viral infection throughout the upper and lower respiratory tract (Taubenberger and Morens, 2008). Consequences of increased viral titers throughout the respiratory tract include hyperactive cytokine responses, and patients hospitalized with severe influenza showed significant increases in pro-inflammatory cytokines (Beigel et al., 2005). Elevated expression of type I interferons, TNF-α, IL-1, IL-6, IL-18, and IL-33 have been observed in pathogenic influenza infections, suggesting that inhibition of these cytokines may ameliorate influenza pathology and improve host survival (Guo and Thomas, 2017). However, deletion or blockade of pro-inflammatory cytokine pathways including IFNα, IFNγ, TNF, IL-1, and IL-6 has shown mixed results in mice and humans (Bot et al., 1998;

Dienz et al., 2012; García-Sastre et al., 1998; Hussell et al., 2001; Perrone et al., 2010; Salomon et al., 2007; Seo et al., 2011; Teijaro, 2014; Weiss et al., 2010). General immunosuppression with corticosteroids has also shown little to no effect on patient outcome in clinical trials (Brun-Buisson et al., 2011; Teijaro, 2014; Tisoncik et al., 2012). These failures have renewed efforts to identify novel pro-inflammatory host mediators that contribute to influenza pathogenesis. One such family of pro-inflammatory mediators are the IL-36 family of cytokines, IL-36α, -β, and -γ, which are recently-discovered members of the IL-1 family. These proteins have been shown to be important in several different inflammatory conditions including asthma, colitis, and psoriasis (Medina-Contreras et al., 2015; Ramadas et al., 2011; Tortola et al., 2012). In addition, IL-36γ administration has been shown to increase mucus production and neutrophil migration into the lungs of mice (Ramadas et al., 2011). A recent study showed that IL-36γ-deficient mice were more susceptible to pulmonary *S. pneumonia* infection, demonstrating an important role for IL-36γ in lung immunity (Kovach et al., 2017). In addition, deletion of IL-36 receptor improves survival during lethal influenza challenge in mice (Aoyagi et al., 2017a). However, the role of individual IL-36 cytokines in immunity against respiratory virus infections has not been investigated.

In the present study, we investigated the regulation of IL-36 cytokines during mild and severe influenza infections in mice. *Il36g* mRNA was significantly increased in the lung during the initial stages of influenza infection, suggesting that inhibition of IL-36γ production may prevent excessive inflammation during severe influenza infection and improve host survival. Surprisingly, infection of IL-36γ-deficient mice with influenza virus showed the opposite effect, as IL-36γ-deficient mice had significantly

increased weight loss, mortality, and viral titers during both mild and severe influenza infection. Analysis of innate immune cell subsets in the lung revealed a rapid and dramatic loss of lung alveolar macrophages in IL-36γ-deficient mice compared to their wild-type counterparts. Finally, the decreased survival in IL-36γ-deficient mice could be rescued through the transfer of wild-type alveolar macrophages into the lung prior to influenza infection. Overall, these data demonstrate an unexpected protective role for IL-36γ during influenza infection by promoting the survival of lung alveolar macrophages.

Materials and Methods

Mice. C57BL/6J (WT) and B6.SJL-Ptprc^{a} Pepc^{b}/BoyJ (CD45.1) were purchased from The Jackson Laboratory and bred in house under specific pathogen free conditions at Emory University. For some experiments WT and CD45.1 mice were crossed to produce CD45.1^{+}CD45.2^{+} F1 offspring. Cryopreserved sperm of the line B6;129S5-Il1f9^{tm1Lex}/Mmucd (*Il36g*$^{-/-}$ mice) was purchased from the Knockout Mouse Project, injected into a C57Bl6/J oocyte and backcrossed in house as previously described (Supplementary Table 1) (Harusato et al., 2017). Intranasal infection with influenza A/HKx31 (H3N2) at 30,000 or 300,000 50% egg infectious dose (EID_{50}) and PR8 (H1N1) at 450 PFU was performed under isoflurane anesthesia. For all mortality experiments, mice were monitored with daily weighing and euthanized when they reached 25% weight loss. All experiments were completed in accordance with the Institutional Animal Care and Use Committee guidelines of Emory University.

Whole lung mRNA isolation for viral titers and Il36 qPCR. Infected mice were euthanized by 2,2,2-tribromoethanol overdose and brachial exsanguination. Lungs were harvested into RNA later (Sigma) and stored at 4 degrees C overnight and then at -

80 degrees C until processing. Lungs were homogenized in Trizol (Ambion) by either Tissue Tearor or Bead Bug according to the manufacturer's directions. RNA was purified from the homogenized lung using Ambion spin columns by a modified manufacturer's protocol. cDNA was synthesized from RNA using reverse transcriptase (Applied Biosystems) and viral titers were determined by digital droplet PCR and Quantasoft software (Biorad) using primers and probes directed at the Influenza *NP* gene, which is conserved between x31 and PR8. The sequences were X-31 NP Forward: 5'-GCA TGC CAT TCT GCC GCA TT-3', X-31 NP Reverse: 5'-GCT GAT TTG GCC CGC AGA TG-3', Probe: 5'- /5HEX/TA+G T+CT +CCA TAT TTT CAT T+G+G AA+G C/3BHQ_1/ -3'. Expression levels of IL-36 family members were determined by real time qPCR on a Biorad CFX96 Real time system and CFX manager v3.1 using primers against *Il36a*, *Il36b*, *Il36g*, and *Hprt*. Sequences were *Il36a* forward: 5'-TAG TGG GTG TAG TTC TGT AGT GTG-3', *Il36a* reverse: 5'-GTT CGT CTC AAG AGT GTC CAG ATA T-3', *Il36b* forward: 5'-ACA AAA AGC CTT TCT GTT CTA TCA T-3', *Il36b* reverse: 5'-CCA TGT ATT TAC TTC TCA GAC T-3', *Il36g* forward: 5'-AGA GTA ACC CCA GTC AGC GTG-3', *Il36g* reverse: 5'-AGG GTG GTG GTA CAA ATC CAA-3', *Hprt* forward: 5'-CAC AGG ACT AGA ACA CCT GC-3', *Hprt* reverse: 5'-GCT GGT GAA AAG GAC CTC T-3'. For *Il36g* expression in sorted immune cells, cDNA was synthesized with the iScript cDNA synthesis kit before real time qPCR (Biorad). Real time qPCR Data were analyzed using CFX Manager before export to Microsoft Excel.

Lung harvest for pathological examination. Mice were euthanized as above and the ribcage carefully removed. A small incision was made in the trachea and the lungs were inflated with 0.75 mL formalin. The lungs, heart, and thymus were removed *en bloc* and placed into a cassette and then into formalin jars. Lungs were embedded in

paraffin, sectioned and stained with hematoxylin and eosin by the Winship Research Pathology Core Lab at Emory University. Lungs were scored for bronchiolar and alveolar necrosis, perivascular infiltrates, and alveolar exudates and infiltrates by a pathologist blinded to treatment conditions.

Isolation of immune cells from lungs, flow cytometry, and cytokine analysis. For isolation and quantification of immune cells from lungs, mice were euthanized as above. Bronchoalveolar lavage was performed using 1 mL of compete RPMI delivered via an 18-gauge IV catheter into a small incision into the trachea. The airways were washed five times before the lungs were harvested into HBSS. Lungs were finely minced with scissors before digestion (30 minutes, 37 degrees C) with warm HBSS containing 4E5 units/mL DNase (Sigma) and 500 mg/L Collagenase D (Roche). Lungs were further homogenized via swishing with a 3-mL syringe before and after digestion and every 10 minutes during digestion. Following digestion, immune cells were purified via 40 %/80 % isotonic Percoll gradient centrifugation. Live/dead staining was performed with Zombie Yellow, Zombie Ultraviolet or Zombie Near Infrared (Biolegend) and Fc blocking was done with anti-CD16/32 clone 2.4G2 in FACS buffer consisting of 2 % w/v BSA and 0.05 % w/v sodium azide in PBS. The hybridoma expressing 2.4G2 was purchased from ATCC and cultured in our lab. The antibody was purified from the supernatant by standard techniques. Cells were stained with fluorescently labeled antibodies purchased from Abcam, Biolegend, BD Biosciences or eBioscience in FACS buffer. Antibodies were anti-CD45.2-A488 [104, Biolegend], anti-CD45.2-A647 [104, Biolegend], anti-CD86-PE [GL1, Biolegend] anti-CD11c-PE/CF594 [HL3, BD Biosciences], anti-CD103-PerCP/Cy5.5 [2E7, Biolegend], anti-I-A/I-E-PE/Cy7 [M5/114.15.2, Biolegend], anti-CD45R-APC [RA3-6B3, Biolegend], anti-Ly6C-APC/Cy7

[AL-21, BDBiosciences], anti-SiglecF-BV421 [E50-2440, BD Biosciences], anti-Ly6G-BV510, [1A8, Biolegend], anti-NK1.1-BV650 [PK136, Biolegend], anti-CD11b-BV711 [M1/70, Biolegend], anti-CD90.2-BV785 [30-H12, Biolegend], anti-CD206-A700 [C068C2, Biolegend], anti-CD200R-PE [OX-110, Biolegend] anti-TREM2-FITC [78.18, Abcam], anti-CCR5-PerCP/e710 [7A4, eBioscience], and anti-CD45.1-BUV395 [A20, BD Biosciences]. Cells were sorted on a BD Aria II or were fixed with 1 % paraformaldehyde before analysis on a BD LSRII or BD Fortessa X20. Annexin V (Biolegend) staining was performed according to manufacturer's instructions immediately before flow cytometric analysis. Cell numbers were determined by counting live cells on a hemocytometer in the presence of trypan blue (Sigma). Flow cytometry data was initially analyzed using FlowJo v10.0.8r1 before exporting data to Microsoft Excel for further calculations. For cytokine analysis, the first BAL pull was kept separate and spun at 700 x g for 5 minutes to remove cells. The supernatant was stored at -80 degrees C while the cells were combined with the remaining BAL pulled. Cytokine levels in the BAL supernatant were determined by a Biolegend LEGENDPlex Mouse Inflammation Panel by manufacturer's instructions.

Cell isolation and adoptive transfer. For transfer of alveolar macrophages, lungs were harvested from naïve B6 or *Il36g*$^{-/-}$ mice and digested (30 minutes, 37 degrees C) with Collagenase type II (625 units/mL, Worthington) and DNase (4E5 units/mL, Sigma) and swished as above. Percoll purification was performed as above. Alveolar macrophages were isolated via positive selection on CD11c and SiglecF with MACS columns per manufacturer's instructions (Miltenyi). The bound fraction was collected and an aliquot was stained to determine purity. 500,000 alveolar macrophages in 50 μL PBS were administered intranasally to recipient mice under isoflurane anesthesia. WT

controls received PBS intranasally. For survival experiments, mice were infected with high dose x31 the following day and monitored daily for 14 days. For next day analysis of transfer efficiency or phenotypic analysis of *Il36g*$^{-/-}$ alveolar macrophages transferred to WT mice, the mice were not infected.

Statistics. Statistical analysis was performed in GraphPad Prism and the tests used to determine significance are listed in the appropriate figure legends. Asterisks in the figures denote significance (* $p \leq 0.05$, ** $p < 0.01$, *** $p < 0.001$, **** $p < 0.0001$).

Results

IL-36γ is induced during influenza infection and protects against morbidity and mortality. To determine the expression level of IL-36 family members following influenza infection, B6 mice were infected with influenza A/HK-x31 (H3N2) and expression of the IL-36 cytokine family genes *Il36a*, *Il36b*, and *Il36g* in whole lungs were measured by RT-PCR (Figure 1A-C). *Il36a* expression was not altered following infection, and *Il36b* was significantly increased only on day 3 following influenza infection. We observed *Il36g* expression in the lung was significantly increased by day 3 after infection, and increased expression of *Il36g* was maintained through day 6. In addition, expression levels of *Il36g* in naïve (d0) whole lungs were higher than either *Il36a or Il36b* (Supplemental Figure 1). *Il36g* expression has previously been reported in bronchial epithelial cells following infection with respiratory viruses or bacteria, but which immune cells produce the cytokine during influenza infection is not known. (Bochkov et al., 2010; Kovach et al., 2017). As *Il36g* expression has been observed in multiple immune cell types in different models of inflammation, we examined several types of leukocytes for *Il36g* RNA 6 days after influenza infection, when *Il36g* was uniquely upregulated among *Il36* genes. Surprisingly, among immune cells examined,

neutrophils were the highest producers of *Il36g* mRNA at day 6 post-infection (Figure 1D). These data show that IL-36 family members, most notably IL-36γ, are induced in the lung following influenza infection and suggest a potential role of IL-36γ in mediating influenza immunity.

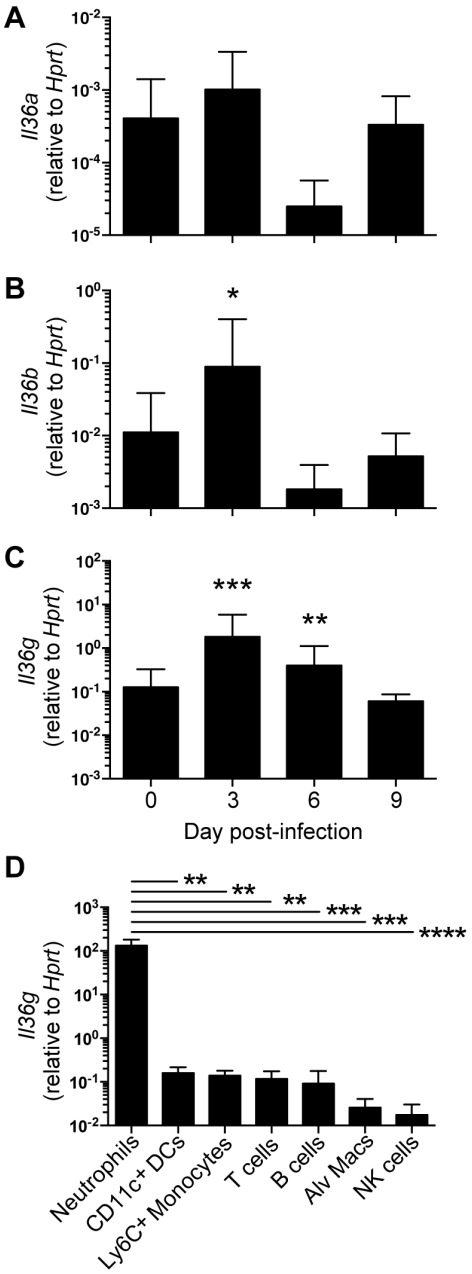

Figure 1: RT-PCR of whole lung homogenate or sorted cells for expression of *Il36* cytokines.
The expression levels of (A) *Il36a*, (B) *Il36b*, and (C) *Il36g* were determined by real-time qPCR relative to the housekeeping gene *Hprt* in naïve C57Bl/6J mice and at days 3, 6, and 9 post-infection with 30,000 EID_{50} of influenza A/HK-x31. Data are combined from three independent replicates of at least 5 mice per group. Males and females were used in equal proportions. Expression levels of *Il36g* (D) from several immune cell types as indicated below the x axis. Asterisks indicate significantly different expression from uninfected lungs by Student's t test on logarithmically transformed data (A-C) or ANOVA followed by Holm-Sidak multiple comparisons test on log-transformed data (D).

Highly pathogenic influenza infections are associated with high levels of pro-inflammatory cytokines such as TNFα and IL-1, and some studies have shown that blocking these cytokines limited immunopathology and improved survival in murine models (Hussell et al., 2001; Perrone et al., 2010). Given the pro-inflammatory role for IL-36γ in other diseases, we examined whether deletion of *Il36g* could decrease morbidity and mortality following influenza A/PR8 (H1N1) infection. As shown in Figure 2A, *Il36g*$^{-/-}$ mice had significantly greater mortality following infection, indicating that IL-36γ had a protective rather than pathogenic role in influenza immunity. To confirm a protective role for IL-36γ during influenza infection, we measured survival following infection with the less pathogenic influenza x31 (H3N2) virus. Compared to WT mice, *Il36g*$^{-/-}$ KO mice showed significantly increased weight loss beginning on day 3 post-infection, as well as significantly greater mortality, with two different doses of influenza x31 (Figures 2B and 2C). Together, these data demonstrate a surprising protective role for IL-36γ in improving survival following influenza infection with different strains and doses.

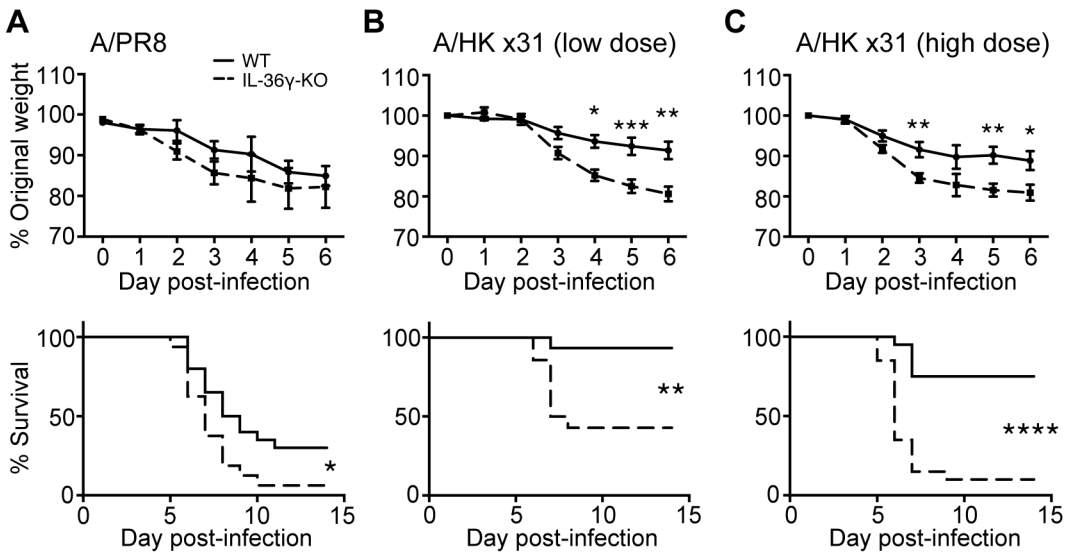

Figure 2: Survival and weight loss of WT and *Il36g*$^{-/-}$ mice following influenza infection.
Age- and sex-matched C57Bl/6J (solid lines) and *Il36g*$^{-/-}$ mice (dashed lines) were infected with (A) influenza PR8, (B) 30,000 EID_{50} x31, or (C) 300,000 EID_{50} x31 and monitored daily for weight loss. Data are combined from 2-3 independent replicate experiments of at least 10 mice per group per replicate. Male and female mice were used in equal proportions. Asterisks indicate significant differences in survival by the log-rank test or differences in weight loss by Student's t test.

The absence of IL-36γ results in increased viral replication and immunopathology. We next examined whether the decreased survival in mice lacking IL-36γ was associated decreased control of viral replication during influenza infection. As shown in Figure 3A, we found that *Il36g*$^{-/-}$ mice have increased viral load by digital droplet PCR 6 days after infection with PR8. Likewise, following infection with a low dose of x31 influenza, *Il36g*$^{-/-}$ mice have increased viral load at days 6 and 9 post-infection (Figure 3B). *Il36g*$^{-/-}$ mice which were infected with the high dose of x31 had increased viral titers as soon as 3 days post-infection and continued to have increased titers until 6 days post-infection, when the majority of the mice reach humane endpoints (Figure 3C). We also analyzed the cytokines present in the bronchoalveolar lavage (BAL) fluid of WT and *Il36g*$^{-/-}$ mice infected with high dose x31, since these mice have a

large difference in viral titers early in infection. We found that compared to WT mice, the BAL of *Il36g*$^{-/-}$ mice had increased IFNβ and IL-6, but not IFNγ, TNF, or IL-1α (Figure 3D). To further understand the role of IL-36γ during influenza infection, formalin-fixed lungs from WT and *Il36g*$^{-/-}$ KO mice infected with high-dose x31 were evaluated for inflammation and damage by an independent pathologist blinded to treatment conditions. On day 6 post-infection, *Il36g*$^{-/-}$ mice had more diffuse immune infiltrate around the bronchioles compared to WT mice (Figure 3E). Together, these data pointed to a role for IL-36γ in controlling the early viral replication and limiting the resulting immunopathology following influenza infection.

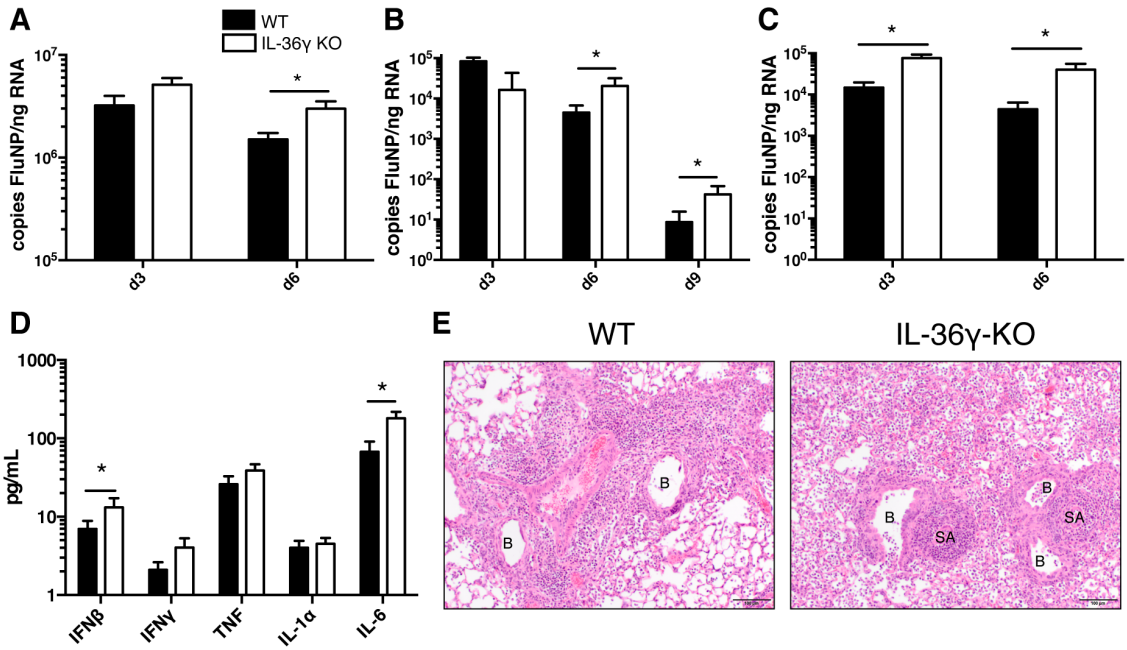

Figure 3: Viral titers, cytokine levels, and pathology of WT and *Il36g*$^{-/-}$ mice following influenza infection.
Age- and sex-matched C57Bl/6J (filled bars) and *Il36g*$^{-/-}$ mice (open bars) were infected with (A) influenza PR8, (B) 30,000 EID_{50} x31, or (C) 300,000 EID_{50} x31 and lungs were analyzed for influenza NP copy number. (D) Bronchoalveolar lavage fluid was analyzed for expression of proinflammatory cytokines on day 3 post-infection in C57Bl/6J (filled

bars) and *Il36g*$^{-/-}$ mice (open bars). (E) Example images of formalin-fixed, paraffin-embedded, H&E-stained lungs from C57Bl/6J and *Il36g*$^{-/-}$ mice. Inflamed bronchioles (B) and small arterioles (SA) are noted on the images. For A-D, data are combined from 2-3 independent replicate experiments of at least 5 mice per group per replicate. Males and females were used in equal proportions. Asterisks indicate significant differences by Student's t test on log-transformed data.

Alveolar macrophages are rapidly depleted following influenza infection in IL-36γ-deficient mice. The increased morbidity and viral titers observed in *Il36g*$^{-/-}$ mice were evident within three days post-infection, suggesting a defect in early innate immunity. As many different immune cell types contribute to the early response during influenza infection (Pulendran and Maddur, 2014), we examined multiple innate and adaptive immune cell subsets in WT and *Il36g*$^{-/-}$ mice following influenza x31 infection using a 13-color flow cytometry panel (Supplemental Figure 2). As shown in Figures 4A and 4B, the number of alveolar macrophages was significantly decreased in *Il36g*$^{-/-}$ mice on days 3 and 6 post-infection, whereas no other immune cell subsets examined showed any differences across both time points. Although there were increased numbers of CD11b^{Hi} DCs in *Il36g*$^{-/-}$ mice on day 3 post-infection, this difference was not evident at day 6, and seemed unlikely to account for the increased severity of influenza infection in IL-36γ-KO mice. To determine whether the decrease in alveolar macrophages was the result of a homeostatic defect in *Il36g*$^{-/-}$ mice, we next compared the frequency and number of lung alveolar macrophages in WT and *Il36g*$^{-/-}$ mice prior to, or following, influenza infection. As shown in Figures 4C and 4D, alveolar macrophage frequency and numbers are similar in naïve WT and *Il36g*$^{-/-}$ mice, but rapidly decline in *Il36g*$^{-/-}$ mice following infection. Thus, in the absence of IL-36γ, lung alveolar macrophages are rapidly lost following influenza infection.

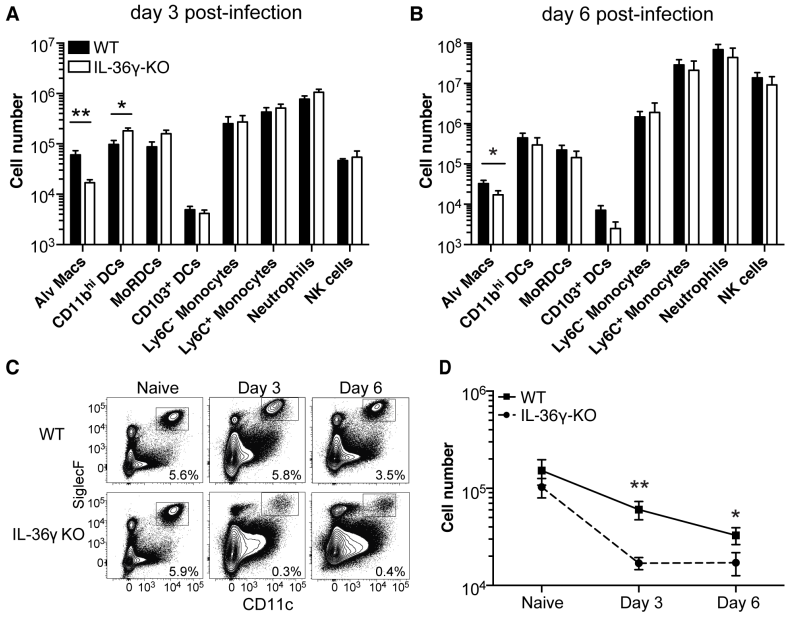

Figure 4: Analysis of innate immune subsets in the lung by flow cytometry. C57Bl/6J (filled bars) and *Il36g*$^{-/-}$ mice (open bars) were infected with 300,000 EID_{50} x31 influenza and the numbers of different immune cell subsets in the lung were assessed at (A) day 3 and (B) day 6 post-infection. (C) Representative flow plots of live CD45.2+ cells are shown with gates denoting alveolar macrophages. (D) The number of alveolar macrophages in C57Bl/6J (solid line) and *Il36g*$^{-/-}$ mice (dashed line) over time following influenza infection. Data are combined from two-three independent replicates of at least 5 mice per group per replicate. Males and females were used in equal proportions. Asterisks indicate significant differences in cell number by Student's t test on log-transformed data.

Alveolar macrophages from Il36g$^{-/-}$ *mice have an M2-like phenotype.* We next investigated the potential mechanism governing alveolar macrophage loss in *Il36g*$^{-/-}$ mice following influenza infection. In naïve mice, there was no difference in the frequency of live or early apoptotic alveolar macrophages by Annexin V and live/dead staining (Figure 5A). However, within one day of influenza infection, we observed a significant decrease in live alveolar macrophages in *Il36g*$^{-/-}$ mice compared to WT mice, with a corresponding increase in early apoptotic cells (Figure 5B). To better understand this difference in apoptosis, and since M1-like macrophages are more resistant to

apoptosis, we next examined if there were differences in M1/M2 macrophage skewing between WT and *Il36g*$^{-/-}$ mice (Pachulec et al., 2017). We examined the surface expression of classical M1 proteins CD86 and MHCII, M2 proteins CD206 and CD200R, the pro-survival proteins TREM2 and CCR5, as well as CD11b on alveolar macrophages form WT and *Il36g*$^{-/-}$ mice (Rőszer, 2015; Tyner et al., 2005; Wu et al., 2015). Alveolar macrophages isolated from *Il36g*$^{-/-}$ mice had a statistically significant increase in the expression of CD206 and CD200R, markers associated with an M2-like macrophage (Figure 5C). To confirm this result, we sorted out alveolar macrophages from naïve WT and *Il36g*$^{-/-}$ mice and performed real time qPCR for the hallmark M2 gene *Retnla*. We found that *Il36g*$^{-/-}$ alveolar macrophages had greater expression of *Retnla* compared to their WT counterparts, supporting our flow cytometric results (Figure 5D). We next isolated and transferred *Il36g*$^{-/-}$ alveolar macrophages into WT mice and allowed the cells to rest for 10 days (Figure 5E). When the phenotype of the transferred cells was compared to the input cell mix, levels of surface CD200R and CD206 decreased over the 10 days in the presence of IL-36γ (Figure 5F). In fact, CD200R expression was equivalent to the endogenous cells while CD206 expression remained slightly elevated. Together, these data show the loss of alveolar macrophages in *Il36g*$^{-/-}$ mice following influenza infection was associated with a rapid increase in apoptosis, and alveolar macrophages in *Il36g*$^{-/-}$ mice had a phenotype consistent with a more M2-like macrophage polarization that may have contribute to their decline following influenza infection. Additionally, transfer of *Il36g*$^{-/-}$ alveolar macrophages to an IL-36γ-replete environment restores the phenotype of the cells as measured by decreased surface CD206 and CD200R.

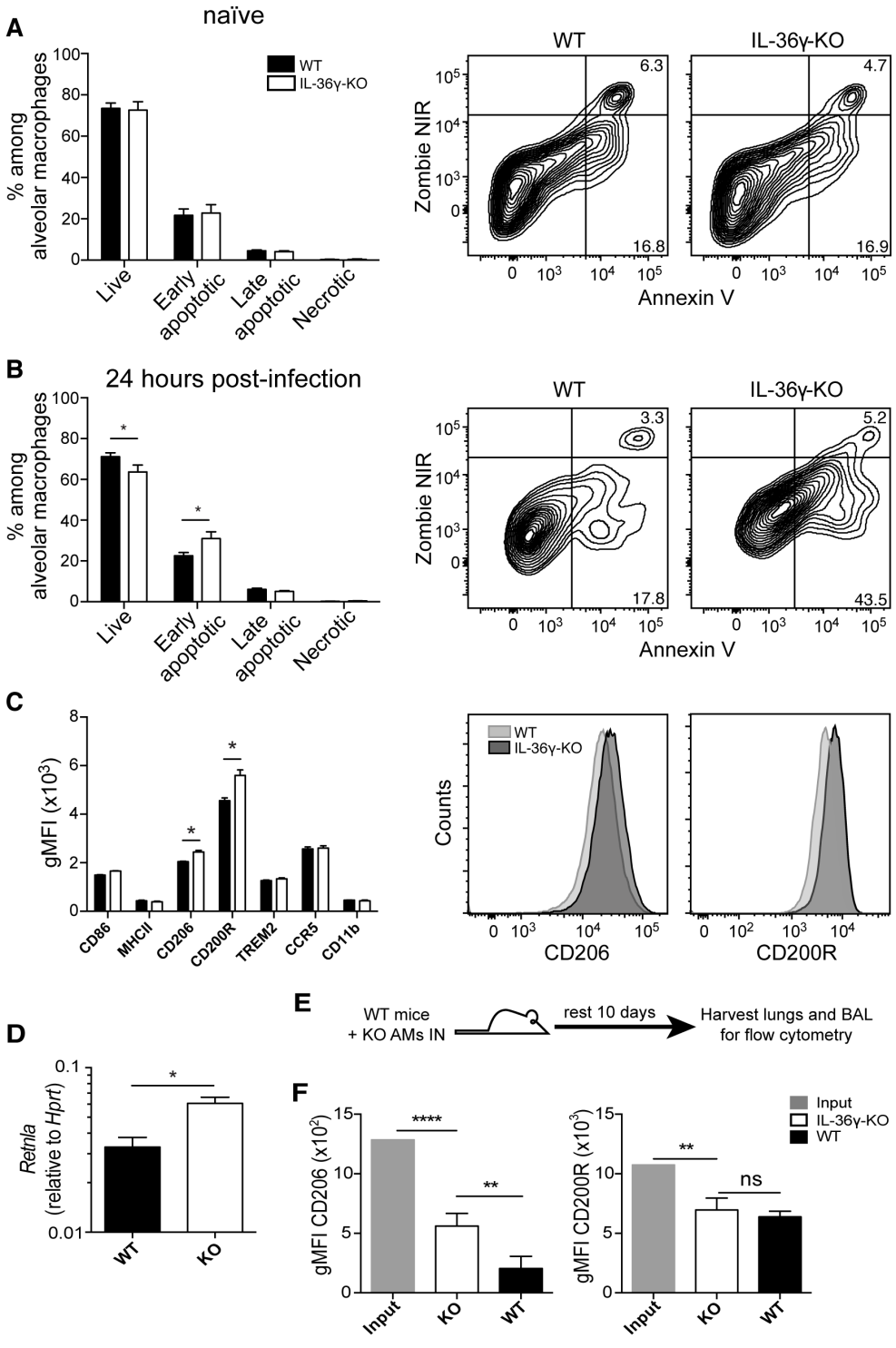

Figure 5: Apoptosis and surface marker expression of WT and *Il36g*$^{-/-}$ mice. The apoptosis of alveolar macrophages from C57Bl/6J (filled bars) and *Il36g*$^{-/-}$ mice (open bars) was measured using live/dead and Annexin V staining in (A) naïve mice or (B) 24 hours post-infection. Representative staining is shown gated on alveolar macrophages. (C) Phenotype of alveolar macrophages in naïve C57Bl/6J and *Il36g*$^{-/-}$

mice for markers associated with M1 and M2 macrophages subsets. (D) Expression of *Retnla* in alveolar macrophages isolated from naïve WT (black bars) and *Il36g*$^{-/-}$ (open bars) alveolar macrophages. (E and F) Geometric mean fluorescence intensity of CD206 and CD200R on input *Il36g*$^{-/-}$ alveolar macrophages (grey bars), *Il36g*$^{-/-}$ alveolar macrophages after 10 days in a WT mouse (open bars), or the host alveolar macrophages (black bars). Data are combined from 2-3 independent replicates of at least 5 mice per group per replicate. Males and females were used in equal proportions. Asterisks indicates significant differences in cell number by ANOVA followed by Tukey's multiple comparisons test (A and B), Student's t test (C, D WT vs KO), or the one-sample T test (D, input vs KO).

Transfer of wild-type alveolar macrophages restores protection against influenza infection in IL-36γ-deficient mice. Alveolar macrophages were critical for the early control of viral replication and protection against severe influenza infection (Cardani et al., 2017; Schneider et al., 2014). Therefore, we sought to determine if complementing *Il36g*$^{-/-}$ mice with WT alveolar macrophages prior to influenza infection would be sufficient to protect against severe influenza disease. To confirm our method transferred alveolar macrophages in physiologically relevant numbers, WT alveolar macrophages were transferred to IL-36γ-KO mice and the BAL and lung were harvested the next day (Figure 6A). We found that 30 % of alveolar macrophages in the BAL and 15 % of those in the lung were transferred WT cells, confirming that physiological numbers of cells were transferred (Figure 6B). Next, we isolated alveolar macrophages from the lungs of naïve WT or *Il36g*$^{-/-}$ mice, and transferred them intranasally to separate cohorts of *Il36g*$^{-/-}$ mice one day prior to influenza infection (Figure 6C). As shown in Figure 6D, *Il36g*$^{-/-}$ mice that received WT alveolar macrophages showed a significant increase in survival compared to *Il36g*$^{-/-}$ mice that received *Il36g*$^{-/-}$ alveolar macrophages. The survival of *Il36g*$^{-/-}$ mice that received WT alveolar macrophages was equivalent to WT mice. Thus, the defect in influenza immunity observed in *Il36g*$^{-/-}$ mice

resulting in severe disease could be rescued by the presence of WT alveolar macrophages.

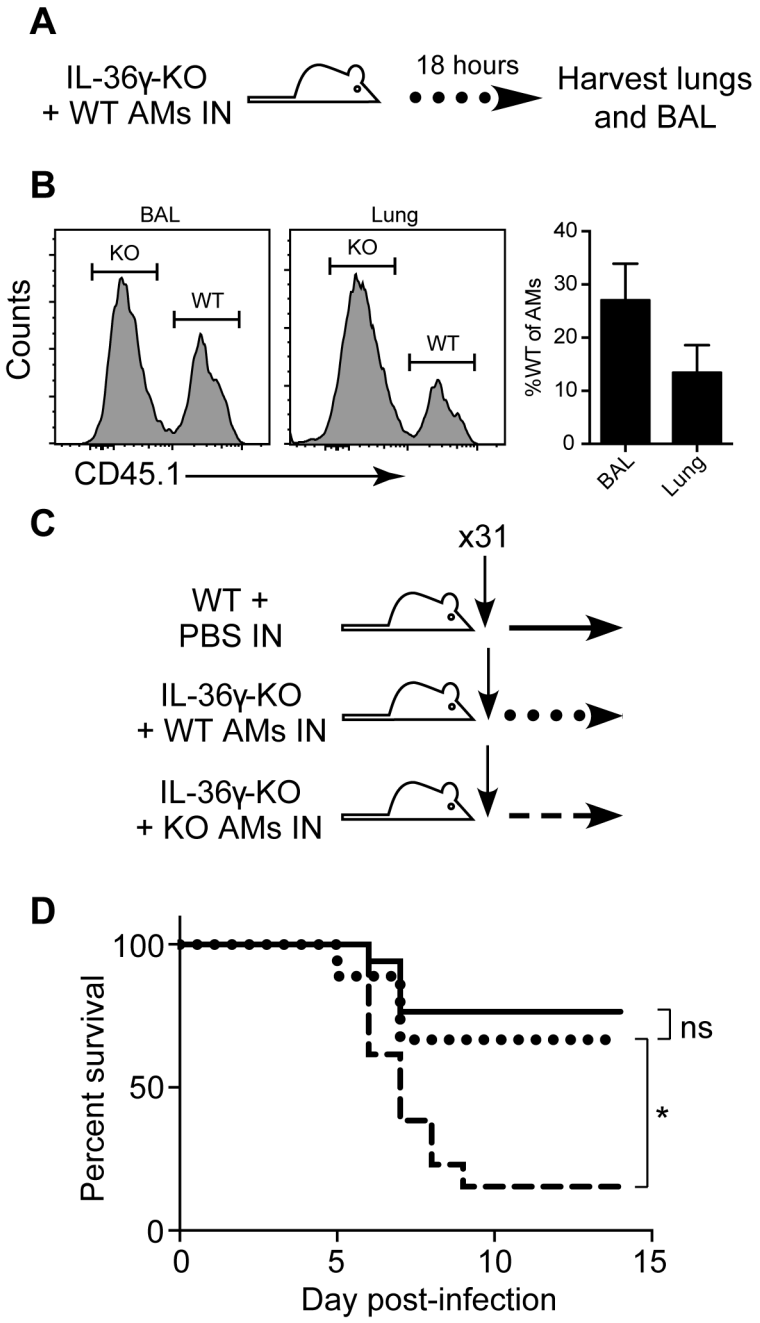

Figure 6: Transfer of WT alveolar macrophages rescues mortality in IL-36γ-KO mice.
(A) *Il36g*$^{-/-}$ mice were transferred with 5×10^5 purified WT alveolar macrophages intranasally and (B) lungs were harvested the next day for identification of the transferred cells on the congenic marker CD45.1. Representative staining gated on live

alveolar macrophages and percentage WT (transferred cells) are shown. (C) Age- and sex-matched *Il36g*$^{-/-}$ mice were transferred with 5×10^5 purified *Il36g*$^{-/-}$ alveolar macrophages intranasally (dashed line), and a matched cohort of *Il36g*$^{-/-}$ mice (dotted line) received 5×10^5 purified WT alveolar macrophages intranasally. C57Bl/6J (solid line) mice were mock transferred with PBS. Data are combined from 2 independent replicate experiments of at least 4 mice per group. All recipients were male mice to prevent rejection on Y antigens. Asterisk indicate a significant difference in survival by the log-rank test.

Discussion

We have shown that *Il36g* was uniquely upregulated among IL-36 cytokines during the first 6 days of influenza infection. Mice lacking *Il36g* had increased morbidity and mortality following influenza infection and this increase was associated with increased viral titers, higher levels of inflammatory cytokines in the airways, and more diffuse pathology in *Il36g*$^{-/-}$ mice. Analysis of innate cell subsets revealed a significant decrease in alveolar macrophages in *Il36g*$^{-/-}$ mice as soon as 3 days post-infection that continues through day 6 post infection. Compared to their WT counterparts, alveolar macrophages in *Il36g*$^{-/-}$ mice were skewed towards an M2-like phenotype by surface marker and gene expression prior to influenza infection, and showed increased apoptosis within 24 hours of infection. Transfer of WT alveolar macrophages into the lungs of *Il36g*$^{-/-}$ mice increased survival compared to *Il36g*$^{-/-}$ mice that received *Il36g*$^{-/-}$ alveolar macrophages, and the survival of WT-transferred *Il36g*$^{-/-}$ mice was equivalent to mock-transferred WT mice.

Early control of viral replication in the lung is key to preventing dissemination of the virus throughout the lung. Several cell types have been shown to have a role in the innate immune response to influenza, including neutrophils, natural killer cells, and alveolar macrophages. However, of these, only alveolar macrophages are situated within the respiratory tract prior to infection and can respond immediately without the need for recruitment from the vasculature or bone marrow (Lim et al., 2015; Schultz-

Cherry, 2015; Weiss et al., 2010). Our data and previously published studies indicated a role for alveolar macrophages in controlling viral replication during the first three days of infection, before neutrophils and natural killer cells arrive to the lungs *en masse*. *Il36g*$^{-/-}$ mice, which rapidly lost alveolar macrophages during influenza infection, have increased viral titers, presumably leading to increased inflammation and immunopathology. Indeed, we detected more IL-6 and IFNβ in the airways of IL-36γ-KO mice at day 3 post-infection. A more robust cytokine response early during infection correlated with more diffuse immune infiltrate late in the infection, presumably leading to an ARDS-like state in *Il36g*$^{-/-}$ mice and increased mortality.

Cytokines function as key factors for communication between immune cells during influenza infection. The outcome of influenza infection is not only dependent on the presence or absence of particular cytokines, but also their levels within the tissue. For example, production of IFNα is correlated with symptom onset in humans and can boost the production of other inflammatory mediators, but in mice, deletion of its receptor in mice led to increased IL-8 production, increased neutrophil recruitment, and greater mortality upon lethal influenza challenge (Hayden et al., 1998; Seo et al., 2011). Another example of the importance of maintaining a balanced cytokine response for proper immune function comes from studies of IL-1. Deletion of *Il1r* led to decreased pathology and neutrophil recruitment, but also delayed viral clearance and increased mortality (Schmitz et al., 2005). IL-1 was thus key to survival of influenza infection, but also contributed to the development of ARDS in humans (Pugin et al., 1996). We found that lack of IL-36γ has a similar effect to deletion of IL-1R on the outcome of influenza infection, albeit by a different mechanism. In both cases, the mice without the cytokine pathway of interest have an extended viremia and suffer greater

morbidity and mortality. However, in IL-36γ-KO mice, alveolar macrophages are rapidly lost from the lung due to increased apoptosis. This removes a key blockade to early viral replication and induces greater proinflammatory cytokines (similar to observations in IFNαR-KO mice) leading to increased pathology as the infection progresses. We find that in naïve mice, *Il36g* mRNA is produced at much higher levels than either *Il36a* or *Il36b* and other reports have found that IL-36γ protein is detectable in the BAL of naïve mice (Aoyagi et al., 2017b; Kovach et al., 2017). This baseline production of IL-36γ likely acts on alveolar macrophages to maintain a more M1-like phenotype in the absence of infection. Following influenza infection, neutrophils have the highest expression of *Il36g* among immune cells, which differed from the dogmatic production of the cytokine by epithelium, dendritic cells, or $CD4^+$ T cells (Gabay and Towne, 2015). *Il36g* production by neutrophils has only been observed in experimental autoimmune encephalitis, a mouse model of multiple sclerosis, and it is very interesting that full length IL-36γ was cleaved to its more active form by neutrophil-derived elastase and proteinase-3 (Bozoyan et al., 2015b; Henry et al., 2016). If neutrophils produce both the cytokine and activating protease, it is possible that neutrophils release cleaved IL-36γ, but confirming that hypothesis requires further work. While baseline production of IL-36γ was important for macrophage phenotype in naïve mice, it was likely the IL-36γ produced by neutrophils contributed to the survival of alveolar macrophages during the early stages of influenza infection.

IL-36 family cytokines had a key role in pulmonary immune responses to bacterial and viral infection as well as the development of asthma. In mice, a SNP regulating expression of IL-36γ determined the asthma sensitivity or resistance of two

inbred mouse lines, and HDM administration causes rapid expression of IL-36γ in experimental asthma models (Ramadas et al., 2006; 2011). Respiratory infection of mice with either Gram-positive or Gram-negative bacteria induced production of IL-36γ, and antibody blockade or genetic deletion of *Il36g* caused greater morbidity and mortality after infection with *S. pneumoniae* (Kovach et al., 2017). In this model, mice lacking IL-36γ had greater bacterial load in the lung as well as systemic dissemination. In agreement with our observed increase in surface expression of M2-like markers in naïve mice, that study also found that interstitial and alveolar macrophages from the lungs of *Il36g*$^{-/-}$ mice had decreased expression of classical M1-like genes. Based on our PCR and transfer experiments, IL-36γ from a macrophage-extrinsic source was acting on the alveolar macrophages to maintain a more M1-like transcription profile since transfer of *Il36g*$^{-/-}$ alveolar macrophages to WT hosts reduced their expression of M2-like markers and WT macrophages did not make the cytokine. While the skewing of *Il36g*$^{-/-}$ KO alveolar macrophages towards an M2-like cell was not complete, it would explain the decreased survival and increased apoptosis of the cells following influenza infection. Collectively, these data, point towards a key role for IL-36γ in macrophage polarization in the lung.

Deletion of *Il36r* led to increased survival and decreased pathology in a lethal influenza infection with PR8 (Aoyagi et al., 2017a). Mice lacking IL-36R also had an extended viremia, but decreased pathology and pro-inflammatory cytokines compared to WT mice. Analysis of immune cell subsets in the lungs of *Il36r*$^{-/-}$ mice showed decreased neutrophils and monocytes following infection, in contrast to our findings in *Il36g*$^{-/-}$ mice. The differences in survival and cell recruitment between *Il36r*$^{-/-}$ and

Il36g$^{-/-}$ mice following influenza infection may indicate differential roles for the various IL-36 family members in the immune response. Despite similar EC_{50} values *in vitro*, IL-36γ had weaker affinity than IL-36α (K_D= 1800 vs 480 nM, respectively) for IL-36 receptor, possibly affecting how the ligands signal through their receptor (Towne et al., 2011; Zhou et al., 2017). Higgins et al. showed differential effects of IL-36α and IL-36β in conditioning MDDCs for T cell stimulation (Higgins et al., 2015). Aoyagi et al. showed that *Il36r*$^{-/-}$ and *Il36g*$^{-/-}$, but not *Il36a*$^{-/-}$ mice were protected during lethal pulmonary infection with *P. aeruginosa* (Aoyagi et al., 2017b). These data together with our findings suggest differential roles for IL-36 family members during infection. It is possible that IL-36γ acts to oppose signaling from another IL-36 family member, or has an effect in the lungs of naïve mice which is only seen with genetic deletion of the cytokine and not of the receptor. Future studies are necessary to dissect the roles of individual IL-36 family members in regulating lung immune function during homeostasis and following infection.

In conclusion, we observed that the rapid apoptosis of alveolar macrophages in *Il36g*$^{-/-}$ mice following influenza infection resulted in increased viral load, increased proinflammatory cytokines, and enhanced immunopathology, leading to decreased survival. Importantly, this defect was corrected by the transfer of wild-type alveolar macrophages into the lungs of *Il36g*$^{-/-}$ mice. Overall, we demonstrated a critical role for IL-36γ in the immune response to influenza infection.

Supplemental Materials

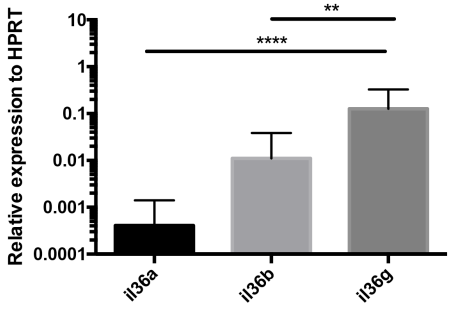

Supplemental Figure 1: Expression of *Il36* family members in naïve mice as reported in Figure 1 A-C.
Expression of the three *Il36* genes in naïve mice was compared to each other using ANOVA followed by Holm-Sidak multiple comparisons test.

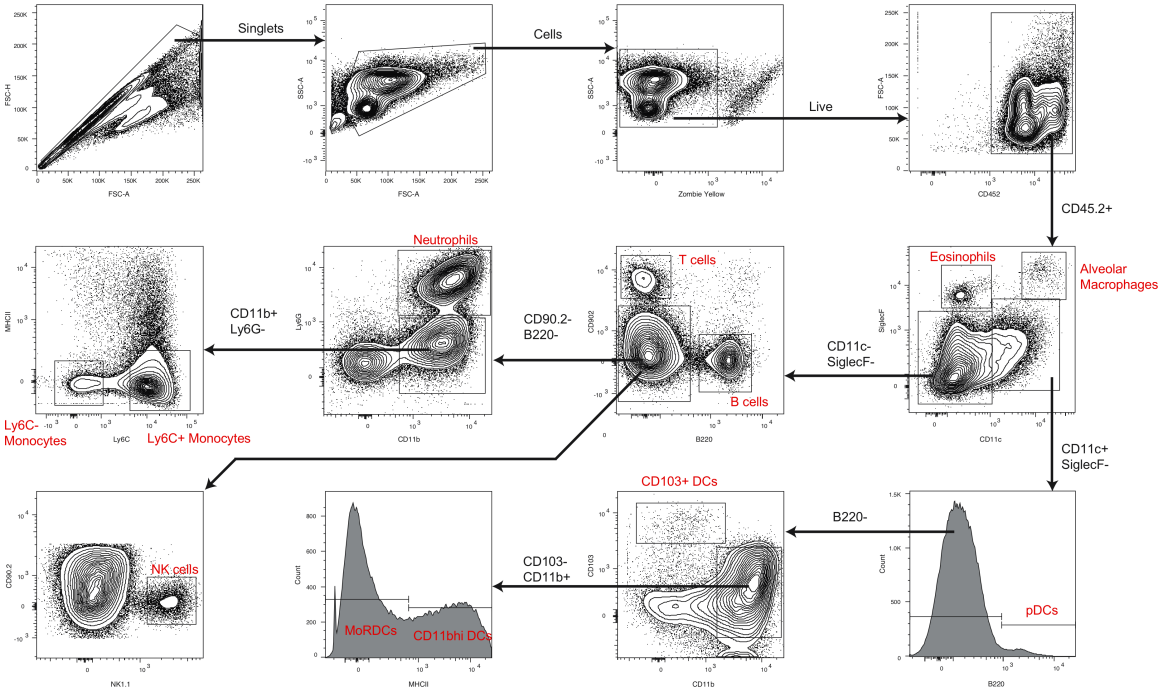

Supplemental Figure 2: Gating strategy for innate immune cell subsets.
Example flow cytometry staining for the analysis of lung immune cell subsets. Gating strategy is noted by black arrows and cell subsets analyzed are identified in red text adjacent to gates.

	C57BL/6J	304/304		300/304	300/304	152/304	152/304	

Panel Info				129S1/SvImJ	/304	304/304	4/304	4/304	152/304	152/304	
				C57BL/6J	100.00%	0.00%	98.68%	98.68%	50.00%	50.00%	
				129S1/SvImJ	0.00%	100.00%	1.32%	1.32%	50.00%	50.00%	
SNP_ID		Expected SNPs									
Chromosome-bp	RS_ID	C57BL/6J	129S1/SvImJ		B6	129	KO #1	KO #2	Het	Het	NTC
01-005230167-M	rs3708040	C	T		C	T	C	C	T/C	T/C	
01-026072256-M	rs3666554	G	T		G	T	G	G	T/G	T/G	
01-046003967-M	rs3654040	A	C		A	C	A	A	C/A	C/A	
01-065042402-M	rs3697376	G	A		G	A	G	G	A/G	A/G	
01-086182722-M	rs3678377	A	G		A	G	A	A	G/A	G/A	
01-102073421-M	rs3720366	G	C		G	C	G	G	C/G	C/G	
01-122978406-M	rs3676992	G	T		G	T	G	G	T/G	T/G	
01-143006008-M	rs3663996	A	G		A	G	A	A	G/A	G/A	
01-162977516-M	rs3706326	G	A		G	A	G	G	A/G	A/G	
01-178701443-M	rs3668273	A	G		A	G	A	A	G/A	G/A	
01-193173300-M	rs3715125	G	A		G	A	G	G	A/G	A/G	
02-003179310-M	rs3713997	G	A		G	A	G	G	A/G	A/G	
02-020551513-M	rs4139548	A	G		A	G	G	G	G/A	G/A	
02-041042651-M	rs3697051	C	G		C	G	G	G	G/C	G/C	
02-061161692-M	rs3714030	T	C		T	C	T	T	C/T	C/T	
02-078062303-M	rs3670874	T	G		T	G	T	T	G/T	G/T	
02-101074874-M	rs3686727	A	G		A	G	A	A	G/A	G/A	
02-119931810-M	rs3691456	A	T		A	T	A	A	T/A	T/A	
02-139603599-M	rs3726475	T	A		T	A	T	T	A/T	A/T	
02-161858323-M	rs3693259	C	A		C	A	C	C	C/A	C/A	
02-179086475-M	rs3680965	G	T		G	T	G	G	T/G	T/G	
03-011350737-M	rs3680834	G	C		G	C	G	G	C/G	C/G	
03-032431792-M	rs3659585	G	A		G	A	G	G	A/G	A/G	
03-053161686-M	rs3685081	T	C		T	C	T	T	C/T	C/T	
03-073214161-M	rs3681493	A	T		A	T	A	A	T/A	T/A	
03-088155864-N	rs4224040	T	C		T	C	T	T	C/T	C/T	
03-110268748-M	rs3712218	C	T		C	T	C	C	T/C	T/C	
03-131286062-N	rs3089257	C	T		C	T	C	C	C/T	C/T	
03-151125653-M	rs3725806	A	T		A	T	A	A	T/A	T/A	
03-160287200-M	rs3665134	G	A		G	A	G	G	A/G	A/G	
04-003163167-M	rs3694594	G	T		G	T	G	G	T/G	T/G	
04-022875524-M	rs4138316	C	T		C	T	C	C	T/C	T/C	
04-039199957-M	rs3723778	C	G		C	G	C	C	G/C	G/C	
04-061409675-M	rs3656076	G	T		G	T	G	G	T/G	T/G	
04-084241978-M	rs3659971	T	C		T	C	T	T	C/T	C/T	
04-106314110-M	rs3664065	C	A		C	A	C	C	A/C	A/C	
04-120122875-M	rs3702270	G	A		G	A	G	G	A/G	A/G	
04-141084977-M	rs3718220	A	G		A	G	A	A	G/A	G/A	
04-151168886-M	rs3680364	G	T		G	T	G	G	T/G	T/G	
05-003188964-M	rs3676096	C	T		C	T	C	C	T/C	T/C	
05-023890459-M	rs3664933	C	G		C	G	C	C	G/C	G/C	
05-044010971-M	rs3663092	T	G		T	G	T	T	G/T	G/T	
05-065734378-N	rs4225249	A	G		A	G	A	A	G/A	G/A	
05-082050497-M	rs3705373	C	A								

05-106058057-M	rs3656524	T	C		T	C	T	T	C/T	C/T
05-125054661-M	rs3705399	T	C		T	C	T	T	C/T	C/T
05-139966164-M	rs3717290	T	C		T	C	T	T	C/T	C/T
05-149044358-M	rs3722801	C	A		C	A	C	C	A/C	A/C
06-003167392-M	rs3661828	C	T		C	T	C	C	T/C	T/C
06-017592278-N	rs3023064	G	T		G	T	G	G	G/T	G/T
06-045126062-M	rs3706944	A	G		A	G	A	A	G/A	G/A
06-062599520-M	rs3706318	A	G		A	G	A	A	G/A	G/A
06-083216741-M	rs3707989	G	T		G	T	G	G	T/G	T/G
06-106057600-M	rs3665833	C	T		C	T	C	C	T/C	T/C
06-122941044-M	rs3727110	T	A		T	A	T	T	A/T	A/T
06-135955068-M	rs3684061	C	A		C	A	C	C	A/C	A/C
06-149052281-M	rs3711088	C	G		C	G	C	C	G/C	G/C
07-004201219-N	rs4226386	A	G		A	G	A	A	G/A	G/A
07-022997618-M	rs3662246	C	T		C	T	C	C	T/C	T/C
07-044964980-M	rs3671564	G	C		G	C	G	G	C/G	C/G
07-064095712-M	rs3672773	G	T		G	T	G	G	T/G	T/G
07-085095955-M	rs3670440	C	T		C	T	C	C	T/C	T/C
07-106153798-M	rs3654689	G	T		G	T	G	G	T/G	T/G
07-135024189-M	rs3664224	C	T		C	T	C	C	T/C	T/C
08-003089774-M	rs3701395	T	C		T	C	T	T	C/T	C/T
08-025034424-M	rs3684251	C	T		C	T	C	C	T/C	T/C
08-045080531-M	rs4137370	T	C		T	C	T	T	C/T	C/T
08-067470102-N	rs3089230	G	C		G	C	G	G	G/C	G/C
08-086985036-M	rs3706660	C	T		C	T	C	C	T/C	T/C
08-107088585-M	rs3683511	A	G		A	G	A	A	G/A	G/A
08-123021323-M	rs3693295	T	C		T	C	T	T	C/T	C/T
09-003938578-M	rs3694533	T	C		T	C	T	T	C/T	C/T
09-016198772-M	rs3719348	G	T		G	T	G	G	T/G	T/G
09-034961903-M	rs3659084	G	A		G	A	G	G	A/G	A/G
09-052894456-M	rs3654569	C	A		C	A	C	C	A/C	A/C
09-077792491-M	rs3676260	T	A		T	A	T	T	A/T	A/T
09-098865563-M	rs3692530	T	C		T	C	T	T	C/T	C/T
09-115037423-M	rs3721068	G	A		G	A	G	G	A/G	A/G
09-125082704-M	rs3706619	G	A		G	A	G	G	A/G	A/G
10-003233934-M	rs3724192	G	C		G	C	G	G	C/G	C/G
10-023127952-M	rs3665690	A	G		A	G	A	A	G/A	G/A
10-034328321-G	rs13480578	C	A		C	A	C	C	A/C	A/C
10-072471838-G	rs13480647	A	G		A	G	A	A	A/G	A/G
10-093476458-N	rs4228405	T	C		T	C	T	T	C/T	C/T
10-117629082-M	rs3670118	A	G		A	G	A	A	G/A	G/A
10-129117100-M	rs3719409	G	A		G	A	G	G	A/G	A/G
11-005661856-N	rs4222040	T	A		T	A	T	T	A/T	A/T
11-024515722-M	rs3673413	G	A		G	A	G	G	A/G	A/G
11-047224208-M	rs3686921	C	A		C	A	C	C	A/C	A/C
11-070331570-M	rs3668244	T	C		T	C	T	T	C/T	C/T
11-090199967-M	rs3682081	T	C		T	C	T	T	C/T	C/T
11-111226923-M	rs3712384	A	C		A	C	A	A	C/A	C/A
11-122195777-M	rs3675603	C	T		C	T	C	C	T/C	T/C
12-003567042-M	rs3675632	G	T		G	T	G	G	T/G	T/G

12-022232159-M	rs3712523	C	G		C	G	C	C	G/C	G/C
12-041270227-M	rs3665793	A	G		A	G	A	A	G/A	G/A
12-061271925-M	rs3677704	A	T		A	T	A	A	T/A	T/A
12-069389027-M	rs3655558	A	G		A	G	A	A	G/A	G/A
12-092440423-M	rs3719660	G	C		G	C	G	G	C/G	C/G
12-107536049-N	rs4229611	A	G		A	G	A	A	G/A	G/A
12-112276179-M	rs3686631	A	T		A	T	A	A	T/A	T/A
13-003966099-M	rs3695486	A	G		A	G	A	A	G/A	G/A
13-023105764-M	rs3679575	A	G		A	G	A	A	G/A	G/A
13-043995023-N	rs3023382	T	G		T	G	T	T	G/T	G/T
13-065339791-N	rs3023384	C	T		C	T	C	C	C/T	C/T
13-084819885-M	rs3666540	G	A		G	A	G	G	A/G	A/G
13-101929792-M	rs3687254	C	T		C	T	C	C	T/C	T/C
13-117094028-M	rs3710370	G	A		G	A	G	G	A/G	A/G
14-005055006-M	rs3689508	T	A		T	A	T	T	A/T	A/T
14-024063411-M	rs3719262	A	G		A	G	A	A	G/A	G/A
14-040017031-M	rs3659053	G	C		G	C	G	G	C/G	C/G
14-060626617-N	rs4230429	T	C		T	C	T	T	C/T	C/T
14-077156430-M	rs3666728	C	T		C	T	C	C	T/C	T/C
14-097042967-M	rs3677639	A	G		A	G	A	A	G/A	G/A
14-114403652-M	rs3685710	C	T		C	T	C	C	T/C	T/C
15-003094890-M	rs3687235	A	G		A	G	A	A	G/A	G/A
15-020280219-M	rs3662097	G	T		G	T	G	G	T/G	T/G
15-043015319-M	rs3667271	G	C		G	C	G	G	C/G	C/G
15-059754938-N	rs4230758	C	T		C	T	C	C	T/C	T/C
15-102788257-N	rs3023429	G	T		G	T	G	G	T/G	T/G
16-005053446-C	rs4153115	G	T		G	T	G	G	T/G	T/G
16-019621494-C	rs4165081	A	G		A	G	A	A	A/G	A/G
16-037994236-C	rs4174474	G	A		G	A	G	G	G/A	G/A
16-057482753-C	rs4189277	A	G		A	G	A	A	A/G	A/G
16-075684315-C	rs4205499	T	C		T	C	T	T	T/C	T/C
16-096070057-C	rs4221067	C	T		C	T	C	C	T/C	T/C
17-003335010-M	rs3694565	G	C		G	C	G	G	C/G	C/G
17-023157746-M	rs3673763	A	T		A	T	A	A	T/A	T/A
17-043164647-M	rs3677240	G	A		G	A	G	G	A/G	A/G
17-066532305-N	rs3023456	T	G		T	G	T	T	G/T	G/T
17-083294998-M	rs3707550	T	A		T	A	T	T	A/T	A/T
17-092673068-N	rs3023460	T	G		T	G	T	T	T/G	T/G
18-005066417-M	rs3706767	T	C		T	C	T	T	C/T	C/T
18-022053385-M	rs3707236	A	G		A	G	A	A	G/A	G/A
18-043081750-M	rs3676196	C	T		C	T	C	C	T/C	T/C
18-054835717-M	rs3715080	T	A		T	A	T	T	A/T	A/T
18-067972780-M	rs3657976	T	C		T	C	T	T	C/T	C/T
18-078813035-M	rs3686065	A	C		A	C	A	A	C/A	C/A
18-090060367-M	rs3663208	G	T		G	T	G	G	T/G	T/G
19-018239318-M	rs3691881	T	G		T	G	T	T	G/T	G/T
19-021081804-M	rs3692864	A	G		A	G	A	A	G/A	G/A
19-038092479-M	rs3695591	T	C		T	C	T	T	C/T	C/T
19-048069669-N	rs3023496	C	T		C	T	C	C	C/T	C/T
19-060823449-N	rs3023498	A	G		A	G	A	A	G/A	G/A
X-016114535-G	rs13483721	C	A		C	A	C	C	A/C	A/C
X-025132696-G	rs13483729	C	G		C	G	C	C	G/C	G/C
X-054650362-N	rs3161045	T	A		T	A	T	T	A/T	A/T
X-068494838-M	rs3664154	C	T		C	T	C	C	T/C	T/C
X-087817653-G	rs13483918	A	T		A	T	A	A	T/A	T/A
X-100413449-M	rs3690903	T	G		T	G	T	T	G/T	G/T
X-114340727-M	rs3702256	A	G		A	G	A	A	G/A	G/A
X-133535206-G	rs13484074	T	C		T	C	T	T	T/C	T/C
X-143466659-M	rs3698078	A	C		A	C	A	A	C/A	C/A

Supplemental Table 1: SNP analysis of *Il36g*$^{-/-}$ mice.

Two Il36g$^{-/-}$ mice from different litters were analyzed for B6 vs 129 DNA content by a

150 marker Jackson Labs analysis. Single SNPs are listed in rows and identified by chromosome location and RS ID. Columns represent samples tested. 455187 1 and 455187 2 are Il36g$^{-/-}$ mice from our colony, other columns are no template, B6, 129, and B6/129 heterozygous controls. B6 loci are shown in green, 129 in tan, and heterozygous in yellow. *Il36g* is located at chr2-24186746 thru chr2-24193567.

Originally published in *The Journal of Immunology*. Alexander N. Wein, Paul R. Dunbar, Sean R. McMaster, Zheng-Rong Tiger Li, Timothy L. Denning, and Jacob E. Kohlmeier. 2018. IL-36γ protects against severe influenza infection by promoting lung alveolar macrophage survival and limiting viral replication. *J. Immunol.* 201: pp-pp.

Chapter 3. CXCR6 regulates partitioning of lung-resident memory CD8 T cells between the airways and parenchyma and maintains the airway T cell memory pool

Over the past decade, resident memory T cells (T_{RM}) have been recognized as a distinct population from either central (T_{CM}) or effector memory (T_{EM}) T cells (Schenkel and Masopust, 2014). T_{RM} are uniquely situated to immediately respond to reinfection of a tissue and proliferate locally without the requirement for priming in the lymph node (Beura et al., 2018; Park et al., 2018; Wakim et al., 2008). The cues that lead to the development of resident vs. effector vs. central memory cells are still being investigated and are subject to debate, but it is recognized that T_{RM} are a distinct population compared to T_{EM} and T_{CM}. Regulation of T_{RM} seeding in distinct tissues is less well characterized, but several reports have shown the tissue tropism of T_{RM} are determined by expression of signature chemokine receptors and adhesion molecules (Mackay et al., 2013). These enable migration to different mucosal sites and assist in retaining cells in the tissue by preventing tissue egress into the circulation or lymphatics. Classically, CCR9 and integrin $\alpha4\beta7$ are expressed on memory T cells destined to home to the gut, where the ligands CCL25 and MadCAM1 are constitutively expressed (Mora et al., 2003). CCR4/CCL17, CCR8/CCL1, and CCR10/CCL27 enable migration to the skin and cutaneous lymphocyte antigen (CLA) allows them to bind to local selectins (Campbell et al., 1999; Schaerli et al., 2004; Sigmundsdottir et al., 2007). However, it is unknown whether similar combinations of chemokine receptors and adhesion molecules direct the preferential migration or retention of memory T cells to other peripheral tissues.

Following influenza virus infection, memory CD8 T cells can persist in the lung for months and these T_{RM} are required for effective immunity against heterosubtypic influenza challenge (Hogan et al., 2001; Wu et al., 2014). Studies on CD8 T cell homing

to the lung has lagged behind that of other tissues due to the unique problems of identifying resident cells within such a vascularized organ, but intravital labeling with fluorescent antibodies has enabled the identification of intra- vs. extravascular cells within the lung (Anderson et al., 2012). The lung T_{RM} pool can be divided into two populations, airway T_{RM} and parenchyma T_{RM}, that differ not only based on localization within the tissue, but also in their effector functions and homeostatic maintenance. Airway T_{RM} are poorly cytolytic compared to T_{RM} in the parenchyma, yet are sufficient to protect against respiratory virus challenge through the rapid production of cytokines (Jozwik et al., 2015; McMaster et al., 2015; Zhao et al., 2016). Furthermore, airway T_{RM} have a limited lifespan and must be maintained via a process of continual recruitment that remains poorly understood (Ely et al., 2006; Kohlmeier et al., 2007). Despite the importance of both airway and parenchyma T_{RM} for cellular immunity against respiratory pathogens, critical questions regarding the ontogeny and maintenance of these two lung T_{RM} populations remain unanswered.

Several reports have identified molecules important for $CD8^+$ T cell homing to the lung. Integrins such as CD11a/CD18 (LFA-1) and CD49a (VLA-1) are required for $CD8^+$ T cell entry into and retention in the lung, respectively (Galkina et al., 2005; Ray et al., 2004). Chemokine receptor such as CXCR3 and CCR5 have been shown to effect cellular localization of effector or memory $CD8^+$ T cells in the lung during acute infection as well as steady-state memory (Galkina et al., 2005; Kohlmeier et al., 2008; Slütter et al., 2013). However, these chemokine receptors are required for T cell trafficking to inflammation in a diverse range of tissues, and thus seem unlikely to direct the preferential homing of $CD8^+$ T cells to the lung mucosa in the absence of inflammation. Furthermore, it is also unclear whether the same chemotactic signals are

required to draw cells into the lung parenchyma and airways, or whether these populations are separated based on differential migratory cues within the tissue.

CXCL16 and CXCR6 are a chemokine and receptor pair with exclusive binding between ligand and receptor (Matloubian et al., 2000). CXCL16 can be produced in multiple isoforms including a small, soluble chemokine and a membrane-tethered protein that is cleaved and released by the metalloprotease ADAM10 (Abel et al., 2004). CXCR6 has been shown to draw $CD8^+$ T cells to the liver in GvHD and is required for the maintenance of liver-resident $CD8^+$ T cells following infection (Sato et al., 2005; Tse et al., 2014). Its expression level on $CD8^+$ T cells in the lung correlated with disease severity in patients with COPD and was upregulated on T cells in the lungs of patients with asthma, sarcoidosis, or interstitial lung disease (Agostini et al., 2005; Freeman et al., 2007; Morgan et al., 2005). In mice, CXCR6 drew antigen-specific $CD8^+$ T cells to the lung after vaccination against ESAT6 or infection with *M. tuberculosis* (Lee et al., 2011). Finally, CXCR6 was recently shown to be part of a core cluster of genes that define $CD69^+$ $CD8^+$ T_{RM} cells in mice and humans (Hombrink et al., 2016; Kumar et al., 2017; Mackay et al., 2013). Despite these reports on CXCR6 function in T_{RM} in various tissues and infection models, the role of CXCR6 in the establishment and maintenance of different T_{RM} populations within the lung following respiratory viral infection has not been investigated.

In the present study, we investigated the expression of homing molecules on flu-specific $CD8^+$ T_{RM} to identify processes that regulate the establishment and/or maintenance of these cells in the different compartments of the lung. We found that CXCR6 was highly expressed on T_{RM} in the lung parenchyma in both mice and humans, but largely absent from T_{RM} in the airways and T_{EM} in the circulation. Expression of

CXCR6 on flu-specific memory T cells required cognate antigen encounter in the lung, demonstrating that pulmonary imprinting maintained CXCR6 expression. Interestingly, *Cxcr6*-deficient mice had a significant defect in the number of flu-specific T_{RM} in the lung airways, but not the lung parenchyma or systemic T_{EM} populations, and this finding was confirmed in mixed bone marrow chimeras. Analysis of CXCL16 showed it was constitutively expressed in the lung and localized primarily to the airway epithelium in both mice and humans. In addition, *Cxcl16*-deficient mice showed a similar defect in the number of flu-specific T_{RM} in the airways but not the lung parenchyma. Microscopic localization of WT and *Cxcr6*-deficient cells in the lung showed that WT $CD8^+$ T_{RM} were more abundant around the large conducting airways, whereas *Cxcr6*-deficient $CD8^+$ T_{RM} were spread more diffusely throughout the parenchyma. A more detailed analysis of CXCR6 expression on airway T_{RM} showed that CXCR6 was highly expressed on cells that had recently migrated into the airways and CXCR6 expression decreased over time with exposure to the airway environment. Finally, we found that transiently blocking CXCR6-CXCL16 interactions following the establishment of flu-specific CD8 T cell memory significantly decreased the steady-state migration of T_{RM} into the airways. Together, these data demonstrate a critical role for CXCR6 in the migration of lung T_{RM} from the parenchyma into the airways and show the requirement for continued CXCR6 signaling in maintaining the airway T_{RM} pool.

Results

CXCR6 is expressed on mouse and human lung resident $CD8^+$ T cells. To determine which chemokine receptors may be important for the homing of $CD8^+$ T_{RM} to the lungs and airways, we infected mice with influenza A/HK-x31 and waited until immunological memory was established. The mice were i.v. injected with a

fluorescently-conjugated antibody before sacrifice to distinguish between cells in the lung vasculature and those in the parenchyma. Comparison of the influenza nucleoprotein (FluNP)-specific memory CD8 T cells in the lung vasculature and lung parenchyma identified CXCR3 and CXCR6 as uniquely upregulated on T_{RM} in the parenchyma compared to T_{EM} in the lung vasculature (Figures 7A and B). We next divided the lung-resident (i.v.$^-$) cells into three populations based on the canonical residency markers CD69 and CD103 (Figure 7C). First, we sorted the three populations from the total CD8$^+$ T_{RM} pool (i.v.$^-$ CD44^{Hi} CD62L$^-$) for qPCR analysis of CXCR6 expression. We found that CD69$^+$CD103$^+$ T_{RM} had the highest expression of *Cxcr6*, followed by the CD69$^+$CD103$^-$ T_{RM}. The CD69$^-$CD103$^-$ cells, which may have represented a transiently-resident population of circulating T_{EM}, had significantly lower expression of *Cxcr6* than either the CD69$^+$ or CD69$^+$CD103$^+$ T_{RM}. Staining of the FluNP-specific lung T_{RM} for surface expression of CXCR6 using a CXCL16-Ig fusion protein showed that surface protein levels matched RNA levels (Matloubian et al., 2000). We also examined co-expression of CXCR3 and CXCR6 to determine if CXCR6$^+$ cells also had higher expression of CXCR3. As shown in Figure 7D, CXCR6$^+$ antigen-specific CD8+ T_{RM} had higher expression of CXCR3 than CXCR6$^-$ cells. Next, we compared levels of CXCR6 expression in the airways (BAL) and spleen to the lung resident and lung systemic populations. Unlike lung parenchyma CD8$^+$ T_{RM}, FluNP-specific airway T_{RM} and FluNP-specific memory CD8$^+$ T cells in the pulmonary circulation (lung sys) and spleen had significantly decreased CXCR6 expression. (Figure 7E). However, CXCR6 expression was highly variable in the airways, with a subset of cells expressing CXCR6 at levels comparable to lung parenchyma T_{RM}. We also investigated the expression of CXCR6 on memory CD8$^+$ T cell subsets resident in the

human lung (Figure S3). Similar to our observations in mice, CXCR6 expression was significantly higher on $CD69^{+}CD103^{+}$ T_{RM} and $CD69^{+}$ T_{RM} compared to $CD69^{-}CD103^{-}$ memory CD8 T cells (Figure 7F). In total, T_{RM} within the lung parenchyma have higher CXCR6 expression than those cell transiting through the lung, in the airways, in the pulmonary vasculature, or in the systemic circulation, suggesting a potential role for CXCR6 in lung T_{RM} establishment or maintenance.

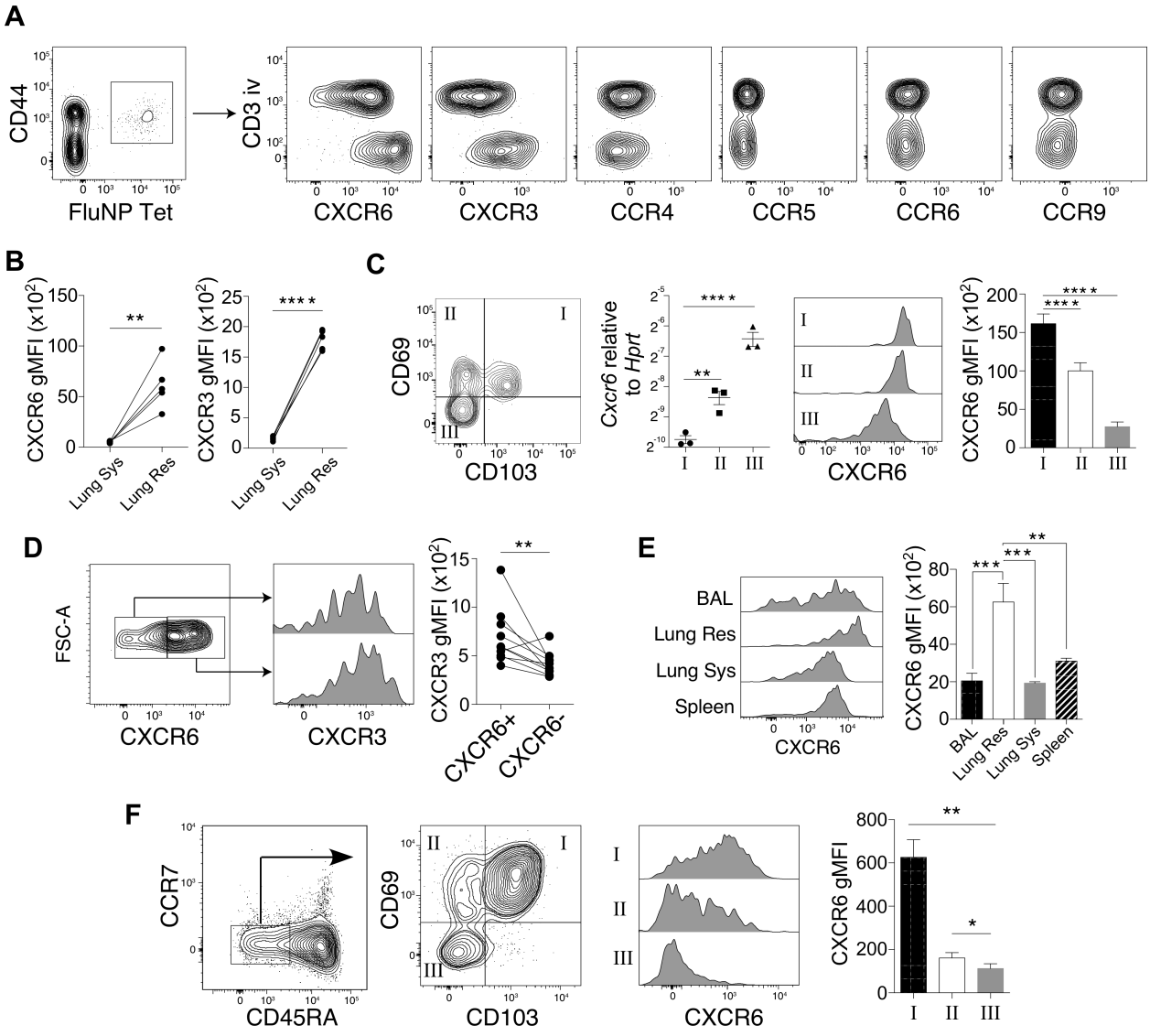

Figure 7: CXCR6 is upregulated on lung-resident memory CD8 T cells. (A) Chemokine receptor expression of $CD8^+$ T cells showing gating on $CD44^+$ and $FluNP_{366\text{-}374}D^{b+}$ cells. Y-axis of plots of chemokine expression of antigen-specific cells separates cells on CD3 i.v.$^+$ (lung systemic) and CD3 i.v.$^-$ (lung resident). Staining is concatenated from 5 mice and representative of 2 experiments of 5 mice each. (B) Quantification of gMFI of CXCR6 and CXCR3 on lung systemic and lung resident cells. Values are from lung-resident and lung-systemic cells in the same mouse. Data is representative of 2 experiments of 5 mice each (C) Expression of CXCR6 by influenza-specific CD3 i.v.$^-$ $CD8^+$ T cells are divided into three populations based on expression of CD69 and CD103 with example flow plots. Populations are designated by roman numerals I ($CD69^+CD103^+$), II ($CD69^+CD103^-$), and III ($CD69^-CD103^-$). qPCR for *Cxcr6* is graphed relative to *Hprt*. CXCR6 surface expression is shown as representative flow plots and quantification of gMFI. qPCR data is combined from three independent infections and sorts. Staining is concatenated from 5 mice and representative of 2 experiments of 5 mice each. (D) CXCR3 surface expression on $CXCR6^+$ and $CXCR6^-$ antigen-specific lung-resident T cells are shown as representative flow plots and quantification of gMFI. Data is combined from 2 replicates of 5 mice each (E) Surface expression of CXCR6 on antigen-specific $CD8^+$ T cells from the BAL (black bar), lung-resident (open bar), lung-systemic (grey bar), and splenic (hashed bar) populations. CXCR6 surface expression is shown as representative flow plots and quantification of gMFI. Data are representative of 2 experiments of 5 mice each. (F) Staining of human memory $CD8^+$ T cells from explanted human lungs for CXCR6 expression. $CD45RA^-$ $CCR7^-$ $CD8^+$ T cells were divided into three populations based on expression of CD69 and CD103 using roman numerals I ($CD69^+CD103^+$) II ($CD69^+CD103^-$) and III ($CD69^-$ $CD103^-$). CXCR6 surface expression is shown as representative flow plots and quantification of gMFI. Data are from 5 individual donors (F). gMFI data was analyzed by paired Student's t test (panels B, D) or one-way repeated measures ANOVA followed by Holm-Sidak multiple comparisons test (panel C, E, F). qPCR data was analyzed using one-way ANOVA followed by Holm-Sidak multiple comparisons test (Panel C).

Antigen re-encounter in the lung maintains CXCR6 expression on developing T_{RM}. We next investigated the kinetics of CXCR6 expression on lung and vascular flu-specific CD8 T cells over the duration of the response to influenza. We harvested mice at early acute phase (D7), peak acute response (D10), resolution and contraction (D12, D14, D21), and memory (D45) and examined the expression levels of CXCR6 on lung-resident and systemic populations. We found higher expression of CXCR6 on the lung-resident population throughout the course of infection, peaking during the early phase of resolution, but continuing out to memory (Figure 8A). Because some of the i.v.$^-$ cells

are transiently-resident effector memory T cells, we divided lung-resident cells based on CD69 expression and examined the levels of CXCR6 expression. We observed that among the lung-resident cells, $CD69^+$ cells have much higher expression of CXCR6 than $CD69^-$ cells over the entire course of infection, resolution, and establishment of memory (Figure 8B). These differences in CXCR6 expression between resident and vascular cells, and between $CD69^+$ and $CD69^-$ resident cells, suggested that antigen encounter in the lung environment may be important for maintaining CXCR6 expression. Antigen exposure in the lung is essential for establishing T_{RM} cells following influenza infection (McMaster et al., 2018). Using a method to establish systemic effector T cells and "pulling" them to the lungs, we asked if pulmonary antigen exposure was also necessary for CXCR6 upregulation. Mice were intramuscularly infected with a live influenza virus and after 7 days, they were dosed intranasally with either CpG to induce local inflammation or CpG with cognate antigen to induce inflammation and expose T cells to antigen in the lung (Figure 8C). Three days after intranasal dosing, expression levels of CXCR6 in the lung were equivalent between the group that had seen antigen in the lung and those that had not (Figure 8D). However, at memory, T cells in the lung resident population that encountered cognate antigen in the pulmonary environment had significantly increased expression of CXCR6 compared to cells that did not. Overall, these data indicate that CXCR6 expression was sustained on lung-resident CD8 T cells throughout the cellular response to influenza infection, and maintenance of CXCR6 expression on lung T_{RM} is dependent on antigen exposure within the lung.

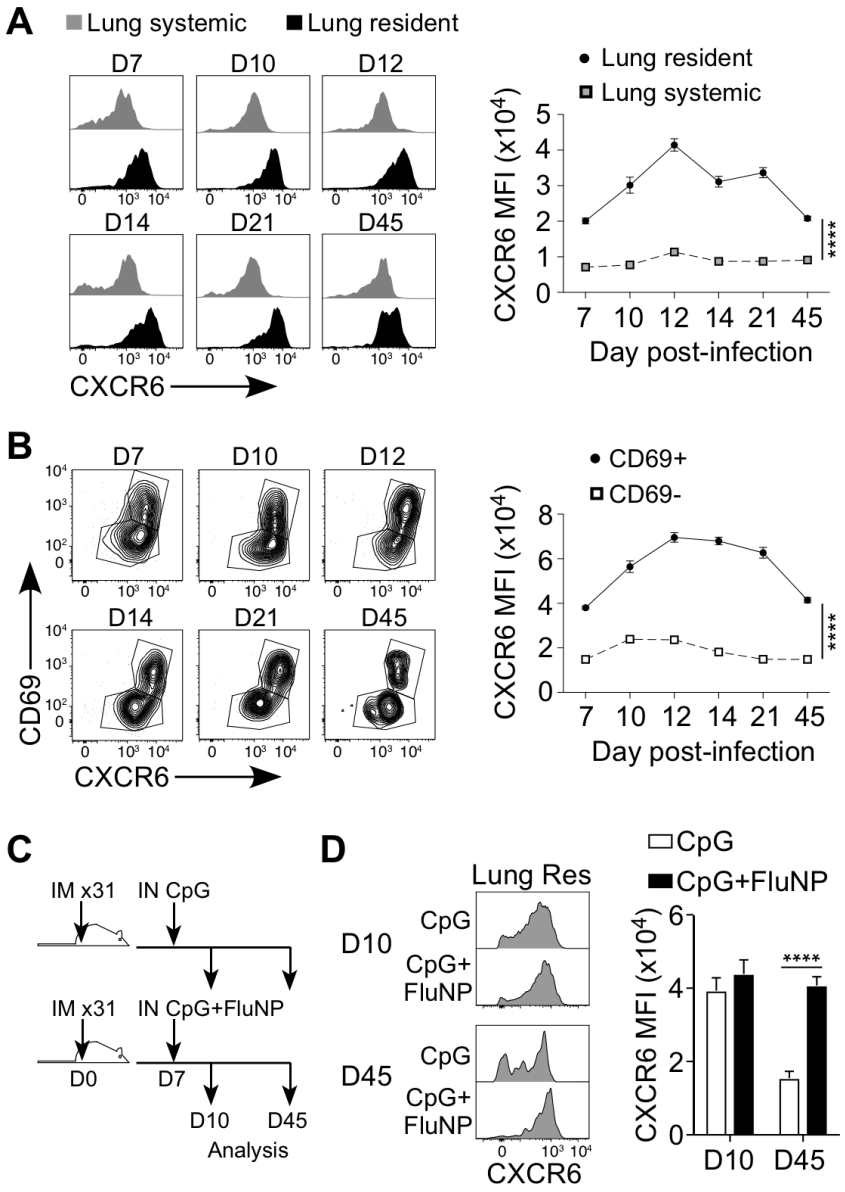

Figure 8: CXCR6 expression on lung-resident memory T cells occurs throughout infection and is antigen-dependent.
(A) CXCR6 expression of lung systemic (grey histograms, grey boxes) and lung resident (black histograms, black circles) antigen-specific $CD8^+$ T cells at indicated times post-infection. Data are combined from 2 experiments of 5 mice each and shown as representative flow histograms (left) and gMFI is quantified (right). (B) CXCR6 expression of lung resident antigen-specific CD8 T cells that are $CD69^+$ (black circles) and $CD69^-$ (open boxes) at indicated times post-infection. Data are combined from 2 experiments of 5 mice each and are shown as representative flow histograms (left) and gMFI is quantified (right). (C) Experimental design diagram showing "pull" method of establishing lung-resident CD8 T cells. (D) CXCR6 expression on antigen-specific CD8 T cells after dosing intranasally with either CpG (top histograms, open bars) or CpG and FluNP peptide (bottom histograms and black bars). Data are combined from 3

experiments of 5 mice per group and shown as representative histograms and gMFI is quantified. Data were analyzed by Student's T test (A, B) or one-way ANOVA followed by Holm-Sidak multiple comparisons test (D).

Cxcr6$^{-/-}$ mice have decreased numbers of antigen-specific T cells in the airways. To determine the importance of CXCR6 for recruitment of flu-specific CD8^{+} T cells to the lung, we infected WT and *Cxcr6$^{-/-}$* mice with x31 influenza and assessed the number of antigen-specific T cells in the airways (BAL), lungs (Lung Res), and spleen during the acute and memory phases of infection. At 10 days post-infection, there was no difference in the number of FluNP-specific CD8^{+} T cells in the spleen or lung parenchyma. However, the BAL revealed a significant decrease in the number of FluNP-specific CD8^{+} T cells in the airways of *Cxcr6$^{-/-}$* mice (Figure 9A). At 50 days post-infection, there were still significantly fewer FluNP-specific CD8^{+} T cells airways of *Cxcr6$^{-/-}$* mice, while the numbers of cells in the lung and spleen between WT and *Cxcr6$^{-/-}$* mice were similar (Figure 9B). We also examined the frequency of CD8^{+} T cells that were specific to the FluNP$_{366\text{-}374}$D^{b} epitope to determine if the phenotype we observed in the airways of *Cxcr6$^{-/-}$* mice could be explained by a skewing of the virus-specific response to different influenza antigens, but there was no difference in the frequency of memory CD8^{+} T cells recognizing the FluNP epitope between WT and *Cxcr6$^{-/-}$* mice (Figure 9C). Furthermore, the number of total memory CD8^{+} T cells was significantly decreased in the airways of *Cxcr6$^{-/-}$* mice (Figure 9D), suggesting a global effect of *Cxcr6* deficiency on the memory CD8^{+} T cell pool in the airways. Thus, despite the increased expression of CXCR6 on T$_{RM}$ in the parenchyma, these data show that CXCR6 is important for regulating the number of memory CD8^{+} T cells in the airways, but not the lung parenchyma.

As CXCR3 has been reported to be important for T cell trafficking to the lungs and airways, and we observed that high expression of CXCR6 associated with increased CXCR3 expression, we also examined the expression of CXCR3 on WT and *Cxcr6*$^{-/-}$ FluNP-specific CD8^{+} T cells in the lung (Kohlmeier et al., 2009; Medoff et al., 2006; Slütter et al., 2013). However, there was no difference in the frequency of CXCR3^{+} FluNP-specific cell in the BAL, lung-resident compartment, or in the spleen, indicating the decreased number of airway cells observed in *Cxcr6*$^{-/-}$ mice was not due to defects in CXCR3-mediated trafficking (Figure 9E). To determine the impact of decreased airway T_{RM} in *Cxcr6*$^{-/-}$ mice on cellular immune protection, we challenged naïve or x31 influenza-immune WT and *Cxcr6*$^{-/-}$ mice with influenza A/PR8. While we observed no difference in weight loss between naïve mice, x31-immune *Cxcr6*$^{-/-}$ mice showed significantly greater weight loss compared to WT mice on days 3 and 5 post-challenge (Figure 9F). Thus, the decreased number of flu-specific airway T_{RM} capable of immediately responding to a secondary challenge in *Cxcr6*$^{-/-}$ mice results in impaired cellular immunity to influenza virus.

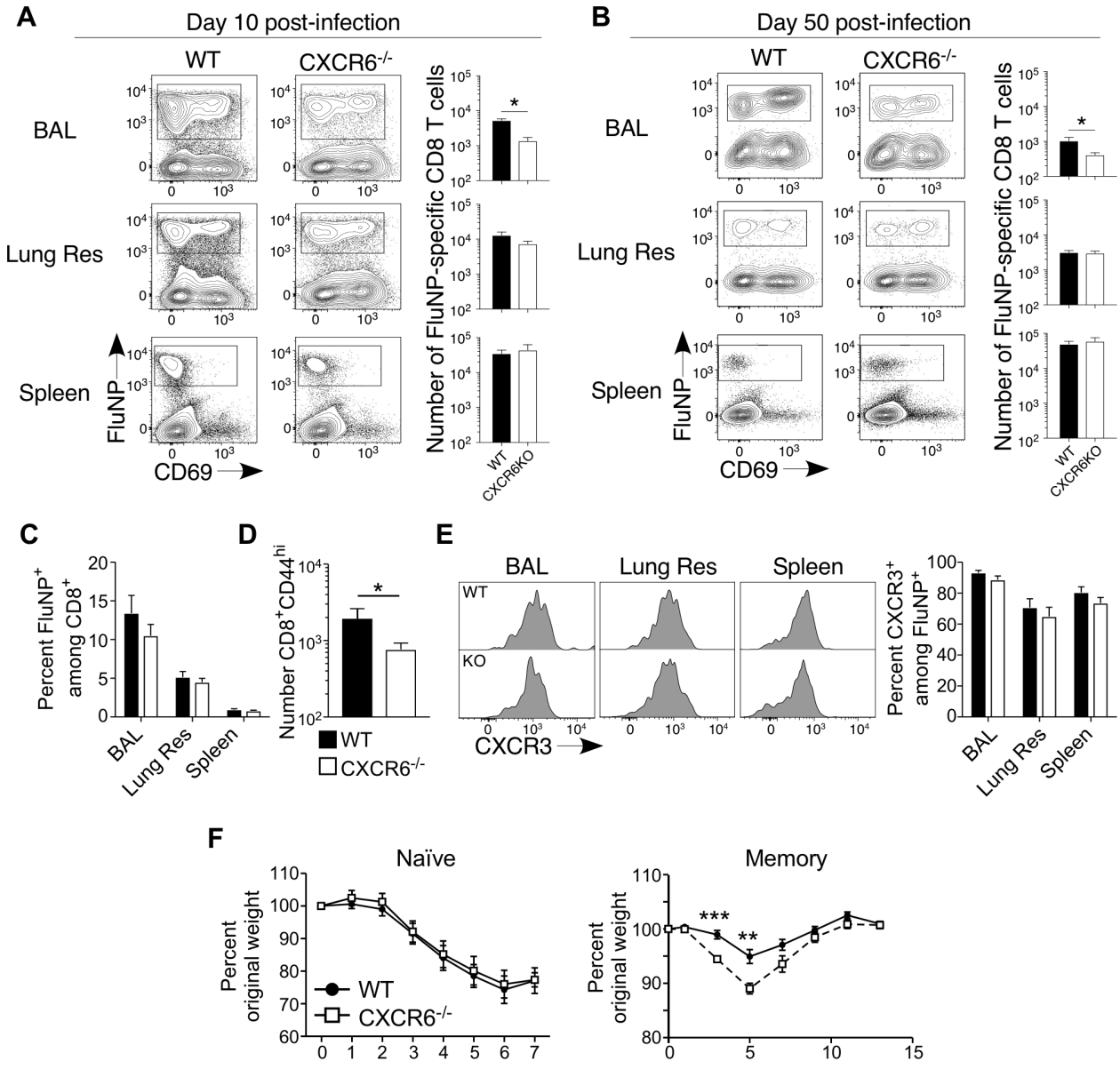

Figure 9: Mice lacking *Cxcr6* have decreased airway-resident cells following influenza infection.

(A and B) Analysis of the antigen-specific response of WT (black bars) and *Cxcr6*$^{-/-}$ (open bars) mice at 10 (A) and 50 (B) days post-infection. Example CD69 and FluNP$_{366-374}$D^{b} staining of the CD8^{+}CD44^{+} T cells population (left) and quantification of the FluNP-specific response in the BAL, lung-resident, and splenic compartments (right) are shown. (C) Percent of WT (black bars) and *Cxcr6*$^{-/-}$ (open bars) CD8^{+} T cells in the BAL, lung resident, and spleen that are specific for FluNP at day 50 post-infection. (D) Number of total CD8^{+}CD44^{+} cells in the BAL of WT (black bar) and *Cxcr6*$^{-/-}$ (open bars) mice at day 50 post-infection. (E) CXCR3 expression of WT (top histograms, black bars) and *Cxcr6*$^{-/-}$ (bottom histogram, open bars) FluNP-specific cells at day 50 post-infection. Example histograms (left) and quantification (right) of the percent CXCR3^{+} in the BAL, lung-resident compartment, and spleen are shown. (F) Weight loss of WT

(black circle) and *Cxcr6*$^{-/-}$ (open square) following infection with PR8 influenza without (left) or with (right) pre-existing T cell memory. Data are representative of 4 (A-E, n=12 WT mice 15 KO mice) and 2 (F n=20 mice per group) experiments and were analyzed with Student's t test (A, B, D, F) or two-way ANOVA followed by the Holm-Sidak multiple comparisons test (C, E)

To determine whether these observations were unique to influenza virus infection and control for any potential differences in infection or disease course between intact WT and *Cxcr6*$^{-/-}$ mice, we generated mixed bone marrow chimeras and infected these mice with Sendai virus, a natural mouse parainfluenza virus (Figure 10A). We examined Sendai-specific CD8^{+} T cell responses in the spleen, blood, mediastinal LN, liver, lung, and airways on days 10 and 60 post-infection (Figure 10B). We included analysis of Sendai-specific CD8^{+} T cells in the liver as control due to previous studies that have shown CXCR6 is essential for maintenance of T_{RM} in the liver (Tse et al., 2014). On day 10 post-infection, there were no differences in the localization of Sendai-specific CD8^{+} T cells in any of the tissues examined (Figure 10C). In contrast, on day 60 post-infection the Sendai-specific airway T_{RM} (BAL) were highly skewed toward WT cells, despite equal ratios of WT to *Cxcr6*$^{-/-}$ cells in the lung parenchyma, mediastinal LN, and blood (Figure 10D). In agreement with prior studies, Sendai-specific liver T_{RM} were also skewed toward WT cells, but the level of skewing observed in the liver was significantly less than that observed in the airways. Together, these data show the defect in airway T_{RM} in the absence of CXCR6 is consistent in different respiratory viral infections and when WT and *Cxcr6*$^{-/-}$ cells are subjected to the same infection dynamics *in vivo*.

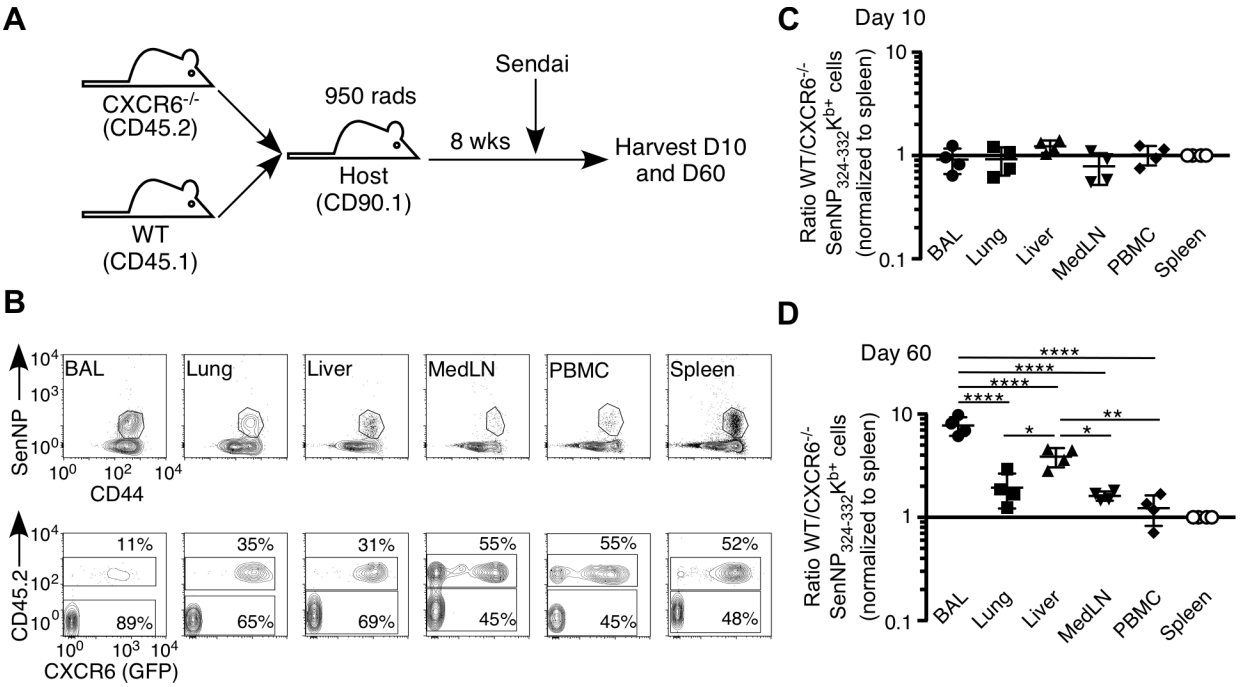

Figure 10: Mixed bone-marrow chimeras show a defect in airway recruitment in *Cxcr6*$^{-/-}$ T cells.
(A) Experimental schema showing setup of chimera experiment. (B) Example flow plots of indicated tissues from chimeric mice at day 60 post-infection showing CD44 by $SenNP_{324-332}K^{b}$ of $CD8^{+}$ cells (top row) and CD45.2 by GFP of $SenNP_{324-332}K^{b+}$ cells (bottom row). WT cells are $CD45.2^{-}$ GFP^{-} and KO cells are $CD45.2^{+}$ $GFP^{+/-}$. (C and D) Ratio of WT to KO $SenNP_{324-332}K^{b+}$ cells in indicated tissues at day 10 (C) and day 50 (D) post-infection, normalized to the spleen. Values greater than 1 indicate more WT cells in tissues. Data are representative of 3 experiments (n=4-5 mice) and were analyzed with a one-way ANOVA followed by Tukey's multiple comparisons test.

CXCL16 is expressed on the airway epithelium and required for airway T_{RM}.

The only known ligand for CXCR6 is CXCL16, which is a membrane anchored chemokine that can be cleaved by proteases to form a chemo-attractive gradient (Matloubian et al., 2000). To investigate whether the expression patterns of CXCL16 could explain the defect in airway T_{RM}, we investigated CXCL16 protein localization in the lung by immunofluorescent microscopy. In naïve and memory mice, CXCL16 staining was limited to the lining of the large airways and co-localized with the epithelial marker EpCAM (Figures 11A and S4). To investigate the kinetics of CXCL16 expression

over the course of an influenza infection, we harvested BAL and assessed levels of CXCL16 and the CXCR3 ligands CXCL9 and CXCL10 (Figure 11B). As expected, influenza infection resulted in a rapid and transient increase of CXCL9 and CXCL10 in the airways, and both were undetectable by day 30 post-infection. In contrast, CXCL16 was constitutively expressed in the airways, with a transient increase during active infection. To further investigate potential cellular sources of CXCL16 in the lung, we sorted several hematopoietic and non-hematopoietic cell types from the lungs of mice 30 days after influenza infection. Consistent with our microscopy data, *Cxcl16* expression was highest on epithelial cells, and alveolar macrophages also showed increased expression compared to other $CD45^+$ hematopoietic cells, endothelial cells and fibroblasts (Figure 11C). Analysis of human lung sections also revealed that CXCL16 protein expression was restricted to the lung epithelium (Figure 11D). Together, these data show that CXCL16 is constitutively expressed in the epithelium lining the lung airways in both mice and humans, and the localized expression of CXCL16 may explain the impact of CXCR6-CXCL16 interactions on airway, but not parenchyma, lung T_{RM}. To test whether the absence of CXCL16 also resulted in decreased airway T_{RM} following influenza infection, we infected WT and *Cxcl16*$^{-/-}$ mice influenza virus and assessed FluNP-specific CD8 T cell numbers in the airways and parenchyma on days 10 and 60 post-infection (Figure 11E). Similar to *Cxcr6*$^{-/-}$ mice, *Cxcl16*$^{-/-}$ mice had significantly decreased numbers of FluNP-specific $CD8^+$ T_{RM} in the airways but not the parenchyma (Figure 11F). Thus, direct interactions between CXCR6 and its ligand CXCL16 at the respiratory epithelium are required for T_{RM} in the lung airways.

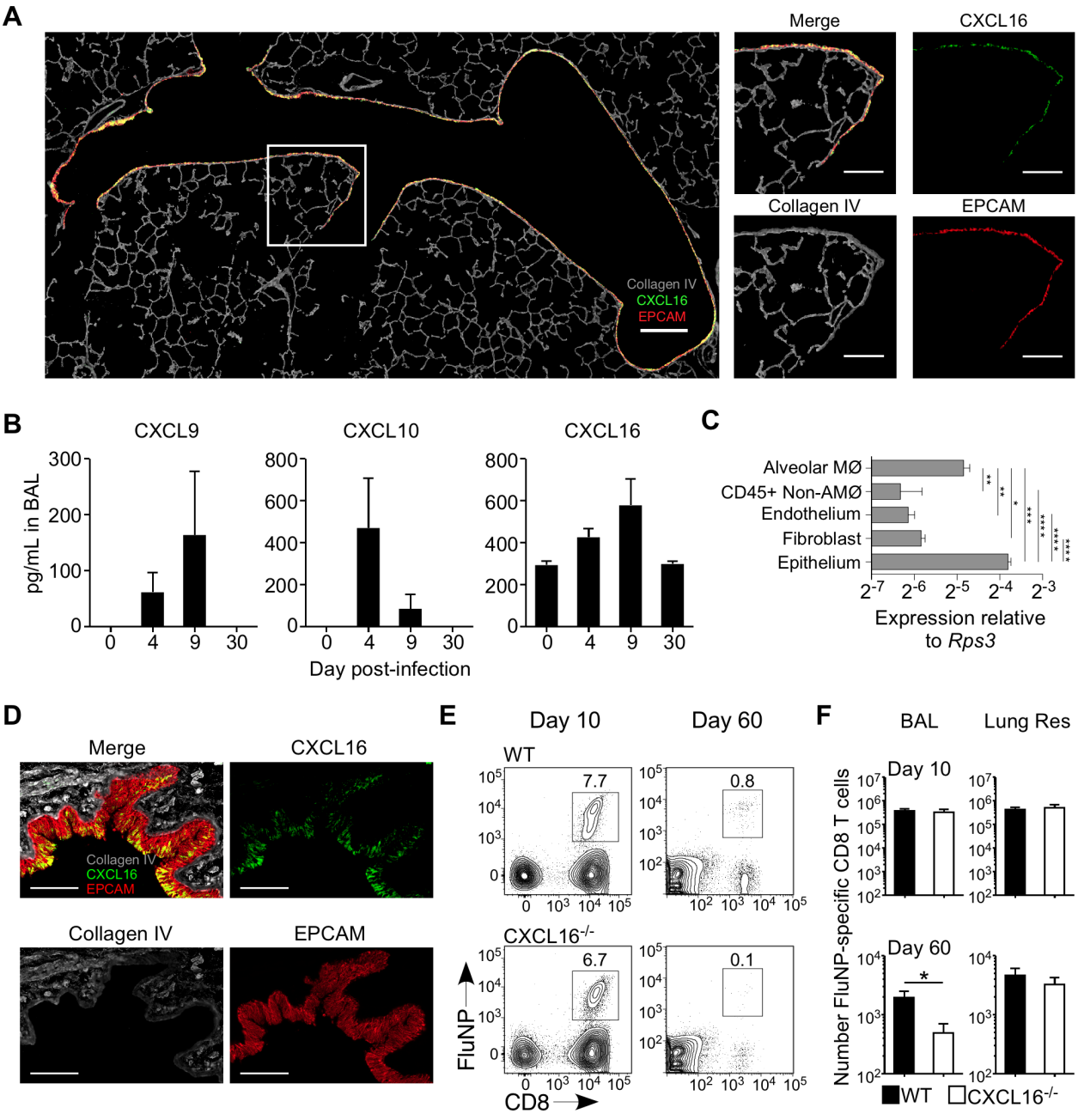

Figure 11: CXCL16 is expressed in the lung and is required for T cell recruitment to the airways.

(A) Immunofluorescence microscopy of mouse lung at immunological memory showing CXCL16 (green), EpCAM (red) and Collagen IV (grey). Original image is at 200x magnification. (B) ELISA of BAL fluid for the chemokines CXCL9 (left), CXCL10 (center), and CXCL16 (right) at indicated times post-infection. Data are representative of 2 experiments (n=3-4 mice). (C) qPCR of listed cell types for *Cxcl16* mRNA levels in day 30 post-infection mice. Data are relative to the housekeeping gene *Rps3*. Data are representative of 2 experiments (n=3 mice). (D) Immunofluorescence microscopy of explanted human lung showing CXCL16 (green), EpCAM (red), and Collagen IV (grey). Original image is at 200x magnification. (E) Analysis of the antigen-specific response of

WT (black bars) and CXCL16$^{-/-}$ (open bars) mice at 10 (left) and 60 (right) days post-infection. Example CD8 and FluNP$_{366-374}$D^{b} staining of lung-resident T cell population and quantification of the FluNP-specific response in the BAL and lung-resident compartments are shown. Data are representative of 2 experiments (n=3-4 mice). Data were analyzed by one-way ANOVA and Holm-Sidak multiple comparisons test (C) or Student's t test (E).

CXCR6 mediates localization, but not survival, of lung T_{RM}. Potential explanations for the reduced number airway T_{RM} in *Cxcr6*$^{-/-}$ and *Cxcl16*$^{-/-}$ mice are that CXCR6 may be anchoring virus-specific cells to the epithelium and promoting their survival in the airway environment, or that CXCR6-CXCL16 interactions are directing the localization of T_{RM} within the lung tissue. To test these possibilities, we first performed dual adoptive transfers of congenic WT and *Cxcr6*$^{-/-}$ T_{EM} directly into the airways via intratracheal administration and assessed survival (Figure 12A). Eight days post-transfer, both WT and *Cxcr6*$^{-/-}$ cells were detectable in the airways, and the ratio of recovered cells showed no survival defect in cells deficient in CXCR6 expression (Figure 12B and 12C). To investigate the localization of *Cxcr6*$^{-/-}$ T_{RM} in the lung, we took advantage of the transgenic OT-I system to compare the localization of congenic WT and *Cxcr6*$^{-/-}$ cells within the tissue. Congenic (CD45.1) mice were seeded with equal numbers of naïve WT (CD45.2^{+}CD90.1^{+}) and *Cxcr6*$^{-/-}$ (CD45.2^{+}CD90.2^{+}) CD8^{+} T cells and infected with influenza x31-OVA (Figure 12C). Tile scans were taken of whole lung sections 45 days post-infection and WT and *Cxcr6*$^{-/-}$ OT-I cells were identified by congenic marker staining (Figure 6D). The distance of each cell to the nearest airway was measured and the mean distance of WT and *Cxcr6*$^{-/-}$ cells was calculated (Figure S5). Compiled measurements from multiple lung sections showed that WT cells were, on average, 146 microns closer to the airways than *Cxcr6*$^{-/-}$ cells (757 vs 903 microns, respectively, Figure 12E). To more clearly visualize any CXCR6-mediated defect of

localization near the airways, we determined the ratio of WT to *Cxcr6*$^{-/-}$ OT-I T cells at discrete distances from the nearest airway (Figure 12F). At distances greater than 200 microns the ratio of WT to *Cxcr6*$^{-/-}$ OT-I T cells was 1:1. However, within 50 microns to the closest airway, WT cells were present at a 3:1 ratio compared to *Cxcr6*$^{-/-}$ cells. Together, these data show in airway T_{RM} in the absence of CXCR6 is not due to altered survival in the airway environment, but due to defective trafficking to the airways.

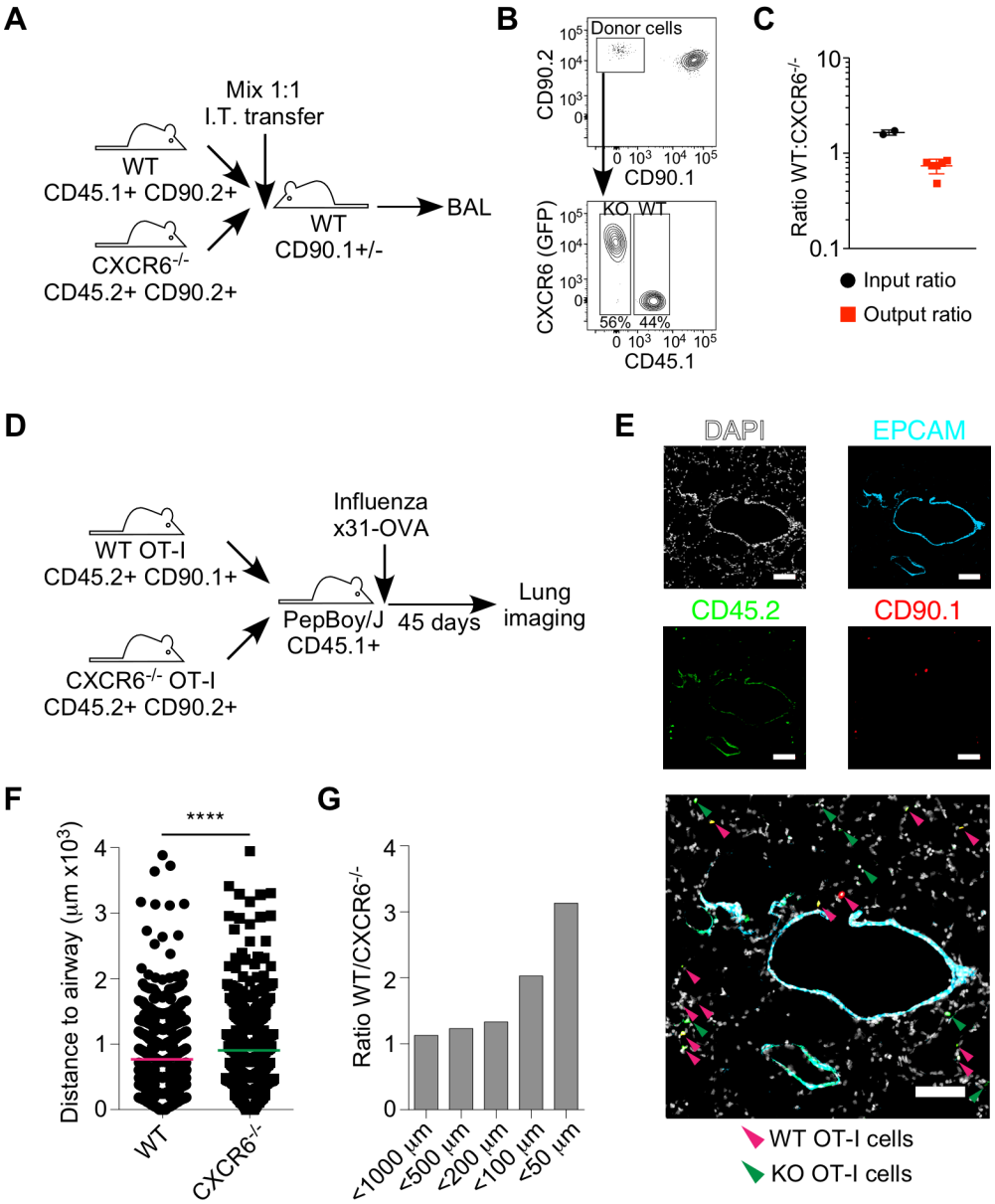

Figure 12: OT-I T cells lacking CXCR6 are located further from the airways than WT cells.
(A) Experimental diagram showing setup of intratracheal transfer experiment. (B) Example staining of WT and CXCR6$^{-/-}$ donor cells from the airways eight days post-transfer. (C) Ratio of WT:CXCR6$^{-/-}$ cells pre-transfer (black circles) or after eight days in the airways (red squares). (D) Experimental diagram showing setup of OT-I transfer experiment. (E) Example image of a mouse lung section showing WT (pink arrows) and *Cxcr6*$^{-/-}$ (green arrows) OT-I T cells. All transferred cells are CD45.2^{+} (green) and WT cells are also CD90.1^{+} (red). EpCAM (cyan) and DAPI (white) were used to define airways. (F) Quantification of the distance of WT (circles) and CXCR6$^{-/-}$ (squares) OT-I T cells to the nearest airway. Data were analyzed by Mann-Whitney test. (G) Ratio of WT to CXCR6$^{-/-}$ OT-I cells in bins based on distance to the nearest airway. Ratios greater than 1 indicate more WT cells. Data are representative of 2 experiments with 4-5 recipient mice (B,C) or were compiled from whole lung sections from 6 individual mice from 2 independent replicates (E-G).

CXCR6 is expressed on T_{RM} recently recruited to the airways and is required for airway T_{RM} maintenance. Although the impact of CXCR6-mediated trafficking on lung T_{RM} is limited to airways, surface expression of CXCR6 on airway T_{RM} was significantly lower than parenchyma T_{RM}. Airway T_{RM} are a dynamic population with a relatively high rate of turnover that must be replaced by a steady influx of cells from the established memory T cell pool (Ely et al., 2006). This raised the possibility that high levels of CXCR6 expression on parenchyma T_{RM} may guide cells to the airways, and upon entry into the airways CXCR6 is downregulated. To test this, we first compared transcriptional activity from the *Cxcr6* locus to CXCR6 protein expression by crossing *Cxcr6*$^{-/-}$ and WT mice to generate one allele that drives eGFP expression from the *Cxcr6* promoter and one allele that can produce CXCR6 protein. A comparison of CXCR6 protein expression between airway (BAL) and parenchyma (Lung Res) T_{RM} confirmed our previous results of decreased surface CXCR6 expression on airway T_{RM} (Figure 13A). However, airway T_{RM} showed continued, but diminished, *Cxcr6* transcription as measured by GFP expression (Figure 13B). To investigate when the loss of CXCR6

surface expression is occurring on airway T_{RM}, we compared expression of CXCR6 and the integrin CD11a, which is highly expressed on circulating memory T cells but is downregulated within 48 hours after airway entry (Kohlmeier et al., 2007). Strikingly, the expression of CXCR6 was significantly higher on $CD11a^{Hi}$ airway T_{RM} which have recently entered the airway environment (Figure 13C). In contrast, $CD11a^{Lo}$ airway T_{RM} were uniformly negative for CXCR6 surface expression. As these findings suggested that CXCR6 may be important for the continual recruitment that sustains the airway T_{RM} pool, we investigated whether blocking CXCR6-CXCL16 interactions after T cell memory had been established would impact the maintenance of airway T_{RM} (Figure 13D). Intranasal administration of anti-CXCL16 significantly reduced the frequency of recently recruited $CD11a^{Hi}$ FluNP-specific T_{RM} in the airways compared to PBS controls (Figure 13E). In addition, limiting the influx of cells into the airways by blocking CXCL16 resulted in a significant decrease in the overall number of FluNP-specific airway T_{RM}, but had no effect of the number of FluNP-specific T_{RM} in the lung parenchyma (Figure 13F). Thus, CXCR6-CXCL16 interactions maintain the airway T_{RM} pool through the continual recruitment of lung T_{RM} into the airways.

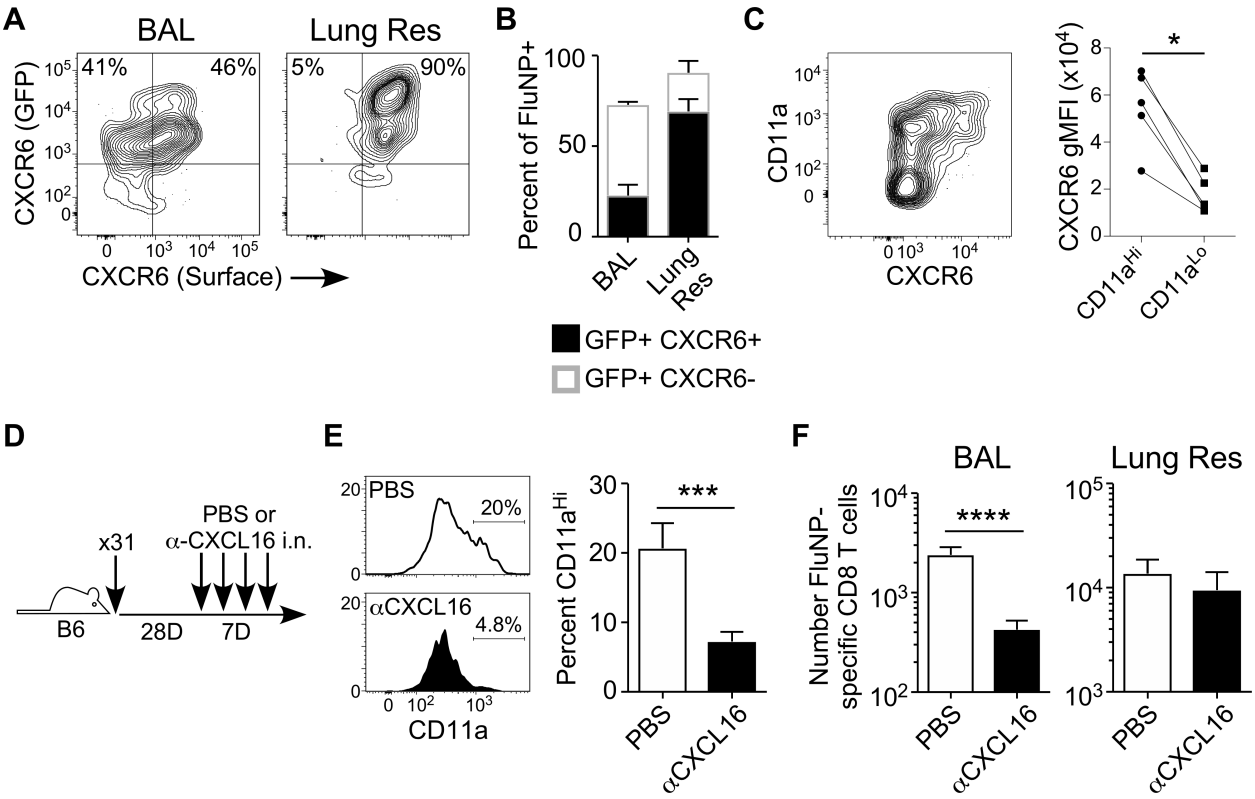

Figure 13: CXCR6 expression is downregulated upon entry into the airways. (A) Example flow plots showing GFP expression of CXCR6$^{GFP/+}$ CD8 T cells versus surface expression of CXCR6 in the BAL and lung-resident compartments. (B) Quantification of GFP expression based on surface CXCR6 expression (black, CXCR6^{+}; open, CXCR6^{-}) in the BAL and lung-resident populations. (C) Flow staining and gMFI quantification of CXCR6 levels based on CD11a expression in CD8 T cells in the BAL. Example staining is concatenated from 5 mice. (D) Experimental setup of CXCL16 blockade experiment. (E) Example staining and quantification of CD11a expression on PBS (open histogram and bar) or αCXCL16-treated (black histogram and bar) mice. (F) Numbers of antigen-specific cells in the BAL and lung-resident compartments of PBS (open histogram and bar) or αCXCL16-treated (black histogram and bar) mice. Data are representative of 2 (A, B), 4 (C), or 3 (E, F) experiments and were analyzed by Student's t test (C, E, F).

Discussion

We have shown that CXCR6 expression was increased on lung T_{RM} compared to T_{EM} in the vasculature, and expression was highest on T_{RM} co-expressing the canonical tissue residency markers CD69 and CD103. The increased expression of CXCR6 on lung CD8 T cells was sustained throughout the immune response to influenza infection and was dependent on pulmonary antigen encounter. Mice lacking CXCR6 had decreased

numbers of virus-specific $CD8^+$ T cells in their airways following influenza or parainfluenza infection despite equal CXCR3 expression, demonstrating a unique role for CXCR6 in regulating the airway T_{RM} pool. In the absence of CXCR6, immune mice had increased morbidity following a heterosubtypic respiratory viral challenge. Mixed bone marrow chimeras showed that the effects on airway T_{RM} observed in *Cxcr6*$^{-/-}$ mice were not due to differences in the immune response between intact WT and *Cxcr6*$^{-/-}$ mice, and that the effect was broadly applicable to T_{RM} formed by other respiratory viruses. In addition to decreased numbers within the airways, lung $CD8^+$ T cells lacking CXCR6 were located further from the airways than WT cells. CXCL16, the ligand for CXCR6, was expressed exclusively in the airways and blockade or genetic deletion of CXCL16 led to decreased recruitment of virus-specific $CD8^+$ T_{RM} to the airways. Finally, $CD69^+CD103^+$ $CD8^+$ T_{RM} cells in human lungs also had increased CXCR6 expression compared to $CD69^-CD103^-$ cells and CXCL16 was expressed by human bronchial epithelial cells lining the airways. Together, these findings identified a critical role for CXCR6-CXCL16 interactions in controlling the localization of virus-specific $CD8^+$ T_{RM} in the lung and maintaining the airway T_{RM} pool.

Previous genomic analyses of $CD8^+$ T_{RM} cells have shown increased *Cxcr6* expression is a common trait of T_{RM} in many mucosal sites, but the biological importance of CXCR6 expression on T_{RM} in these tissues is less well defined (Hombrink et al., 2016; Kumar et al., 2017; Mackay et al., 2016). CXCR6 was important in the maintenance of T_{RM} in the liver following malaria infection in mice and was highly expressed on intrahepatic $CD69^+$ $CD103^+$ HBV-specific CD8 T_{RM} in humans (Fernandez-Ruiz et al., 2016; Tse et al., 2014). CXCR6 was expressed on skin T_{RM} in humans, and important for the maintenance of skin T_{RM} in mice where $CXCR6^{-/-}$ cells

formed fewer $CD69^+CD103^+$ T_{RM} in the skin at memory (Zaid et al., 2017). Notably, direct injection into the skin resulted in a similar decrease in *Cxcr6*$^{-/-}$ skin T_{RM}, suggesting CXCR6 may be important for retention rather than recruitment of $CD8^+$ T cells in the skin. Although a role for CXCR6 in the localization of gut T_{RM} has not been reported, CXCR6 regulated the topography of $NKp46^+$ ILC3s in the intestine by directing their interaction with CXCL16-expressing $CX3CR1^+$ intestinal dendritic cells (Satoh-Takayama et al., 2014). These studies, together with our reported data, suggest that CXCR6-CXCL16 interactions may have a primary role of controlling localization of lymphocytes within tissues, rather than directly recruiting them into the tissue from the circulation.

Previous studies investigating mechanisms controlling T cell localization to the lung have identified chemotactic or adhesion molecules that regulate migration or retention of antigen-specific T cells resident in both the lung parenchyma and airways. Integrins such as VLA-1 (CD49a), $\alpha_E\beta_7$ (CD103), or E-cadherin are important for the maintenance of lung T_{RM}. The chemokine receptor CXCR3 has been implicated in the homing and maintenance of lung T_{RM}, but its role in effector T cell recruitment to the parenchyma and airways during the acute response to respiratory infection has complicated evaluation of its role in maintaining lung T_{RM} once they have been established. $CXCR3^{-/-}$ antigen-specific effector T cells fail to accumulate in the lung and airways following influenza or parainfluenza virus infections, resulting in a smaller pool of cells in the tissue that can survive contraction and transition into T_{RM} (Kohlmeier et al., 2009). CXCR3 is important for the recruitment of circulating memory $CD8^+$ T cells to the lung in response to respiratory infection, but a population of $CXCR3^{Lo}$ lung T_{RM} is maintained under homeostatic conditions in the interstitial spaces of the lung. Thus, the

role of CXCR3 in the trafficking and/or maintenance of memory T cells in the lung may largely depend on the presence or absence of localized inflammation, and future studies where CXCR3 can be conditionally ablated at different times during the immune response may help to refine its role in lung T_{RM}. In addition to the role of chemokines in trafficking to the lung, the potential for chemotactic signals to regulate partitioning of T_{RM} between the airways and parenchyma has been largely unexplored. It was previously shown that airway surveilling memory $CD8^+$ T cells expressed high levels of CXCR3 and that CXCR3 was required for the steady-state recruitment of memory T cells to the airways following intravenous transfer, but we found CXCR3 expression was identical between WT and *Cxcr6*$^{-/-}$ flu-specific CD8 T cells and thus unlikely to contribute to the difference we observed in *Cxcr6*$^{-/-}$ airway T_{RM} (Slütter et al., 2013). It should be noted that neither *Cxcr3*$^{-/-}$ or *Cxcr6*$^{-/-}$ memory T cells showed a complete loss of airway T_{RM}, raising the possibility that both chemokine receptors can contribute to the preferential migration of T_{RM} into the airways under steady-state conditions.

Defining mechanisms that differentially regulate these two populations of T_{RM} within the lung is important because they have been shown to have distinct effector functions that synergize to provide optimal cellular immunity in the lung (Jozwik et al., 2015; McMaster et al., 2015). Airway T_{RM} are able to rapidly produce cytokines upon antigen recognition but are poorly cytolytic, and thus likely serve more of a sentinel role to draw additional immune cells to sites of viral infection in the lung. Several reports have shown that pathogen-specific airway T_{RM} numbers correlate with protection against respiratory challenge, and thus identifying mechanisms that regulate airway T_{RM} is central to developing strategies that promote robust cellular immunity against respiratory pathogens. Airway T_{RM} have a short half-life in the lumen of airways (~14

days) and begin to downregulate certain cell surface markers such as CD11a and Ly6C within hours of entering the airway environment (Ely et al., 2006; Kohlmeier et al., 2007). In addition, airway T_{RM} do not undergo homeostatic proliferation and must be continually replenished from the memory T cell pool, but the mechanisms regulating this continual recruitment had not been known. Our data showed that CXCR6 expression on lung-resident $CD8^+$ T cells direct their movement within the tissue toward the CXCL16 gradient from the airway epithelium, resulting in a one-way migration into the airways to replenish and maintain the airway T_{RM} pool. This process raises interesting questions regarding the source of newly-recruited airway T_{RM}, and the impact it may have on other memory $CD8^+$ T cell populations. The most straightforward explanation is that the lung parenchyma T_{RM} population is continually seeding airway T_{RM}, which is supported by the high CXCR6 expression on this population, proximity to the airways, and analysis of recently-recruited airway T_{RM} showing they arrive in the airways expressing T_{RM} markers such as CD69 and CD103. This may also explain the gradual decline of T_{RM} in the lung parenchyma as they are recruited into the airways (Wu et al., 2014). Additional studies are required to fully understand the ontology of the antigen-specific CD8 T cells that continually seed the airway T_{RM} pool.

In summary, we have identified a unique role for the chemokine receptor CXCR6 in directing the migration of T_{RM} in the lung under steady-state conditions and maintaining the airway T_{RM} pool. The differential impact of CXCR6 signaling on the airway and parenchyma T_{RM} populations in the lung was likely due to the localization of CXCL16, the ligand for CXCR6, to the respiratory epithelium. As airway T_{RM} are known to be critical for cellular immunity in the lung, developing vaccination strategies that

induce CXCR6 expression on antigen-specific T cells may increase airway T_{RM} and improve the efficacy of vaccination against respiratory pathogens.

Methods

Mouse Models. C57BL/6J (B6), B6.PL-*Thy1*^{a}/CyJ (CD90.1), B6.SJL-*Ptprc*^{a}*Pepc*^{b}/BoyJ (CD45.1), C.129P2-*Cxcr6*^{tm1Litt}/J (CXCR6$^{-/-}$), and C57BL/6-Tg(TcraTcrb)1100Mjb/J (OT-I) mice were purchased from The Jackson Laboratory. Mice were housed and bred under specific pathogen-free conditions at Emory University. B6 and CD45.1 mice were bred and the F1 mice were used as controls for CXCR6$^{-/-}$ mice for congenic identification. OT-I mice were crossed with CD90.1 or CXCR6$^{-/-}$ mice to give congenic WT OT-I (CD90.1^{+}) and CXCR6$^{-/-}$ OT-I (CD90.2^{+}). Mice were assigned to experimental groups in the order they were weaned and all experiments used both male and female mice at 8-12 weeks of age. The mice were healthy, immune competent, influenza-naïve, with no previous procedures. Mice were housed 5 to a cage in autowater racks before transfer to sterile static cages for infection. All animal procedures and experiments were approved by the Emory University or Kindai University Animal Care and Use Committees.

Human Lungs. Non-transplantable but otherwise healthy human lungs were provided by LifeLink of Georgia. Lungs were explanted by LifeLink personnel after transplantable organs were harvested and transported on ice to Emory University for further processing. Informed consent was obtained from next-of-kin prior to explant. This study was exempt from IRB review since the donors were deceased at time of collection.

Virus Strains. Sendai virus, Influenza A/PR8, Influenza A/HK-x31, and Influenza A/HK-x31-Ova_{I} were grown in embryonated chicken eggs for 72 hours before harvest

and pooling of the allantoic fluid. The 50 % egg infectious dose (EID_{50}) or plaque forming units (PFU) of pooled virus stocks was determined prior to use. For PR8, the LD_{50} was determined previously by infection of WT C57BL6/J mice with varying amounts of virus.

2,2,2-tribromoethanol solution. To make 2,2,2-tribromoethanol solution, 12.5 g 2,2,2-tribromoethanol was slowly dissolved in 25 mL of tert-amyl alcohol using a magnetic stir bar and stir plate. Following complete dissolution, 1 L deionized water was added in 100 mL fractions every 5 minutes with continued stirring. The solution was sterile filtered, aliquoted into brown glass bottles, and stored in the refrigerator until use.

Ack buffer. To make Ack lysis buffer, 32.96 g ammonium chloride, 4 g potassium bicarbonate, and 0.149 g sodium EDTA were dissolved in 4 L deionized water. The solution was sterilized by autoclave before use.

MACS buffer. To make MACS buffer, 16 mL of 0.5-M sodium EDTA was combined with 20 mL fetal bovine serum, 400 mL 10x PBS, and 3.564 L deionized water and mixed completed. The solution was filter sterilized before use.

Digestion media for mouse lungs. For digestion media, Hank's Balanced Salt Solution was armed in a 37-degree C water bath. 1mL DNase stock solution (2E3 units/mL in PBS) and 5 mL Collagenase D stock (5g/mL in RPMI with 10% FBS, 1% Penn/Strep/Glut) were added to 44 mL of warm Hank's and used immediately.

Intranasal animal infection. For sub-lethal infection with influenza HK-x31 or Sendai viruses, mice were anesthetized with 300-400 μL 2,2,2-tribromoethanol solution and virus was administered dropwise intranasally in 30 μL of PBS. Sendai was used at 3×10^3 EID_{50} per mouse, influenza A/HK-x31 and Influenza A/HK-x31-Ova_I were used at

3×10^4 EID_{50}. For challenge experiments with PR8, mice were anesthetized with isoflurane before intranasal dosage of virus in 50 μL. Primary infection with PR8 was at 250 PFU (1x LD_{50}) and secondary infection with PR8 was at 1250 PFU (5x LD_{50}). During lethal infection, mice were monitored daily for weight loss and euthanized at 25 % weight loss as required by Emory IACUC.

Intramuscular animal infection and "pull". To establish a circulating pool of influenza-specific T cells, mice were infected intramuscularly in the right thigh with 1×10^6 EID_{50} influenza A/HK-x31 in 50 μL HBSS. The thighs were wiped with 70 % ethanol following injection to prevent intranasal infection. 7 days after infection, mice were anesthetized with 300-400 μL 2,2,2-tribromoethanol and dosed intranasally with 50 μL of PBS containing 5 μg ODN-1826 with or without 5 μg of the immunodominant CD4 and CD8 influenza peptides NP 311-325 and 366-374.

Generation of mixed bone marrow chimeras. To generate mixed bone marrow (BM) chimeras, donor mice were euthanized and the femurs were harvested into complete RPMI. BM was washed out of the femur and stored in complete RPMI until just before transfer, when the cells were spun down and suspended in PBS at $1x10^8$ cells per mL and the two genotypes were mixed at a 1:1 ratio. BM was transferred i.v. to recipient mice via the tail vein. Before receiving BM, recipient mice were given two doses of 475 rads of gamma irradiation from a ^{131}Cs irradiator with 6 hours between doses. Chimeras were maintained on a solid food diet with 1.2% sulfamethoxazole and 0.2% trimethoprim (Purina TestDiet 5TYG) for four weeks and given wet food and Napa Nectar every other day for the first two weeks. Mice were rested for an additional two weeks prior to use, allowing for immune reconstitution.

General mouse harvest, cell isolation, staining, and flow cytometry. When appropriate, mice were injected i.v. with 1.5 mcg CD3e-PE/CF594 in 200 μL sterile PBS via the tail vein. After 5 minutes, mice were injected with 500 μL 2,2,2-tribromoethanol solution i.p. and exsanguinated brachially. Bronchoalveolar lavage (BAL) was harvested directly from euthanized mice via insertion of an 18-ga catheter into an incision in the trachea and 5 x 1-mL washes were performed with RPMI 1640 supplemented with 10% fetal bovine serum, and 1x penicillin/streptomycin/glutamine (complete RPMI). Lung, mediastinal lymph node, and spleen were harvested and placed into appropriate tubes filled with 5 mL Hank's balanced saline solution (HBSS).

Spleens were inserted into sterile mesh pouch in a tissue culture dish and homogenized with tweezers before transferring back to tube. Cells were pelleted via centrifugation and resuspended in 3 mL ACK buffer and allowed to sit at r.t for 3 min. The reaction was quenched with 10 mL HBSS and spun down. The cells were resuspended in 5 mL complete RPMI for counting and staining. Cells were resuspended to a final concentration of $1x10^7$ cells/mL in complete RMPI and 200 μL of cells were stained for flow ($2x10^6$ cells).

Mediastinal lymph nodes were processed similarly except for the Ack lysis step. Lymph nodes were resuspended in 200 μL complete RPMI for counting and the entire sample was stained.

BAL samples were spun down and resuspended in 200 μL of complete RPMI for counting and staining.

Lungs were transferred to a 6-well plate, and media was aspirated. Lungs were chopped with scissors before digestion with 5 mL digestion media. Samples were further homogenized by syringing up and down with a 3-mL syringe 10 times per well.

Lungs were incubated at 37°C for 30 minutes, syringing every 10 minutes. Lung suspension was transferred back to original tubes, the reaction was quenched by addition of 10 mL HBSS, and cells were pelleted. Pellets were resuspended in 3 mL of 80 % isotonic Percoll at r.t. and overlaid with 40 % isotonic Percoll at r.t. Tubes were spun for 25 minutes with low brake (setting 3 on Sorvall ST-40R). Lung cells were resuspended in 200-600 µL of complete RPMI for counting and staining. 2E6 cells were stained per well.

For staining, samples were transferred to a 96-well V-bottom plate and spun down. For live/dead staining, cells were resuspended 200 µL PBS and spun down. Cells were washed with additional 200 mcl PBS. Cells were resuspended in 100 µL PBS with Zombie UV or Zombie NIR at a 1:200 dilution and stained 30 minutes at r.t. in the dark. Following staining, 100 µL PBS was added and the cells were spun down. Cells were washed with 200 µL FACS wash (PBS with 2 % BSA and 0.05 % sodium azide) and spun down. For blocking of Fc receptors, 100 µL murine FC block 2.4G2 (1 mcg/mL) in FACS wash was added and cells were incubated on ice for 25 min. Cells were spun down and 50 µL of tetramer cocktail was added to each well and stained for 60 min at r.t. in the dark. 150 µL FACS wash buffer was added and cells were spun down. 50 µL of antibody cocktail was added to each well and samples were stained for 30 min on ice in the dark. 150 µL FACS wash buffer was added and cells were spun down. Cells were fixed for 20 minutes in the dark using 100 µL of 1% paraformaldehyde. The fixation was quenched with 100 µL FACS wash and cells were spun down and resuspended in 150 µL FACS wash for flow cytometry.

Specific cell staining procedures. For experiments using the CXCL16-hFc fusion protein to stain cells, the fusion protein solution was mixed 1:1 with Fc block solution

and cells were incubated for 30 minutes before addition of 150 μL FACS ash and spinning down cells. 50 μL of secondary reagent (anti-human FCγ-APC, 1:50) was added to cells and incubated on ice for 20 minutes before addition of 150 μL FACS wash and spinning down of cells. The staining continued with the surface antibody stain as above.

Staining of CCR5 required intracellular staining. Following surface stain, cells were incubated with 100 μL Cytofix/Cytoperm for 20 minutes at room temperature in the dark before the addition of 100 μL Perm/Wash Buffer and spinning down cells. Cells were resuspended in 50 μL Perm/Wash buffer containing antibodies against intracellular antigens and incubated on ice for 30 minutes in the dark. An additional 150 μL of Perm/Wash was added and the cells were spun down. The cells were washed twice more with 200 μL of Perm/Wash before resuspension in FACS wash for flow cytometry.

Isolation of human lung leukocytes. Digestion media was made with 300 mL RMPI 1640, 3 mL non-essential amino acid solution, 3 mL 100x sodium pyruvate, 30 mL collagenase D solution, 6 mL DNase I solution, and 7.5 mL of trypsin inhibitor solution (40 mg/mL in PBS). Digestion media was warmed to 37 degrees C in a water bath.

Blocks of tissue from the lung parenchyma were removed and flash frozen using liquid nitrogen in OCT for microscopy. The remainder of the lung was cut into 1 inch pieces and homogenized by mechanical disruption with a meat grinder. Approximately 20 mL of homogenized lung was transferred to a 50-mL conical tube and 20 mL of digestion media was added. The lungs were digested for 2 hours at 37 degrees C with shaking at 100 rpm. The digested lungs were filtered through a mesh strainer with 1 x

100-mL wash using complete RPMI. The suspension was aliquoted into 50 mL conical tubes and spun down. Red blood cells were lysed using 5 mL of warm Ack media for 5 minutes and the reaction was quenched with 25 mL HBSS and spun down. The cell pellets were resuspended in 12 mL of 80 % isotonic Percoll and moved to 2x15-mL conical tubes. The suspension was overlaid with 40 % isotonic Percoll and tubes were spun as above. The cells were counted and resuspended at $2x10^7$ cells/mL in 90% FBS/10% DMSO and frozen at -80°C before transfer to a liquid nitrogen tank for long-term storage.

Staining of human lung leukocytes. For staining, samples were thawed, immediately transferred to 14 mL of warm complete RPMI, and spun down. Cell pellets were transferred to a 96-well V-bottom plate and spun down.

For live/dead staining, cells were resuspended 200 µL PBS and spun down. Cells were washed with additional 200 µL PBS. Cells were resuspended in 100 µL PBS with Zombie UV at a 1:200 dilution and stained 30 minutes at r.t. in the dark. Following staining, 100 µL PBS was added and the cells were spun down. Cells were washed with 200 µL FACS wash and spun down.

50 µL of antibody cocktail containing human Fc blocking reagent was added to each well and samples were stained for 30 min on ice in the dark. 150 µL FACS wash buffer was added and cells were spun down. Cells were fixed for 20 minutes in the dark using 100 µL of 1% paraformaldehyde. The fixation was quenched with 100 µL FACS wash and cells were spun down. Cells were resuspended in 150 µL FACS wash for flow cytometry.

Cell isolation, sorting, and RNA isolation for Cxcr6 qPCR. Mice were euthanized, BAL and lungs were harvested, and lungs were digested as described in “General Mouse

Harvest" section with the inclusion of the i.v. antibody. For staining, cells were resuspended in 200 μL PBS and spun down. Cells were resuspended in 100 μL PBS with Zombie NIR, CD8a-BV510, CD103-BV421, CD62L-BV605, CD69-PE, CD3-APC, CD44-A700, CD4-APC/Cy7, CD11b-APC/Cy7, F4/80-APC/Cy7, CD19-APC/Cy7 and stained 30 minutes on ice in the dark. Following staining, 100 μL PBS was added and the cells were spun down. Cells were sorted into buffer RLT containing 1% beta-mercaptoethanol on a BD FACS Aria II for live CD4-CD11b-F4/80-CD19-CD3+CD4-CD8a+CD44+CD62L-CD3eiv- cells. These were further divided into three populations based on CD69 and CD103 expression.

RNA was extracted using the QIAGEN RNeasy Kit. cDNA synthesis was performed using the High Capacity cDNA Reverse Transcription Kit from ThermoFisher. Briefly, 10 μL RNA sample was added to 10 μL 2X RT master mix. Thermocycler conditions for RT reaction: 25°C for 10 minutes, 37°C for 120 minutes, 85°C for 5 minutes.

Real time qPCR was performed using SYBR Green PCR Master Mix for *Cxcr6* gene expression using the following primers: *Cxcr6*-F, 5'-CTT CTC TTC TGA TGC CAT GGA-3' and *Cxcr6*-R, 5'-GAA ACA CAT CTG TCA GAG TCC-3'. Expression levels were normalized to hypoxanthine guanine phosphoribosyl transferase (*Hprt*) using the following primers: *Hprt*-F 5'-CAT TAT GCC GAG GAT TTG GAA-3' and *Hprt*-R, 5' CAC ACA GAG GGC CAC AAT GT-3'. Amplification parameters were as follows: 1) 95°C for 10 minutes, 2) 95°C for 15s, 3) 60°C for 30s, 4) 68°C for 30s, repeat steps 2-4 forty times.

OT-I transfer. WT and CXCR6$^{-/-}$ OT-I mice were euthanized by 2,2,2-tribromoethanol overdose and brachial exsanguination. Spleens were harvested into 5

mL HBSS and homogenized by mechanical disruption. Cells were pelleted via centrifugation. Cells counted and resuspended at $1x10^8$ cells/mL in a 5-mL FACS tube. CD8 T cells were purified via negative section using Stem Cell CD8+ T cell negative selection kit. 50 μL of CD8 isolation cocktail was added per 1mL of cell suspension and incubated at r.t. for 10 minutes. Anti-biotin beads were resuspended by vigorous vortexing before adding 125 mL per mL of sample and incubation at r.t. for 5 minutes. Cells were brought up to 2.5 mL of media and placed in the Stem Cell magnet for 5 minutes. Liquid was transferred to a new tube via stripette and the cells were spun down. The cells were resuspended in 1 mL complete RPMI for counting and a 20 μL aliquot was stained for purity with TCRVα2-PE, CD45.1-PE/CF594, CD11b-PerCP/Cy5.5, TCRVβ5-APC, CD90.1-A700, CD45.2-BV421, CD4-BV510, CD90.2-BV785, and CD8a-BV711. Cells were resuspended at $1x10^5$ OT-I cells per mL and the two suspensions were mixed 1:1 for injection of 200 μL of cells ($1x10^4$ per genotype) i.v. tail vein. A small aliquot of the injection mixed was stained with the same antibodies to determine the exact ratio of the infected cells.

Lung harvest for immunofluorescence microscopy. Mice were euthanized with 500 μL 2,2,2-tribromoethanol i.p. and brachially exsanguinated. The skin was removed from the upper body and the ribcage was removed to allow for removal of the organs *en bloc*. The trachea was exposed and a small incision made. The lungs were inflated with 0.7 mL OCT via an 18 gauge i.v. catheter. Silk suture was used to tie off the trachea before removal of the catheter. The trachea was cut above the suture and the lungs were removed and placed in a plastic mold with OCT and covered in OCT. The lungs were floated in a cell culture dish on liquid nitrogen until set and then transferred to dry ice. The lungs were stored at -80°C until sectioning.

Immunofluorescent microscopy staining. Lungs were sectioned at 7 microns on a cryostat and transferred to positively-charged microscope slides. Slides were stored at -80°C until staining.

For staining, slides were removed from the freezer and dried on the grate of a biosafety cabinet (BSC) for 10 minutes. Slides were then fixed in 75:25 acetone/ethanol for 10 minutes and washed 4 x 30 seconds in PBS. Slides were dried on the BSC and outlined with a pap pen. The slides were blocked with FACS wash with 1µg/mL anti-mouse CD16/32 clone 2.4G2, 10% mouse serum, 10% rat serum and 10% donkey serum for 30 minutes at room temp in the dark. The blocking buffer was flicked off and primary stain was added. Slides were incubated at room temp in the dark for 30 minutes. If necessary, slides were washed 4 x 30 seconds in PBS and a secondary stain was performed for 15 minutes. The slides were washed 4 x 30 seconds in PBS and dried on the BSC. Coverslips with Prolong Gold were applied and the slides were cured overnight before imaging.

CXCL9/10/16 ELISA. Serum and BAL (1 mL) were harvested from naïve or x31-infected mice at indicated time points. Chemokine concentration was determined using Quantikine ELISA Kit for CXCL9 and CXCL10, and mouse CXCL16 ELISA Kit according to the manufacturer's instructions.

Cxcl16 qPCR. Lungs are harvested from x31-infected mice at day 30 postinfection and digested by collagenase. Lung cell suspensions were fractionated into CD45/TER119$^+$ hematopoietic cells (HPC) and CD45/TER119$^-$ non-HPC by MACS system (Miltenyi Biotec). HPC and non-HPC were then fractionated into CD11c$^+$Siglec-F$^+$ alveolar macrophages (AM) and non-AM or CD31$^+$endothelial cells, CD31-EpCAM-1$^+$ epithelial cells, CD31$^-$PDGFRα$^+$ fibroblasts and CD31$^-$EpCAM-1$^-$PDGFRα$^-$ other stromal

cells, respectively, by cell sorting with a MoFlo Astrios cell sorter (Beckman Coulter). Purity of the isolated cells was more than 92%.

For the quantification of *Cxcl16* expression in lung tissue cell compartments, total RNA was isolated using TRIzol reagent (Life Technologies) and reverse transcribed to cDNA with ReverTra Ace® qPCR RT Master Mix with gDNA Remover (Toyobo). Quantitative PCR was performed on an ABI 7500 Real-Time PCR system (Life Technologies) with THUNDERBIRD SYBR or Probe qPCR Mix (Toyobo). *Rps3* mRNA, a gene equally and stably expressed throughout a variety of lung cell populations and inflammatory conditions (unpublished transcriptome analysis), was used for normalization. Primers and Taqman probes used were as follows: *Rps3* forward, 5'-CGGTGCAGATTTCCAAGAAG-3', *Rps3* reverse, 5'- GGACTTCAACTCCAGAGTAGCC -3'; *Cxcl16* forward, 5'-TGTGGAACTGGTCATGGGAAG-3', *Cxcl16* reverse, 5'-AGCTTTTCCTTGGCTGGAGAG-3'; *Cxcl16* probe, 5'-TGCCTCAAGCCAGTACCCAGACCC-3'.

CXCL16 blockade. Anti-SR-PSOX/CXCL16 mAb IgG1 12-81 was generated as described previously (Shimaoka et al., 2004a). Mice were infected i.n. with x31. Twenty-eight to 35 days later, mice were administered either anti-SR-PSOX/CXCL16 mAb (30 μg/30 μl) or PBS i.n. twice by three days interval. Tissues were harvested, processed and stained as described in the "General Mouse Harvest" section six days after initial treatment.

Statistics. Flow cytometry data was analyzed using Flowjo. Relevant populations were identified and the percent of parent or gMFI statistics were exported to Microsoft Excel. Cell numbers were calculated by using percent of parent data and the live cell count on a hemocytometer. Calculated values were analyzed for significance using

Graphpad Prism. Details of statistical methods are provided in figure legends. Gaussian distributions were tested using the Kolmogorov-Smirnov test of normalcy, parametric tests were used with data that was Gaussian and non-parametric tests were used on non-Gaussian data. Significance was defined as $p<0.05$; * denotes $p<0.05$, ** denotes $P<0.01$, *** denotes $p<0.001$, and **** denotes $p<0.0001$.

Supplemental Materials

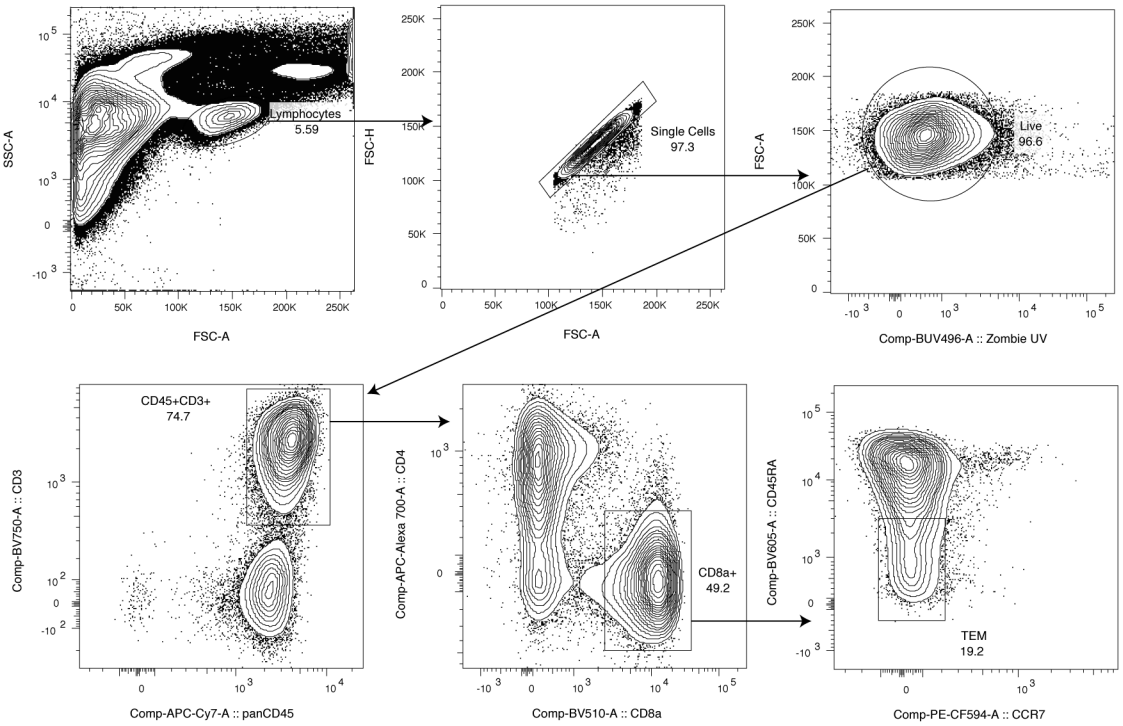

Supplemental Figure 3: Gating strategy for human lung T cells.
Example gates for the donor shown in Figure 1. Live singlet lymphocytes were then gated on $CD45^+CD3^+$ and T cells were divided in $CD4^+$ and $CD8^+$. The effector memory CD8 T cells were then selected based on CCR7 and CD45RA expression.

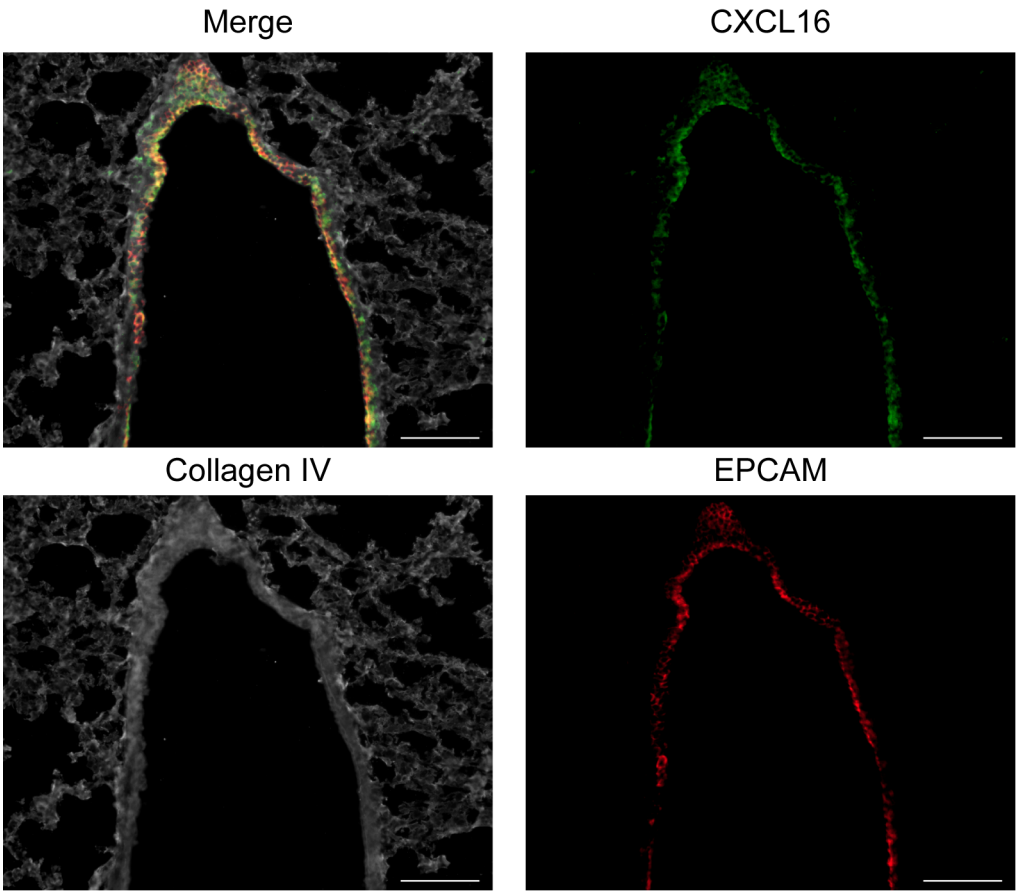

Supplemental Figure 4: Fluorescence microscopy of naïve mouse lungs. Immunofluorescence microscopy of mouse lung showing CXCL16 (green), EpCAM (red) and Collagen IV (grey). Original image is at 200x magnification.

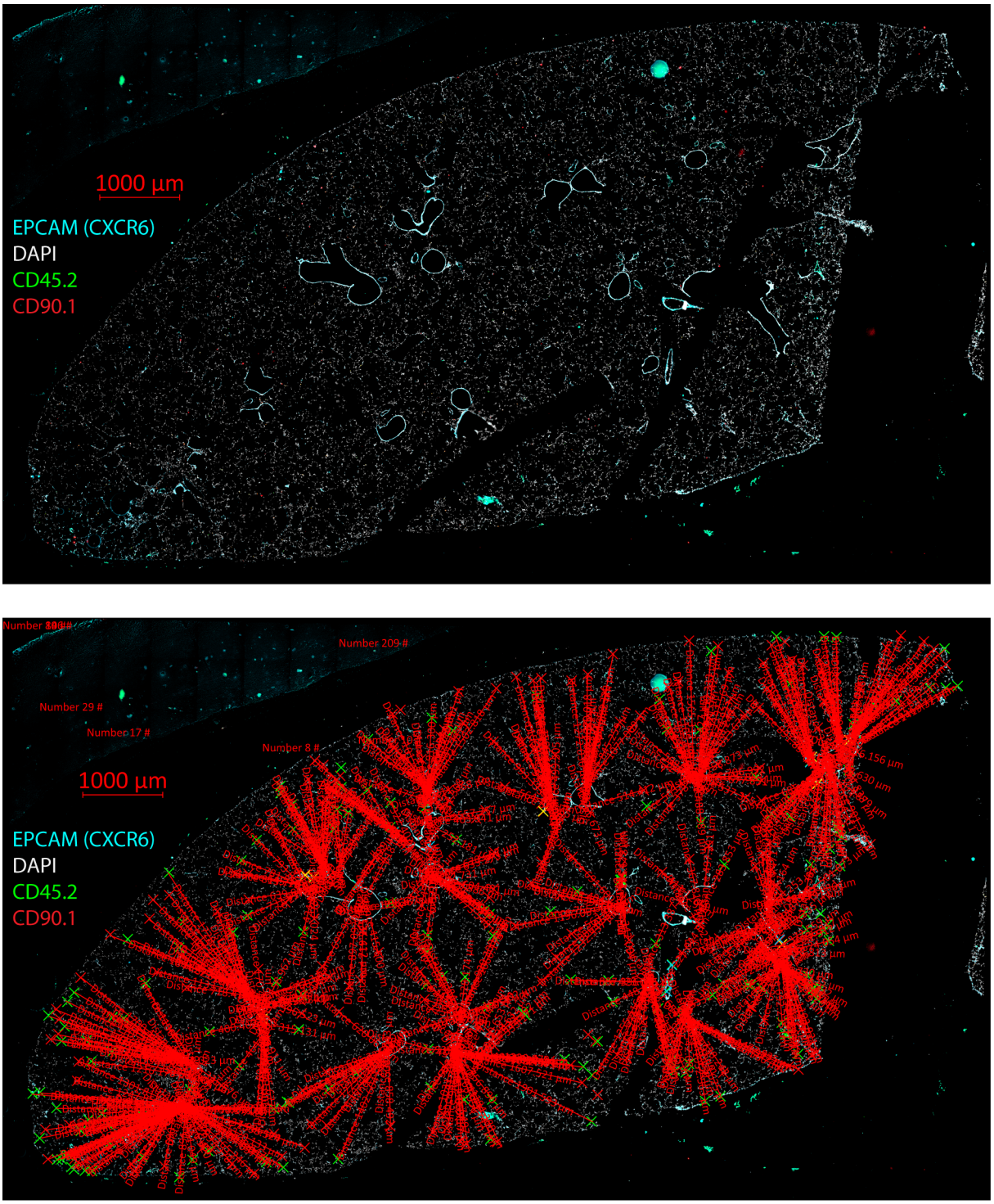

Supplemental Figure 5: Method of measuring distance to the nearest airway by fluorescence microscopy.
Example image of a mouse lung section showing WT (red X) and *Cxcr6*$^{-/-}$ (green X) OT-I T cells. All transferred cells are CD45.2^{+} (green) and WT cells are CD90.1^{+} (red). EpCAM (cyan) and DAPI (white) were used to define airways. Cells were marked and the distance to the nearest EpCAM+ airway was measured using Zen Pro software.

Chapter 4. Discussion, insights, and future directions.

Chapter 1 of this thesis introduced cytokines and chemokines and how they function in the immune system. Additionally, an overview of influenza virus infection and the resulting immune response were presented. An extensive review of the functions of IL-36γ and CXCR6 was included since knowledge of these proteins is necessary to understand the context of Chapters 2 and 3 and evaluate the claims to be made in Chapter 4. However, synthesis of the existing knowledge of these two proteins was reserved until Chapter 4 to allow for the incorporation of new discoveries contained in Chapters 2 and 3.

Chapter 2 explored the role of IL-36γ in the immune response to influenza infection. We showed that *Il36g* is upregulated throughout the course of infection and that *Il36g*$^{-/-}$ mice have increased viral titers, pathology, proinflammatory cytokines, morbidity, and mortality following influenza infection. This striking phenotype correlated with the loss of alveolar macrophages in *Il36g*$^{-/-}$ mice. The alveolar macrophages in *Il36g*$^{-/-}$ mice had increased apoptosis and M2-like gene expression and surface protein markers, but transfer of *Il36g*$^{-/-}$ alveolar macrophages to a WT mouse reduced this skewing. Finally transfer of WT alveolar macrophages to *Il36g*$^{-/-}$ mice rescued the mortality of these mice. Therefore, IL-36γ is a key mediator of alveolar macrophage phenotype at baseline and survival during influenza infection.

Chapter 3 defined CXCR6 as a chemokine receptor responsible for homing of CD8$^+$ T cells to the airways. CXCR6 was expressed at higher levels in lung-resident cells than cells in the lung vasculature and expression was highest in the canonical CD69$^+$CD103$^+$ CD8$^+$ T_{RM} cells in mice and humans. Increased expression was observed over the duration of the immune response to influenza infection and was dependent on

antigen encounter in the lung. *Cxcr6*$^{-/-}$ mice had decreased numbers of influenza-specific CD8^{+} T cells in the airways during the acute infection and this defect continued out to memory. The defect was also seen using Sendai virus, generalizing the findings to respiratory virus infection. CXCL16 protein is produced by the bronchial epithelium in mice and humans. *Cxcl16*$^{-/-}$ mice had a similar defect to *Cxcr6*$^{-/-}$ mice and blockade of CXCL16 after memory was established showed that the chemokine is required for maintenance of the airway-resident cells at steady state. Together, these data demonstrate the importance of CXCR6 and CXCL16 in CD8^{+} T cells trafficking to the airways. Several outstanding questions related to these finding will now be discussed.

Function of individual IL-36 members

Defining the role of individual IL-36 agonists has been difficult since knockout mice for the individual IL-36 cytokines have only recently been reported (Aoyagi et al., 2017a; Kovach et al., 2017; Milora et al., 2015; Ngo et al., 2018). Data from this paper, as well as other works, suggest that different IL-36 family members have different effects in several contexts including lung immunity. One possible explanation is gene regulation instead of gene function. Several of the works reviewed in Chapter 1 showed differential expression of *Il36* genes. In depth analysis of transcription factor binding has only been performed for *Il36a* (Nerlich et al., 2015). Data from *in vitro* and *ex vivo* experiments (many of which are described in Chapter 1) that tested treatments to induce IL-36 proteins give some insight into possible regulatory mechanisms for *Il36b* and *Il36g*, but there is no direct evidence on the topic. In the lungs of naïve mice, the mRNA levels of the three *Il36* genes varied by greater than 100-fold, implying a difference in regulation of these three genes. Examination of the promotors of *Il36b* and *Il36g* to identify transcription factors binding motifs would be a first step in the process.

Additional work could include *in vitro* knockdown of specific transcription factors or deletion of transcription factor binding sites to identify the most important regions and proteins for *Il36b* and *Il36g*.

A second possibility is a difference in the activity of the various IL-36-activating proteases, which would prevent full activity of one or more IL-36 proteins. The presence of enzyme inhibitors, including breakdown products, may block the activity of one or more of the activating proteases (Tyagi and Simon, 1993). This could be tested by use of lung homogenate to inhibit the proteases *in vitro*, or more specifically but also more expensively, by proteomic evaluation of the lungs of mice following influenza infection. Differences in expression of the proteases are another possible mechanism as PU.1 has been shown to control the expression of all three azurophil proteases, but leukocyte elastase is additionally controlled by GABPα and possibly MYB (Sturrock et al., 1996; 2004). ELISA of neutrophil supernatants or RNAseq of neutrophils during influenza infection could provide data on the regulation of the azurophil proteases. Pathogen-specific differences in *Il36g*$^{-/-}$ mice may represent downregulation due to pathogen immune evasion mechanisms or differences in induction of various innate immune pathways by PAMPs (Rivera-Marrero et al., 2004). A difference in release is unlikely since all three proteases are contained in azurophil granules. This line of research also needs to address the activation of IL-36 proteins in the absence of infection. Neutrophils are not present in the airways or lung parenchyma at steady-state, thus it is not clear if the IL-36 proteins are being cleaved in naïve mice. This could be addressed by western blotting of BAL fluid or lung homogenate to determine the size of the IL-36 proteins. If they are indeed cleaved, then other proteases may be acting on the proteins in the absence of neutrophils.

Another possible mechanism is an inherent difference in the three IL-36 proteins that modulate their affinity for the receptor or co-receptor or half-life in the microenvironment. IL-36α has approximately 4-fold higher affinity for IL-36R than IL-36γ, but the affinity of IL-36β has not been reported. Differences in affinity do not appear to affect EC_{50} values of the proteins *in vitro*, but may have an as yet unknown effect *in vivo* (Towne et al., 2011). The stability of the proteins in the local environment has not been studied, but could also affect the strength and duration of IL-36R signaling. Administration of the three cytokines to the lungs or skin of mice would show whether the cytokines have overlapping effects *in vivo* and exclude any differences from gene regulation. If done using tagged proteins or in knockout mice, this would also allow for the tissue half-life of IL-36 cytokines to be determined by serial harvest of tissues for detection of the administered proteins.

Determining the exact reason(s) for differences in the function of IL-36α, IL-36β, and IL-36γ in the lung and elsewhere will require a systematic and comprehensive approach that examines all three IL-36 proteins under the same conditions, which has not been done to date. To extend findings from these experiments *in vivo*, crossing of individual *Il36* knockout mouse lines to generate double-knockout mice which only express one of the cytokines would be a good tool to complement the single knockout models currently available; i.e. experiments with WT mice, *Il36g*$^{-/-}$ mice, and *Il36a*$^{-/-}$ *Il36b*$^{-/-}$ mice. Additionally, crossing the three *Il36* knockout lines to generate a triple-*Il36* knockout mouse would allow for testing of IL-36R-dependence of various phenotypes and effects. While initial characterization of the cytokines showed that IL-

36R and IL-1RAcP were required for the effects of IL-36 cytokines, these studies did not rule out that the cytokines act on the cells producing them without being released.

Development of additional models and tools would also aid the field. Currently, there are no commercially available antibodies against IL-36 proteins that are validated in flow cytometry or immunofluorescence microscopy. This greatly impairs the field since experiments as simple as ELISA cannot be performed correctly without monoclonal antibodies. Additionally, a floxed *Il36* mouse would be useful in determining tissue- and cell type-specific effects. This would be complimented by a lox-STOP-lox *Il36* knock in that would specifically restore expression of cytokine in specific tissues. As interest in these proteins grows, more tools will become available to study the function of IL-36 proteins.

CXCR6 and HIV/AIDS

The effect of SNPs on the function of CXCR6 in humans is not well known. Given the work in this dissertation as well as previous studies on the role of CXC6 in T cell trafficking, those SNPs that negatively affect protein structure, function, or stability could be risk factors for respiratory or skin infection. For example, the CXCR6-E3K allele has been linked to a faster time from *Pneumocystis carinii* pneumonia (PCP) diagnosis to death in a dominant fashion (Duggal et al., 2003). It is unlikely that the E3K allele affects HIV fusion with cells as the time from AIDS diagnosis to death was not affected. We show that CXCR6 deficiency has an effect on morbidity in respiratory viral infection and CXCR6 has been shown to be important in protection against bacterial infection of the lung as well (Lee et al., 2011). The association between CXCR6-E3K and increased mortality in PCP was prior to the field's understanding of the important role of CXCR6 in lung immunity and the authors did not link the mortality to

$CD8^+$ T cell function. It is likely that CXCR6 is important in the response to many respiratory pathogens, including PCP, that require an effective $CD8^+$ T cell response for clearance. However, the dominant nature of CXCR6-E3K suggests that another mechanism could be at play since *Cxcr6*$^{gfp/+}$ mice do not have trafficking defects seen in *Cxcr6*$^{-/-}$ mice.

The effect of CXCR6-E3K on the function of the protein could be tested by several *in vitro* methods. The allele could be introduced into a T cell line and tested for its ability to induce migration on a CXCL16 gradient. Surface expression levels of CXCR6-E3K and CXCR6-E3 should be compared for any differences in protein folding, half-life or localization in the cell. Additionally, purified CXCR6-E3K should be tested for binding to CXCL16 by surface plasmon resonance. These studies should give insight into the effects of the E3K variant on the function of CXCR6 as a chemokine receptor and if they show no defect in the variant CXCR6, then other factors may be at play.

While SNP rs2234358-T in *CXCR6* has shown to be predictive of status as a long-term nonprogressor, the mechanism of the effect is not known (Limou et al., 2010). CXCR6 can serve as a coreceptor for the virus, but the efficiency of CXCR6 seems to be lower than CCR5 or CXCR4 and fewer viruses have been shown to utilize CXCR6 (Deng et al., 1997; Liao et al., 1997; Pöhlmann et al., 1999). rs2234358-T likely influences expression of *CXCR6* via one of several other SNPs in the promoter of CXCR6 that are in linkage disequilibrium with rs2234358-T or by altering mRNA stability or processing since rs2234358-T lies in the 3' UTR.

CXCR6 has not been shown to recruit cells to the female reproductive tract, but the possibility has not been excluded. Altered expression of CXCR6 may play a role in homing of either permissive or cytotoxic cells to sites of HIV replication, thus increasing

or decreasing transmission, respectively. Additionally, CXCR6 seems to be important for DC-T cell interaction and changes in expression of the cytokine could affect the duration or quality of the interaction. These changes in expression could be beneficial to control if they lead to greater induction of cytotoxic T cells or prevent DCs from ferrying infectious virus to $CD4^+$ T cells early in infection.

Testing of rs2234358-T should begin with *in vitro* work to determine the effect of the SNP on gene expression and mRNA stability. This should focus on rs2234358-T in conjunction with the promoter SNPs that it is associated with, and also test each SNP individually to determine their relative effect on expression of CXCR6. Given the unique status of long-term non-progressors and the lack of rodent models of HIV infection, testing of the SNP would need to be done in primates. Genetic alteration of primates is still in its infancy, but it is possible this SNP already exists in one or more primate species which would allow for testing of its effect using SIV models. Otherwise, protection studies involving human subjects to test this SNPs effect are difficult since they are limited to *ex vivo* and *in vitro* methods with human cells.

Relative roles of CXCR3 and CXCR6 in airway homing of T cells

Both CXCR3 and CXCR6 have been reported to traffic memory T cells to the lungs following respiratory viral infection (this work and (Slütter et al., 2013)). Chemokine-dependent homing of cells to a tissue requires production of the chemokine in the destination tissues as well as expression of the chemokine receptor on the cells that are destined to home to the tissue. CXCR6 and CXCR3 are co-expressed on memory T cells in the lungs of mice, fulfilling one half of the requirement for both signaling axes. However, while Slutter et al. found that mRNA of CXCR3 ligands *Cxcl9* and *Cxcl10* are expressed within the lung at memory, we find that at the protein level

CXCL9 and CXCL10 are upregulated during inflammation, but they are not detectable in the airways of naïve or memory mice. Slutter et al. proposed that low level inflammation drive *Cxcl9* and *Cxcl10* in the absence of frank immunological insults, but our data in mice contradicts that hypothesis. It is quite possible that humans produce CXCL9 and CXCL10 based on antigen exposures in the environment, but mice in specific pathogen free housing do not. We show that CXCL16, the ligand for CXCR6, is constitutively produced by bronchial epithelial cells the airways of mice and humans, indicating that it is more likely to serve as a homing chemokine in the absence of inflammation.

Direct comparison between the present work and Slutter 2013 is complicated by the different systems used. While we used infection with the actual influenza virus to prime memory, that paper used either *L. monocytogenes* or Vaccinia expressing the influenza peptide NP147-155. The authors noted differences in the quantity and quality of the responses to the two pathogens, which would also presumably differ from the response with the natural pathogen. That work also predates intravenous antibody labeling to distinguish true lung resident cells from those in the circulation. Perfusion of the tissue does not fully remove T cells from the capillary beds of the lungs and greater than 90 % of the cells that remain in the lung following perfusion are within the capillary beds (Anderson et al., 2012). Thus, the differences seen in the airway compartment of CXCR3-defiencent mice may be based on differences in the lung-resident compartment.

Slutter et al. suffers from several drawbacks. The authors do not specify why they chose to look at mRNA levels of *Cxcl9* and *Cxcl10* in the lungs but not confirm this experiment with measurement of protein levels. They also did not divide T cells by the

then known markers CD69 and CD103 in order to eliminate any contaminating non-resident T cells. This would have been a simple method that was used at the time to identify resident cells in the lung. The authors also did not directly examine the role of CXCR3 in recruiting $CD8^+$ T cells to the lungs or airways during acute infection whereas we find that CXCR6 is involved in T cell homing to the airways at acute and memory phases of the immune response. In addition, we show that genetic deletion of *Cxcr6* and blockade or genetic deletion of CXCL16 also shows an effect on the recruitment of cells to the airways following influenza infection. Investigation of *Cxcl9*$^{-/-}$ and *Cxcl10*$^{-/-}$ as well as *Cxcl9*$^{-/-}$*Cxcl10*$^{-/-}$ mice or blockade of CXCR3 signaling would have been beneficial to support the conclusion of Slutter.

We are planning additional studies with i.v. antibody labeling of circulating cells of *Cxcr3*$^{-/-}$ mice following influenza infection to determine if there is a difference in the truly lung resident cells in the absence of CXCR3. If this experiment shows that there is no difference in the lung-resident cells of WT and *Cxcr3*$^{-/-}$ mice yet the BAL of *Cxcr3*$^{-/-}$ mice has decreased antigen-specific cells following influenza infection, then CXCR3 does play a role in the migration of cells from the lung to the airway. However, if there is also a difference in the lung-resident population, then CXCR3 likely plays a role in homing cells to the lung and without sufficient cells in the lung, the BAL population is also affected. This would be an important finding because it establishes the cytokines that regulate the partitioning of memory T cells between the lung and airways.

Neither this work with *Cxcr6*$^{-/-}$ and *Cxcl16*$^{-/-}$ mice nor Slutter et al.'s paper with *Cxcr3*$^{-/-}$ mice showed a complete absence of T cells within the airways. It is possible that both findings are true and we are in the process of crossing *Cxcr3*$^{-/-}$ and *Cxcr6*$^{-/-}$ mice to generate mice lacking both chemokine receptors. These mice can be used to test if there

are additional chemokine receptors involved in recruitment of T cells to the airways of mice. It is also possible that there is some level of stochastic migration to the airways in the absence of chemokine receptor signaling and that the one-way nature of airway migration retains these cells that randomly enter the airways.

Potential for vaccine design

The creation of a universal influenza vaccine remains one of the holy grails of the infectious disease community. The current vaccination strategy is of limited effectiveness and costs 2-4 billion dollars each year (Cohen and Dolin, 2015; Nabel and Fauci, 2010). Given that antibody responses are necessary for preventing infection, the field has concentrated on developing vaccines that generate broadly neutralizing antibodies against viral HA; however, internal T cell epitopes are conserved within influenza genera since T cell responses are directed, in part, against the NP and M proteins that are used to define genera (Nabel and Fauci, 2010). Thus, vaccines designed to induce T cell immunity may give much broader protection than the current regimen that is designed to induce humoral immunity.

The ability of pre-existing T cells to decrease viral shedding has been known since the 1980's, but vaccine design has largely ignored this finding (McMichael et al., 1983). The current trivalent inactivated vaccine continues to focus on antibodies to HA and NA, but contaminating M1 protein in the vaccine can induce a $CD8^+$ T cell response in individuals carrying HLA-A*02, which is found in 35 % of African-Americans and 50 % of Caucasian-Americans (Ellis et al., 2000; Terajima et al., 2008). The $M1_{58\text{-}66}$ peptide is a well-characterized HLA-A*02 restricted antigen that can confer immunity to influenza infection in humans (Gotch et al., 1987). During the 2009 pandemic, numbers of $CD8^+$ T cells specific for $M1_{58\text{-}66}$ and other conserved internal genes correlated with

decreased severity of symptoms (Sridhar et al., 2013). Additionally, T cells may mediate asymptomatic influenza infections in humans and preexisting T cell immunity to conserved epitopes decreased viral shedding (Hayward et al., 2015). This gives real-world evidence that effective immunity to pandemic influenza strains can be mediated by CD8 T cells; however, localization of T cells within the respiratory mucosa is of the utmost importance in mediating protection against influenza infection (Zens et al., 2016).

Knowledge of the molecules that regulate T cell migration allows the design of future vaccines that may induce expression of CXCR6 to direct T cells to the airways where they can provide protection against infection. This could take several forms. Inclusion of CXCR6-inducing cytokines such as TGF-β may instruct T cells to upregulate CXCR6, especially in the context of boosting. Another option may be DNA- or RNA-based vaccines that express T cell epitopes in conjunction with TGF-β or other cytokines. Novel non-protein adjuvants may be designed in order to shape the immune response to direct T cells to the lungs. Additionally, use of microneedles to establish mucosal-homing T cells may work by itself or in conjunction with the above mechanisms for directing antigen-specific cells to the airways.

CXCR6 as a mechanism of "one mucosa"

Eradication of smallpox is one of the greatest public health achievements of all time. The unique method of skin scarification to inoculate the vaccinia virus contributed to the success of this campaign (Liu et al., 2010). This method provided better protective T cell immunity to challenge at a distant site than intraperitoneal vaccination and complete protection against respiratory challenge with a pathogenic vaccinia virus. Other strategies to protect against intranasal vaccinia challenge required

intranasal dosage of the vaccine (Braxton et al., 2010; Clark et al., 2011). This raises a very simple question of how T cells get to the non-skin sites in numbers sufficient to protect against infection (to be addressed below).

Extending knowledge about respiratory viral infections including influenza to vaccinia challenge would suggest that T_{RM} are required for protection against intranasal vaccinia challenge. Following IN vaccination against vaccinia, depletion of $CD8^+$ T cells using intranasal delivery of anti-CD8 decreased protection against intranasal challenge with vaccinia (Gilchuk et al., 2016). However, there is no literature on the presence or phenotype of T_{RM} in the lung following vaccinia skin scarification. A straightforward experiment to test this would be to use the "pull" system shown in Chapter 3, Figure 2C. An intramuscular vaccination (which was shown to be non-protective) could be followed by intranasal dosage of an adjuvant with or without one or more peptide(s) corresponding to immunodominant CD4 and CD8 vaccinia epitopes. Dosing of antigen and adjuvant should establish T_{RM} cells against vaccinia in the lungs of mice and then challenge of these animals in comparison to mice that received skin scarification would provide insight into the role of T_{RM} cells in protection against intranasal vaccinia infection. If, as is likely given the protection results, T_{RM} cells are established in the lungs following skin scarification with vaccinia, then the skin scarification and adjuvant/antigen groups should show similar levels of protection upon challenge.

It may seem strange that vaccination in the skin would establish T_{RM} in other tissues; however, CXCR6 is involved in T cell homing to the skin and lung (Lee et al., 2011; Zaid et al., 2017). Skin scarification that leads to infection of the dermis and epidermis would generate $CXCR6^+$ memory T cells that are able to home to any tissues that express CXCL16. Following infection with vaccinia virus, T_{RM} disseminate

throughout the skin of mice and are not limited to the site of initial infection (Jiang et al., 2012). During the seeding of the skin, which may be CXCR6-dependent, some of the T_{RM} progenitors would inevitably end up in the lung and airways. These cells may then become resident, though the necessity of antigen encounter in the lung would need to be resolved.

No paper has examined this possibility to date, but flow cytometric analysis of BAL fluid and lung homogenate from animals vaccinated via skin scarification would allow for the identification of any cells that may be present in the lungs or airways. It would also be interesting to examine the liver for vaccinia-specific T cells since that organ also relies on CXCR6 for the recruitment and maintenance of T cells. Additionally, the use of *Cxcr6*$^{-/-}$ mice would directly test the hypothesis that CXCR6 is required for the migration of protective T cells to the lungs following skin scarification. Several other experimental questions would need to be addressed if these experiments are fruitful. Are there differences in phenotype, half-life, or localization between lung T_{RM} established by skin scarification vs intranasal infection? Do both types of cells have equivalent cytokine production and cytolytic potential? Can viruses other than vaccinia induce this type of response? Does intranasal vaccination also induce skin- and liver-resident cells?

Complete characterization of the homing of T cells to the lung following skin scarification is necessary because of the potential benefits to vaccine design. As previously discussed, T cell memory against influenza mediates protection against novel pandemic strains, but there are no currently licensed vaccines that are able to induce such a response in the lung. The “pull” method may be effective in humans, but the risk of adverse events when administering an adjuvant to the lungs of humans is too great to

move this method beyond mice. Skin scarification with modified vaccinia viruses (or other viruses) may be a way to induce protective CD8 T cells in the lung. Use of vaccinia may actually be a benefit due to its large genome. The virus could be edited to express antigens from various respiratory viruses including influenza A and B strains, RSV, parainfluenza virus, and even corona and adenoviruses to generate a single vaccine that is protective against many pathogens.

Conclusion

Influenza virus is a serious threat to public health and despite decades of research and progress in our understanding of the pathogen as well as the immune response against it, there is still much to be learned. Mouse adapted influenza strains provide a powerful tool to understand the immune response to influenza as well as respiratory viruses in general. These findings can be tested for applicability to respiratory viruses in general using Sendai virus, a natural mouse pathogen. To test if the findings apply to humans is more complicated, but correlation with observational studies or explanted human lungs can be beneficial. We have shown that IL-36γ is important for alveolar macrophage survival during influenza infection, but whether that applies to humans remains to be seen. Additionally, we show that CXCR6 is important for homing T cells to the airways following respiratory viral infection, and correlate that with data from explanted human lungs. Research into the roles of chemokines and cytokines in the immune response to influenza infection will remain an active area of investigation for the foreseeable future.

References

Abel, S., Hundhausen, C., Mentlein, R., Schulte, A., Berkhout, T.A., Broadway, N., Hartmann, D., Sedlacek, R., Dietrich, S., Muetze, B., et al. (2004). The transmembrane CXC-chemokine ligand 16 is induced by IFN-gamma and TNF-alpha and shed by the activity of the disintegrin-like metalloproteinase ADAM10. J. Immunol. *172*, 6362–6372.

Adamski, V., Mentlein, R., Lucius, R., Synowitz, M., Held-Feindt, J., and Hattermann, K. (2017). The Chemokine Receptor CXCR6 Evokes Reverse Signaling via the Transmembrane Chemokine CXCL16. Int J Mol Sci *18*, 1468.

Agostini, C., Cabrelle, A., Calabrese, F., Bortoli, M., Scquizzato, E., Carraro, S., Miorin, M., Beghè, B., Trentin, L., Zambello, R., et al. (2005). Role for CXCR6 and its ligand CXCL16 in the pathogenesis of T-cell alveolitis in sarcoidosis. Am J Respir Crit Care Med *172*, 1290–1298.

Anderson, K.G., Sung, H., Skon, C.N., Lefrancois, L., Deisinger, A., Vezys, V., and Masopust, D. (2012). Cutting Edge: Intravascular Staining Redefines Lung CD8 T Cell Responses. The Journal of Immunology *189*, 2702–2706.

Aoyagi, T., Newstead, M.W., Zeng, X., Kunkel, S.L., Kaku, M., and Standiford, T.J. (2017a). IL-36 receptor deletion attenuates lung injury and decreases mortality in murine influenza pneumonia. Mucosal Immunology *10*, 1043–1055.

Aoyagi, T., Newstead, M.W., Zeng, X., Nanjo, Y., Peters-Golden, M., Kaku, M., and Standiford, T.J. (2017b). Interleukin-36γ and IL-36 receptor signaling mediate impaired host immunity and lung injury in cytotoxic Pseudomonas aeruginosa pulmonary infection: Role of prostaglandin E2. PLoS Pathog. *13*, e1006737.

Barton, J.L., Herbst, R., Bosisio, D., Higgins, L., and Nicklin, M.J.H. (2000). A tissue specific IL-1 receptor antagonist homolog from the IL-1 cluster lacks IL-1, IL-1ra, IL-18 and IL-18 antagonist activities. Eur. J. Immunol. *30*, 3299–3308.

Beigel, J.H., Farrar, J., Han, A.M., Hayden, F.G., Hyer, R., de Jong, M.D., Lochindarat, S., Nguyen, T.K.T., Nguyen, T.H., Tran, T.H., et al. (2005). Avian influenza A (H5N1) infection in humans. N. Engl. J. Med. *353*, 1374–1385.

Berglöf, E., Andre, R., Renshaw, B.R., Allan, S.M., Lawrence, C.B., Rothwell, N.J., and Pinteaux, E. (2003). IL-1Rrp2 expression and IL-1F9 (IL-1H1) actions in brain cells. Journal of Neuroimmunology *139*, 36–43.

Bertrand, J.Y., Jalil, A., Klaine, M., Jung, S., Cumano, A., and Godin, I. (2005). Three pathways to mature macrophages in the early mouse yolk sac. Blood *106*, 3004–3011.

Beura, L.K., Mitchell, J.S., Thompson, E.A., Schenkel, J.M., Mohammed, J., Wijeyesinghe, S., Fonseca, R., Burbach, B.J., Hickman, H.D., Vezys, V., et al. (2018). Intravital mucosal imaging of CD8+ resident memory T cells shows tissue-autonomous recall responses that amplify secondary memory. Nat Immunol *19*, 173–182.

Blumberg, H., Dinh, H., Dean, C., Trueblood, E.S., Bailey, K., Shows, D., Bhagavathula, N., Aslam, M.N., Varani, J., Towne, J.E., et al. (2010). IL-1RL2 and Its Ligands Contribute to the Cytokine Network in Psoriasis. J. Immunol. *185*, 4354–4362.

Blumberg, H., Dinh, H., Trueblood, E.S., Pretorius, J., Kugler, D., Weng, N., Kanaly, S.T., Towne, J.E., Willis, C.R., Kuechle, M.K., et al. (2007). Opposing activities of two novel members of the IL-1 ligand family regulate skin inflammation. Journal of Experimental Medicine *204*, 2603–2614.

Bochkov, Y.A., Hanson, K.M., Keles, S., Brockman-Schneider, R.A., Jarjour, N.N., and Gern, J.E. (2010). Rhinovirus-induced modulation of gene expression in bronchial epithelial cells from subjects with asthma. Mucosal Immunology *3*, 69–80.

Boisvert, J., Kunkel, E.J., Campbell, J.J., Keeffe, E.B., Butcher, E.C., and Greenberg, H.B. (2003). Liver-infiltrating lymphocytes in end-stage hepatitis C virus: subsets, activation status, and chemokine receptor phenotypes. J. Hepatol. *38*, 67–75.

Bot, A., Bot, S., and Bona, C.A. (1998). Protective role of gamma interferon during the recall response to influenza virus. J. Virol. *72*, 6637–6645.

Bozoyan, L., Dumas, A., Patenaude, A., and Vallières, L. (2015a). Interleukin-36γ is expressed by neutrophils and can activate microglia, but has no role in experimental autoimmune encephalomyelitis. J Neuroinflammation *12*, 393.

Bozoyan, L., Dumas, A., Patenaude, A., and Vallières, L. (2015b). Interleukin-36γ is expressed by neutrophils and can activate microglia, but has no role in experimental autoimmune encephalomyelitis. J Neuroinflammation *12*, 173.

Braciale, T.J., Sun, J., and Kim, T.S. (2012). Regulating the adaptive immune response to respiratory virus infection. Nat. Rev. Immunol. *12*, 295–305.

Braxton, C.L., Puckett, S.H., Mizel, S.B., and Lyles, D.S. (2010). Protection against lethal vaccinia virus challenge by using an attenuated matrix protein mutant vesicular stomatitis virus vaccine vector expressing poxvirus antigens. J. Virol. *84*, 3552–3561.

Brun-Buisson, C., Richard, J.-C.M., Mercat, A., Thiébaut, A.C.M., Brochard, L., REVA-SRLF A/H1N1v 2009 Registry Group (2011). Early corticosteroids in severe influenza A/H1N1 pneumonia and acute respiratory distress syndrome. Am J Respir Crit Care Med *183*, 1200–1206.

Busfield, S.J., Comrack, C.A., Yu, G., Chickering, T.W., Smutko, J.S., Zhou, H., Leiby, K.R., Holmgren, L.M., Gearing, D.P., and Pan, Y. (2000). Identification and gene organization of three novel members of the IL-1 family on human chromosome 2. Genomics *66*, 213–216.

Calabresi, P.A., Yun, S.H., Allie, R., and Whartenby, K.A. (2002). Chemokine receptor expression on MBP-reactive T cells: CXCR6 is a marker of IFNgamma-producing effector cells. Journal of Neuroimmunology *127*, 96–105.

Califano, D., Furuya, Y., and Metzger, D.W. (2018). Effects of Influenza on Alveolar Macrophage Viability Are Dependent on Mouse Genetic Strain. The Journal of Immunology ji1701406.

Camp, J.V., and Jonsson, C.B. (2017). A Role for Neutrophils in Viral Respiratory Disease. Front Immunol *8*, 550.

Campbell, J.J., Haraldsen, G., Pan, J., Rottman, J., Qin, S., Ponath, P., Andrew, D.P., Warnke, R., Ruffing, N., Kassam, N., et al. (1999). The chemokine receptor CCR4 in vascular recognition by cutaneous but not intestinal memory T cells. Nature *400*, 776–780.

Cardani, A., Boulton, A., Kim, T.S., and Braciale, T.J. (2017). Alveolar Macrophages Prevent Lethal Influenza Pneumonia By Inhibiting Infection Of Type-1 Alveolar Epithelial Cells. PLoS Pathog. *13*, e1006140.

Carroll, K.C., Hobden, J.A., Miller, S., Morse, S.A., Mietzner, T.A., Detrick, B., Mitchell, T.G., McKerrow, J.H., and Sakanari, J.A. (2015). Orthomyxoviruses (Influenza Viruses). In Jawetz, Melnick, & Adelberg's Medical Microbiology, 27e, (New York, NY: McGraw-Hill Education).

Chandrasekar, B., Bysani, S., and Mummidi, S. (2004). CXCL16 signals via Gi, phosphatidylinositol 3-kinase, Akt, I kappa B kinase, and nuclear factor-kappa B and induces cell-cell adhesion and aortic smooth muscle cell proliferation. Journal of Biological Chemistry *279*, 3188–3196.

Chen, H., Wang, Y., Bai, C., and Wang, X. (2012). Alterations of plasma inflammatory biomarkers in the healthy and chronic obstructive pulmonary disease patients with or without acute exacerbation. J Proteomics *75*, 2835–2843.

Chen, R., and Holmes, E.C. (2006). Avian influenza virus exhibits rapid evolutionary dynamics. Mol. Biol. Evol. *23*, 2336–2341.

Chen, W., Calvo, P.A., Malide, D., Gibbs, J., Schubert, U., Bacik, I., Basta, S., O'Neill, R., Schickli, J., Palese, P., et al. (2001). A novel influenza A virus mitochondrial protein that induces cell death. Nature Medicine *7*, 1306–1312.

Chen, X., Liu, S., Goraya, M.U., Maarouf, M., Huang, S., and Chen, J.-L. (2018). Host Immune Response to Influenza A Virus Infection. Front Immunol *9*, 320.

Chu, M., Wong, C.K., Cai, Z., Dong, J., Jiao, D., Kam, N.W., Lam, C.W.K., and Tam, L.S. (2015). Elevated Expression and Pro-Inflammatory Activity of IL-36 in Patients with Systemic Lupus Erythematosus. Molecules *20*, 19588–19604.

Clark, K.M., Johnson, J.B., Kock, N.D., Mizel, S.B., and Parks, G.D. (2011). Parainfluenza virus 5-based vaccine vectors expressing vaccinia virus (VACV) antigens provide long-term protection in mice from lethal intranasal VACV challenge. Virology *419*, 97–106.

Cohen, Y.Z., and Dolin, R. (2015). Influenza. In Harrison's Principles of Internal Medicine, 19e, D. Kasper, A. Fauci, S. Hauser, D. Longo, J.L. Jameson, and J. Loscalzo, eds. (New York, NY: McGraw-Hill Education).

Coulombe, F., Jaworska, J., Verway, M., Tzelepis, F., Massoud, A., Gillard, J., Wong, G., Kobinger, G., Xing, Z., Couture, C., et al. (2014). Targeted prostaglandin E2 inhibition enhances antiviral immunity through induction of type I interferon and apoptosis in macrophages. Immunity *40*, 554–568.

Darash-Yahana, M., Gillespie, J.W., Hewitt, S.M., Chen, Y.-Y.K., Maeda, S., Stein, I., Singh, S.P., Bedolla, R.B., Peled, A., Troyer, D.A., et al. (2009). The chemokine CXCL16 and its receptor, CXCR6, as markers and promoters of inflammation-associated cancers. PLoS ONE *4*, e6695.

Day, C.E., Zhang, S.D., Riley, J., Gant, T., Wardlaw, A.J., and Guillen, C. (2009a). A novel method for isolation of human lung T cells from lung resection tissue reveals increased expression of GAPDH and CXCR6. J. Immunol. Methods *342*, 91–97.

Day, C., Patel, R., Guillen, C., and Wardlaw, A.J. (2009b). The chemokine CXCL16 is highly and constitutively expressed by human bronchial epithelial cells. Exp. Lung Res. *35*, 272–283.

Debets, R., Timans, J.C., Homey, B., Zurawski, S., Sana, T.R., Lo, S., Wagner, J., Edwards, G., Clifford, T., Menon, S., et al. (2001). Two novel IL-1 family members, IL-1 delta and IL-1 epsilon, function as an antagonist and agonist of NF-kappa B activation through the orphan IL-1 receptor-related protein 2. J. Immunol. *167*, 1440–1446.

Deng, H.K., Unutmaz, D., KewalRamani, V.N., and Littman, D.R. (1997). Expression cloning of new receptors used by simian and human immunodeficiency viruses. Nature *388*, 296–300.

Derer, A., Groetsch, B., Harre, U., Böhm, C., Towne, J., Schett, G., Frey, S., and Hueber, A.J. (2014). Blockade of IL-36 receptor signaling does not prevent from TNF-induced arthritis. PLoS ONE *9*, e101954.

Dienz, O., Rud, J.G., Eaton, S.M., Lanthier, P.A., Burg, E., Drew, A., Bunn, J., Suratt, B.T., Haynes, L., and Rincon, M. (2012). Essential role of IL-6 in protection against H1N1 influenza virus by promoting neutrophil survival in the lung. Mucosal Immunology *5*, 258–266.

DiPiazza, A., Nogales, A., Poulton, N., Wilson, P.C., Martinez-Sobrido, L., and Sant, A.J. (2017). Pandemic 2009 H1N1 Influenza Venus reporter virus reveals broad diversity of MHC class II-positive antigen-bearing cells following infection in vivo. Sci. Rep. *7*, 10857.

Dolin, R. (2012). Chapter 187. Influenza. In Harrison's Principles of Internal Medicine, D.L. Longo, A.S. Fauci, D.L. Kasper, S.L. Hauser, J. Jameson, and J. Loscalzo, eds. (New York: McGraw-Hill).

Duggal, P., An, P., Beaty, T.H., Strathdee, S.A., Farzadegan, H., Markham, R.B., Johnson, L., O'Brien, S.J., Vlahov, D., and Winkler, C.A. (2003). Genetic influence of CXCR6 chemokine receptor alleles on PCP-mediated AIDS progression among African Americans. Genes Immun. *4*, 245–250.

Ellingford, J.M., Black, G.C.M., Clayton, T.H., Judge, M., Griffiths, C.E.M., and Warren, R.B. (2015). A novel mutation in IL36RN underpins childhood pustular dermatosis. J Eur Acad Dermatol Venereol *30*, 302–305.

Ellis, J.M., Henson, V., Slack, R., Ng, J., Hartzman, R.J., and Katovich Hurley, C. (2000). Frequencies of HLA-A2 alleles in five U.S. population groups. Predominance Of A*02011 and identification of HLA-A*0231. Hum. Immunol. *61*, 334–340.

Ely, K.H., Cookenham, T., Roberts, A.D., and Woodland, D.L. (2006). Memory T cell populations in the lung airways are maintained by continual recruitment. J. Immunol. *176*, 537–543.

Ettensohn, D.B., Frampton, M.W., Nichols, J.E., and Roberts, N.J. (2016). Human Alveolar Macrophages May Not Be Susceptible to Direct Infection by a Human Influenza Virus. J. Infect. Dis. *214*, 1658–1665.

Farooq, M., Nakai, H., Fujimoto, A., Fujikawa, H., Matsuyama, A., Kariya, N., Aizawa, A., Fujiwara, H., Ito, M., and Shimomura, Y. (2013). Mutation analysis of the IL36RN gene in 14 Japanese patients with generalized pustular psoriasis. Hum. Mutat. *34*, 176–183.

Fernandez-Ruiz, D., Ng, W.Y., Holz, L.E., Ma, J.Z., Zaid, A., Wong, Y.C., Lau, L.S., Mollard, V., Cozijnsen, A., Collins, N., et al. (2016). Liver-Resident Memory CD8+ T Cells Form a Front-Line Defense against Malaria Liver-Stage Infection. Immunity *45*, 889–902.

Foster, A.M., Baliwag, J., Chen, C.S., Guzman, A.M., Stoll, S.W., Gudjonsson, J.E., Ward, N.L., and Johnston, A. (2014). IL-36 Promotes Myeloid Cell Infiltration, Activation, and Inflammatory Activity in Skin. The Journal of Immunology *192*, 6053–6061.

Franzke, C.W., Cobzaru, C., Triantafyllopoulou, A., Loffek, S., Horiuchi, K., Threadgill, D.W., Kurz, T., Van Rooijen, N., Bruckner-Tuderman, L., and Blobel, C.P. (2012). Epidermal ADAM17 maintains the skin barrier by regulating EGFR ligand-dependent terminal keratinocyte differentiation. J. Exp. Med. *209*, 1105–1119.

Freeman, C.M., Curtis, J.L., and Chensue, S.W. (2007). CC chemokine receptor 5 and CXC chemokine receptor 6 expression by lung CD8+ cells correlates with chronic obstructive pulmonary disease severity. Ajpa *171*, 767–776.

Frey, S., Derer, A., Messbacher, M.-E., Baeten, D.L.P., Bugatti, S., Montecucco, C., Schett, G., and Hueber, A.J. (2013). The novel cytokine interleukin-36α is expressed in psoriatic and rheumatoid arthritis synovium. Ann. Rheum. Dis. *72*, 1569–1574.

Friedrich, M., Tillack, C., Wollenberg, A., Schauber, J., and Brand, S. (2014). IL-36γ sustains a proinflammatory self-amplifying loop with IL-17C in anti-TNF-induced psoriasiform skin lesions of patients with Crohn's disease. Inflammatory Bowel Diseases *20*, 1891–1901.

Gabay, C., and Towne, J.E. (2015). Regulation and function of interleukin-36 cytokines in homeostasis and pathological conditions. Journal of Leukocyte Biology 1–8.

Galkina, E., Thatte, J., Dabak, V., Williams, M.B., Ley, K., and Braciale, T.J. (2005). Preferential migration of effector CD8+ T cells into the interstitium of the normal lung. J. Clin. Invest. *115*, 3473–3483.

Gao, W., Kumar, S., Lotze, M.T., Hanning, C., Robbins, P.D., and Gambotto, A. (2003). Innate immunity mediated by the cytokine IL-1 homologue 4 (IL-1H4/IL-1F7) induces IL-12-dependent adaptive and profound antitumor immunity. J. Immunol. *170*, 107–113.

García-Sastre, A., Egorov, A., Matassov, D., Brandt, S., Levy, D.E., Durbin, J.E., Palese, P., and Muster, T. (1998). Influenza A virus lacking the NS1 gene replicates in interferon-deficient systems. Virology *252*, 324–330.

Geissmann, F., Cameron, T.O., Sidobre, S., Manlongat, N., Kronenberg, M., Briskin, M.J., Dustin, M.L., and Littman, D.R. (2005). Intravascular immune surveillance by CXCR6+ NKT cells patrolling liver sinusoids. PLoS Biol. *3*, e113.

Germanov, E., Veinotte, L., Cullen, R., Chamberlain, E., Butcher, E.C., and Johnston, B. (2008). Critical role for the chemokine receptor CXCR6 in homeostasis and activation of CD1d-restricted NKT cells. J. Immunol. *181*, 81–91.

Ghoneim, H.E., Thomas, P.G., and McCullers, J.A. (2013). Depletion of alveolar macrophages during influenza infection facilitates bacterial superinfections. The Journal of Immunology *191*, 1250–1259.

Gilchuk, P., Hill, T.M., Guy, C., McMaster, S.R., Boyd, K.L., Rabacal, W.A., Lu, P., Shyr, Y., Kohlmeier, J.E., Sebzda, E., et al. (2016). A Distinct Lung-Interstitium-Resident Memory CD8(+) T Cell Subset Confers Enhanced Protection to Lower Respiratory Tract Infection. CellReports *16*, 1800–1809.

Gotch, F., Rothbard, J., Howland, K., Townsend, A., and McMichael, A. (1987). Cytotoxic T lymphocytes recognize a fragment of influenza virus matrix protein in association with HLA-A2. Nature *326*, 881–882.

Gresnigt, M.S., Rösler, B., Jacobs, C.W.M., Becker, K.L., Joosten, L.A.B., van der Meer, J.W.M., Netea, M.G., Dinarello, C.A., and van de Veerdonk, F.L. (2013). The IL-36 receptor pathway regulates Aspergillus fumigatus-induced Th1 and Th17 responses. Eur. J. Immunol. *43*, 416–426.

Griffith, J.W., Sokol, C.L., and Luster, A.D. (2014). Chemokines and Chemokine

Receptors: Positioning Cells for Host Defense and Immunity. Annu. Rev. Immunol. *32*, 659–702.

Guilliams, M., De Kleer, I., Henri, S., Post, S., Vanhoutte, L., De Prijck, S., Deswarte, K., Malissen, B., Hammad, H., and Lambrecht, B.N. (2013). Alveolar macrophages develop from fetal monocytes that differentiate into long-lived cells in the first week of life via GM-CSF. Journal of Experimental Medicine *210*, 1977–1992.

Gunther, S., and Sundberg, E.J. (2014). Molecular Determinants of Agonist and Antagonist Signaling through the IL-36 Receptor. The Journal of Immunology *193*, 921–930.

Guo, P., Hirano, M., Herrin, B.R., Li, J., Yu, C., Sadlonova, A., and Cooper, M.D. (2009). Dual nature of the adaptive immune system in lampreys. Nature *459*, 796–801.

Guo, X.-Z.J., and Thomas, P.G. (2017). New fronts emerge in the influenza cytokine storm. Semin Immunopathol *39*, 541–550.

Gursel, M., Gursel, I., Mostowski, H.S., and Klinman, D.M. (2006). CXCL16 influences the nature and specificity of CpG-induced immune activation. J. Immunol. *177*, 1575–1580.

Harusato, A., Abo, H., Ngo, V.L., Yi, S.W., Mitsutake, K., Osuka, S., Kohlmeier, J.E., Li, J.D., Gewirtz, A.T., Nusrat, A., et al. (2017). IL-36γ signaling controls the induced regulatory T cell-Th9 cell balance via NFκB activation and STAT transcription factors. Mucosal Immunology *10*, 1455–1467.

Hashimoto, D., Chow, A., Noizat, C., Teo, P., Beasley, M.B., Leboeuf, M., Becker, C.D., See, P., Price, J., Lucas, D., et al. (2013). Tissue-resident macrophages self-maintain locally throughout adult life with minimal contribution from circulating monocytes. Immunity *38*, 792–804.

Hashimoto, Y., Moki, T., Takizawa, T., Shiratsuchi, A., and Nakanishi, Y. (2007). Evidence for phagocytosis of influenza virus-infected, apoptotic cells by neutrophils and macrophages in mice. J. Immunol. *178*, 2448–2457.

Hayden, F.G., Fritz, R., Lobo, M.C., Alvord, W., Strober, W., and Straus, S.E. (1998). Local and systemic cytokine responses during experimental human influenza A virus infection. Relation to symptom formation and host defense. J. Clin. Invest. *101*, 643–649.

Haynes, B.F., Soderberg, K.A., and Fauci, A.S. (2015). Introduction to the Immune System. In Harrison's Principles of Internal Medicine, 19e, D. Kasper, A. Fauci, S. Hauser, D. Longo, J.L. Jameson, and J. Loscalzo, eds. (New York, NY: McGraw-Hill Education).

Hayward, A.C., Wang, L., Goonetilleke, N., Fragaszy, E.B., Bermingham, A., Copas, A., Dukes, O., Millett, E.R.C., Nazareth, I., Nguyen-Van-Tam, J.S., et al. (2015). Natural T

Cell Mediated Protection Against Seasonal and Pandemic Influenza: Results of the Flu Watch Cohort Study. Am J Respir Crit Care Med 150406071958005–150406071958053.

He, Q., Chen, H.-X., Li, W., Wu, Y., Chen, S.-J., Yue, Q., Xiao, M., and Li, J.-W. (2013). IL-36 cytokine expression and its relationship with p38 MAPK and NF-κB pathways in psoriasis vulgaris skin lesions. J. Huazhong Univ. Sci. Technol. Med. Sci. *33*, 594–599.

He, W., Chen, C.-J., Mullarkey, C.E., Hamilton, J.R., Wong, C.K., Leon, P.E., Uccellini, M.B., Chromikova, V., Henry, C., Hoffman, K.W., et al. (2017). Alveolar macrophages are critical for broadly-reactive antibody-mediated protection against influenza A virus in mice. Nat Commun *8*, 846.

Heesch, K., Raczkowski, F., Schumacher, V., Hünemörder, S., Panzer, U., and Mittrücker, H.-W. (2014). The function of the chemokine receptor CXCR6 in the T cell response of mice against Listeria monocytogenes. PLoS ONE *9*, e97701.

Helft, J., Manicassamy, B., Guermonprez, P., Hashimoto, D., Silvin, A., Agudo, J., Brown, B.D., Schmolke, M., Miller, J.C., Leboeuf, M., et al. (2012). Cross-presenting CD103+ dendritic cells are protected from influenza virus infection. J. Clin. Invest. *122*, 4037–4047.

Henry, C.M., Sullivan, G.P., Clancy, D.M., Afonina, I.S., Kulms, D., and Martin, S.J. (2016). Neutrophil-Derived Proteases Escalate Inflammation through Activation of IL-36 Family Cytokines. CellReports *14*, 1–16.

Heydtmann, M., Lalor, P.F., Eksteen, J.A., Hübscher, S.G., Briskin, M., and Adams, D.H. (2005). CXC chemokine ligand 16 promotes integrin-mediated adhesion of liver-infiltrating lymphocytes to cholangiocytes and hepatocytes within the inflamed human liver. J. Immunol. *174*, 1055–1062.

Higgins, J., Mutamba, S., Mahida, Y., Barrow, P., and Foster, N. (2015). IL-36Î± induces maturation of Th1-inducing human MDDC and synergises with IFN-Î³ to induce high surface expression of CD14 and CD11c. Hum. Immunol. *76*, 1–9.

Hogan, R.J., Usherwood, E.J., Zhong, W., Roberts, A.A., Dutton, R.W., Harmsen, A.G., and Woodland, D.L. (2001). Activated antigen-specific CD8+ T cells persist in the lungs following recovery from respiratory virus infections. J. Immunol. *166*, 1813–1822.

Hojo, S., Koizumi, K., Tsuneyama, K., Arita, Y., Cui, Z., Shinohara, K., Minami, T., Hashimoto, I., Nakayama, T., Sakurai, H., et al. (2007). High-level expression of chemokine CXCL16 by tumor cells correlates with a good prognosis and increased tumor-infiltrating lymphocytes in colorectal cancer. Cancer Research *67*, 4725–4731.

Hombrink, P., Helbig, C., Backer, R.A., Piet, B., Oja, A.E., Stark, R., Brasser, G., Jongejan, A., Jonkers, R.E., Nota, B., et al. (2016). Programs for the persistence, vigilance and control of human CD8+ lung-resident memory T cells. Nat Immunol *17*, 1467–1478.

Hsu, A.C.-Y. (2018). Influenza Virus: A Master Tactician in Innate Immune Evasion and Novel Therapeutic Interventions. Front Immunol *9*, 743.

Huang, F.-F., Barnes, P.F., Feng, Y., Donis, R., Chroneos, Z.C., Idell, S., Allen, T., Perez, D.R., Whitsett, J.A., Dunussi-Joannopoulos, K., et al. (2011). GM-CSF in the lung protects against lethal influenza infection. Am J Respir Crit Care Med *184*, 259–268.

Huang, H., Li, H., Zhou, P., and Ju, D. (2010). Protective effects of recombinant human granulocyte macrophage colony stimulating factor on H1N1 influenza virus-induced pneumonia in mice. Cytokine *51*, 151–157.

Hudspeth, K., Donadon, M., Cimino, M., Pontarini, E., Tentorio, P., Preti, M., Hong, M., Bertoletti, A., Bicciato, S., Invernizzi, P., et al. (2016). Human liver-resident CD56(bright)/CD16(neg) NK cells are retained within hepatic sinusoids via the engagement of CCR5 and CXCR6 pathways. J. Autoimmun. *66*, 40–50.

Hui, D.S.C., Lee, N., and Chan, P.K.S. (2017). A clinical approach to the threat of emerging influenza viruses in the Asia-Pacific region. Respirology *22*, 1300–1312.

Hussell, T., Pennycook, A., and Openshaw, P.J. (2001). Inhibition of tumor necrosis factor reduces the severity of virus-specific lung immunopathology. Eur. J. Immunol. *31*, 2566–2573.

Hydes, T., Noll, A., Salinas-Riester, G., Abuhilal, M., Armstrong, T., Hamady, Z., Primrose, J., Takhar, A., Walter, L., and Khakoo, S.I. (2018). IL-12 and IL-15 induce the expression of CXCR6 and CD49a on peripheral natural killer cells. Immun Inflamm Dis *6*, 34–46.

Ichii, O., Otsuka, S., Sasaki, N., Yabuki, A., Ohta, H., Takiguchi, M., Hashimoto, Y., Endoh, D., and Kon, Y. (2010). Local overexpression of interleukin-1 family, member 6 relates to the development of tubulointerstitial lesions. Lab. Invest. *90*, 459–475.

Ichinohe, T. (2010). Respective roles of TLR, RIG-I and NLRP3 in influenza virus infection and immunity: impact on vaccine design. Expert Rev Vaccines *9*, 1315–1324.

Iuliano, A.D., Roguski, K.M., Chang, H.H., Muscatello, D.J., Palekar, R., Tempia, S., Cohen, C., Gran, J.M., Schanzer, D., Cowling, B.J., et al. (2018). Estimates of global seasonal influenza-associated respiratory mortality: a modelling study. Lancet *391*, 1285–1300.

Iwasaki, A., and Pillai, P.S. (2014). Innate immunity to influenza virus infection. Nat. Rev. Immunol. *14*, 315–328.

Janssen, W.J., Barthel, L., Muldrow, A., Oberley-Deegan, R.E., Kearns, M.T., Jakubzick, C., and Henson, P.M. (2011). Fas determines differential fates of resident and recruited macrophages during resolution of acute lung injury. Am J Respir Crit Care Med *184*, 547–560.

Jiang, X., Clark, R.A., Liu, L., Wagers, A.J., Fuhlbrigge, R.C., and Kupper, T.S. (2012). Skin infection generates non-migratory memory CD8+ T(RM) cells providing global skin immunity. Nature *483*, 227–231.

Jiang, X., Sun, W., Zhu, L., Guo, D., Jiang, H., Ma, D., Jin, J., Zhao, Y., and Liang, J. (2010). Expression of CXCR6 on CD8(+) T cells was up-regulated in allograft rejection. Transpl. Immunol. *22*, 179–183.

Johnston, A., Xing, X., Guzman, A.M., Riblett, M., Loyd, C.M., Ward, N.L., Wohn, C., Prens, E.P., Wang, F., Maier, L.E., et al. (2011). IL-1F5, -F6, -F8, and -F9: a novel IL-1 family signaling system that is active in psoriasis and promotes keratinocyte antimicrobial peptide expression. The Journal of Immunology *186*, 2613–2622.

Jozwik, A., Habibi, M.S., Paras, A., Zhu, J., Guvenel, A., Dhariwal, J., Almond, M., Wong, E.H.C., Sykes, A., Maybeno, M., et al. (2015). RSV-specific airway resident memory CD8+ T cells and differential disease severity after experimental human infection. Nat Commun *6*, 10224.

Kim, C.H., Kunkel, E.J., Boisvert, J., Johnston, B., Campbell, J.J., Genovese, M.C., Greenberg, H.B., and Butcher, E.C. (2001). Bonzo/CXCR6 expression defines type 1-polarized T-cell subsets with extralymphoid tissue homing potential. J. Clin. Invest. *107*, 595–601.

Kim, C.H., Johnston, B., and Butcher, E.C. (2002). Trafficking machinery of NKT cells: shared and differential chemokine receptor expression among V alpha 24(+)V beta 11(+) NKT cell subsets with distinct cytokine-producing capacity. Blood *100*, 11–16.

Kim, H.M., Kang, Y.M., Ku, K.B., Park, E.H., Yum, J., Kim, J.C., Jin, S.Y., Lee, J.S., Kim, H.S., and Seo, S.H. (2013). The severe pathogenicity of alveolar macrophage-depleted ferrets infected with 2009 pandemic H1N1 influenza virus. Virology *444*, 394–403.

Kim, H.M., Lee, Y.-W., Lee, K.-J., Kim, H.S., Cho, S.W., van Rooijen, N., Guan, Y., and Seo, S.H. (2008). Alveolar macrophages are indispensable for controlling influenza viruses in lungs of pigs. J. Virol. *82*, 4265–4274.

Koenen, A., Babendreyer, A., Schumacher, J., Pasqualon, T., Schwarz, N., Seifert, A., Deupi, X., Ludwig, A., and Dreymueller, D. (2017). The DRF motif of CXCR6 as chemokine receptor adaptation to adhesion. PLoS ONE *12*, e0173486.

Kohlmeier, J.E., Cookenham, T., Miller, S.C., Roberts, A.D., Christensen, J.P., Thomsen, A.R., and Woodland, D.L. (2009). CXCR3 directs antigen-specific effector CD4+ T cell migration to the lung during parainfluenza virus infection. The Journal of Immunology *183*, 4378–4384.

Kohlmeier, J.E., Miller, S.C., and Woodland, D.L. (2007). Cutting edge: Antigen is not required for the activation and maintenance of virus-specific memory CD8+ T cells in the lung airways. J. Immunol. *178*, 4721–4725.

Kohlmeier, J.E., Miller, S.C., Smith, J., Lu, B., Gerard, C., Cookenham, T., Roberts, A.D., and Woodland, D.L. (2008). The chemokine receptor CCR5 plays a key role in the early memory CD8+ T cell response to respiratory virus infections. Immunity *29*, 101–113.

Koprak, S., Matheravidathu, S., Springer, M., Gould, S., and Dumont, F.J. (2003). Down-regulation of cell surface CXCR6 expression during T cell activation is predominantly mediated by calcineurin. Cell. Immunol. *223*, 1–12.

Kovach, M.A., Singer, B., Martinez-Colon, G., Newstead, M.W., Zeng, X., Mancuso, P., Moore, T.A., Kunkel, S.L., Peters-Golden, M., Moore, B.B., et al. (2017). IL-36γ is a crucial proximal component of protective type-1-mediated lung mucosal immunity in Gram-positive and -negative bacterial pneumonia. Mucosal Immunology *119*, 1899.

Kumar, B.V., Ma, W., Miron, M., Granot, T., Guyer, R.S., Carpenter, D.J., Senda, T., Sun, X., Ho, S.-H., Lerner, H., et al. (2017). Human Tissue-Resident Memory T Cells Are Defined by Core Transcriptional and Functional Signatures in Lymphoid and Mucosal Sites. CellReports *20*, 2921–2934.

Kumar, S., McDonnell, P.C., Lehr, R., Tierney, L., Tzimas, M.N., Griswold, D.E., Capper, E.A., Tal-Singer, R., Wells, G.I., Doyle, M.L., et al. (2000). Identification and initial characterization of four novel members of the interleukin-1 family. Journal of Biological Chemistry *275*, 10308–10314.

Lamacchia, C., Palmer, G., Rodriguez, E., Martin, P., Vigne, S., Seemayer, C.A., Talabot-Ayer, D., Towne, J.E., and Gabay, C. (2013). ar4192. Arthritis Research & Therapy *15*, R38.

Landrø, L., Damås, J.K., Halvorsen, B., Fevang, B., Ueland, T., Otterdal, K., Heggelund, L., Frøland, S.S., and Aukrust, P. (2009). CXCL16 in HIV infection - a link between inflammation and viral replication. Eur. J. Clin. Invest. *39*, 1017–1024.

Latta, M., Mohan, K., and Issekutz, T.B. (2007). CXCR6 is expressed on T cells in both T helper type 1 (Th1) inflammation and allergen-induced Th2 lung inflammation but is only a weak mediator of chemotaxis. Immunology *121*, 555–564.

Lee, L.N., Ronan, E.O., de Lara, C., Franken, K.L.M.C., Ottenhoff, T.H.M., Tchilian, E.Z., and Beverley, P.C.L. (2011). CXCR6 is a marker for protective antigen-specific cells in the lungs after intranasal immunization against Mycobacterium tuberculosis. Infection and Immunity *79*, 3328–3337.

Lehrke, M., Millington, S.C., Lefterova, M., Cumaranatunge, R.G., Szapary, P., Wilensky, R., Rader, D.J., Lazar, M.A., and Reilly, M.P. (2007). CXCL16 is a marker of inflammation, atherosclerosis, and acute coronary syndromes in humans. J. Am. Coll. Cardiol. *49*, 442–449.

Li, S., Zhu, G., Yang, Y., Jian, Z., Guo, S., Dai, W., Shi, Q., Ge, R., Ma, J., Liu, L., et al. (2017). Oxidative stress drives CD8+ T-cell skin trafficking in patients with vitiligo through CXCL16 upregulation by activating the unfolded protein response in

keratinocytes. J. Allergy Clin. Immunol. *140*, 177–189.e179.

Liang, S., Mozdzanowska, K., Palladino, G., and Gerhard, W. (1994). Heterosubtypic immunity to influenza type A virus in mice. Effector mechanisms and their longevity. J. Immunol. *152*, 1653–1661.

Liao, F., Alkhatib, G., Peden, K.W., Sharma, G., Berger, E.A., and Farber, J.M. (1997). STRL33, A novel chemokine receptor-like protein, functions as a fusion cofactor for both macrophage-tropic and T cell line-tropic HIV-1. J. Exp. Med. *185*, 2015–2023.

Lim, K., Hyun, Y.-M., Lambert-Emo, K., Capece, T., Bae, S., Miller, R., Topham, D.J., and Kim, M. (2015). Neutrophil trails guide influenza-specific $CD8^+$ T cells in the airways. Science *349*, aaa4352–aaa4352.

Limou, S., Coulonges, C., Herbeck, J.T., van Manen, D., An, P., Le Clerc, S., Delaneau, O., Diop, G., Taing, L., Montes, M., et al. (2010). Multiple-cohort genetic association study reveals CXCR6 as a new chemokine receptor involved in long-term nonprogression to AIDS. J. Infect. Dis. *202*, 908–915.

Lin, K.L., Suzuki, Y., Nakano, H., Ramsburg, E., and Gunn, M.D. (2008). CCR2+ monocyte-derived dendritic cells and exudate macrophages produce influenza-induced pulmonary immune pathology and mortality. J. Immunol. *180*, 2562–2572.

Linke, B., Meyer Dos Santos, S., Picard-Willems, B., Keese, M., Harder, S., Geisslinger, G., and Scholich, K. (2017). CXCL16/CXCR6-mediated adhesion of human peripheral blood mononuclear cells to inflamed endothelium. Cytokine.

Liu, L., Zhong, Q., Tian, T., Dubin, K., Athale, S.K., and Kupper, T.S. (2010). Epidermal injury and infection during poxvirus immunization is crucial for the generation of highly protective T cell-mediated immunity. Nature Medicine *16*, 224–227.

Loetscher, M., Amara, A., Oberlin, E., Brass, N., Legler, D., Loetscher, P., D'Apuzzo, M., Meese, E., Rousset, D., Virelizier, J.L., et al. (1997). TYMSTR, a putative chemokine receptor selectively expressed in activated T cells, exhibits HIV-1 coreceptor function. Curr. Biol. *7*, 652–660.

Loo, Y.-M., Fornek, J., Crochet, N., Bajwa, G., Perwitasari, O., Martinez-Sobrido, L., Akira, S., Gill, M.A., García-Sastre, A., Katze, M.G., et al. (2008). Distinct RIG-I and MDA5 signaling by RNA viruses in innate immunity. J. Virol. *82*, 335–345.

Lugthart, G., Melsen, J.E., Vervat, C., van Ostaijen-Ten Dam, M.M., Corver, W.E., Roelen, D.L., van Bergen, J., van Tol, M.J.D., Lankester, A.C., and Schilham, M.W. (2016). Human Lymphoid Tissues Harbor a Distinct CD69+CXCR6+ NK Cell Population. The Journal of Immunology *197*, 78–84.

Lundberg, G.A., Kellin, A., Samnegård, A., Lundman, P., Tornvall, P., Dimmeler, S., Zeiher, A.M., Hamsten, A., Hansson, G.K., and Eriksson, P. (2005). Severity of coronary artery stenosis is associated with a polymorphism in the CXCL16/SR-PSOX gene. J.

Intern. Med. *257*, 415–422.

Mackay, L.K., Minnich, M., Kragten, N.A.M., Liao, Y., Nota, B., Seillet, C., Zaid, A., Man, K., Preston, S., Freestone, D., et al. (2016). Hobit and Blimp1 instruct a universal transcriptional program of tissue residency in lymphocytes. Science *352*, 459–463.

Mackay, L.K., Rahimpour, A., Ma, J.Z., Collins, N., Stock, A.T., Hafon, M.-L., Vega-Ramos, J., Lauzurica, P., Mueller, S.N., Stefanovic, T., et al. (2013). The developmental pathway for CD103(+)CD8+ tissue-resident memory T cells of skin. Nat Immunol *14*, 1294–1301.

Magne, D., Palmer, G., Barton, J.L., Mézin, F., Talabot-Ayer, D., Bas, S., Duffy, T., Noger, M., Guerne, P.-A., Nicklin, M.J.H., et al. (2006). The new IL-1 family member IL-1F8 stimulates production of inflammatory mediators by synovial fibroblasts and articular chondrocytes. Arthritis Research & Therapy *8*, R80.

Marrakchi, S., Guigue, P., Renshaw, B.R., Puel, A., Pei, X.-Y., Fraitag, S., Zribi, J., Bal, E., Cluzeau, C., Chrabieh, M., et al. (2011). Interleukin-36-receptor antagonist deficiency and generalized pustular psoriasis. N. Engl. J. Med. *365*, 620–628.

Martin, U., Scholler, J., Gurgel, J., Renshaw, B., Sims, J.E., and Gabel, C.A. (2009). Externalization of the leaderless cytokine IL-1F6 occurs in response to lipopolysaccharide/ATP activation of transduced bone marrow macrophages. The Journal of Immunology *183*, 4021–4030.

Matloubian, M., David, A., Engel, S., Ryan, J.E., and Cyster, J.G. (2000). A transmembrane CXC chemokine is a ligand for HIV-coreceptor Bonzo. Nat Immunol *1*, 298–304.

McAuley, J.L., Hornung, F., Boyd, K.L., Smith, A.M., McKeon, R., Bennink, J., Yewdell, J.W., and McCullers, J.A. (2007). Expression of the 1918 influenza A virus PB1-F2 enhances the pathogenesis of viral and secondary bacterial pneumonia. Cell Host Microbe *2*, 240–249.

McMaster, S.R., Wein, A.N., Dunbar, P.R., Hayward, S.L., Cartwright, E.K., Denning, T.L., and Kohlmeier, J.E. (2018). Pulmonary antigen encounter regulates the establishment of tissue-resident CD8 memory T cells in the lung airways and parenchyma. Mucosal Immunology *31*, 137.

McMaster, S.R., Wilson, J.J., Wang, H., and Kohlmeier, J.E. (2015). Airway-Resident Memory CD8 T Cells Provide Antigen-Specific Protection against Respiratory Virus Challenge through Rapid IFN-γ Production. The Journal of Immunology *195*, 203–209.

McMichael, A.J., Gotch, F.M., Noble, G.R., and Beare, P.A. (1983). Cytotoxic T-cell immunity to influenza. N. Engl. J. Med. *309*, 13–17.

McNamee, L.A., and Harmsen, A.G. (2006). Both influenza-induced neutrophil dysfunction and neutrophil-independent mechanisms contribute to increased

susceptibility to a secondary Streptococcus pneumoniae infection. Infection and Immunity *74*, 6707–6721.

Medina-Contreras, O., Harusato, A., Nishio, H., Flannigan, K.L., Ngo, V., Leoni, G., Neumann, P.-A., Geem, D., Lili, L.N., Ramadas, R.A., et al. (2015). Cutting Edge: IL-36 Receptor Promotes Resolution of Intestinal Damage. The Journal of Immunology *196*, 1501312–1501338.

Medoff, B.D., Wain, J.C., Seung, E., Jackobek, R., Means, T.K., Ginns, L.C., Farber, J.M., and Luster, A.D. (2006). CXCR3 and its ligands in a murine model of obliterative bronchiolitis: regulation and function. J. Immunol. *176*, 7087–7095.

Milora, K.A., Fu, H., Dubaz, O., and Jensen, L.E. (2015). Unprocessed Interleukin-36α Regulates Psoriasis-Like Skin Inflammation in Cooperation With Interleukin-1. Journal of Investigative Dermatology *135*, 2992–3000.

Minami, M., Kume, N., Shimaoka, T., Kataoka, H., Hayashida, K., Akiyama, Y., Nagata, I., Ando, K., Nobuyoshi, M., Hanyuu, M., et al. (2001). Expression of SR-PSOX, a novel cell-surface scavenger receptor for phosphatidylserine and oxidized LDL in human atherosclerotic lesions. Arterioscler. Thromb. Vasc. Biol. *21*, 1796–1800.

Mora, J.R., Bono, M.R., Manjunath, N., Weninger, W., Cavanagh, L.L., Rosemblatt, M., and Andrian, Von, U.H. (2003). Selective imprinting of gut-homing T cells by Peyer's patch dendritic cells. Nature *424*, 88–93.

Morgan, A.J., Guillen, C., Symon, F.A., Huynh, T.T., Berry, M.A., Entwisle, J.J., Briskin, M., Pavord, I.D., and Wardlaw, A.J. (2005). Expression of CXCR6 and its ligand CXCL16 in the lung in health and disease. Clin. Exp. Allergy *35*, 1572–1580.

Morgan, A.J., Guillen, C., Symon, F.A., Birring, S.S., Campbell, J.J., and Wardlaw, A.J. (2008). CXCR6 identifies a putative population of retained human lung T cells characterised by co-expression of activation markers. Immunobiology *213*, 599–608.

Nabel, G.J., and Fauci, A.S. (2010). Induction of unnatural immunity: prospects for a broadly protective universal influenza vaccine. Nature Medicine *16*, 1389–1391.

Nakai, N., Sugiura, K., Akiyama, M., and Katoh, N. (2015). Acute generalized exanthematous pustulosis caused by dihydrocodeine phosphate in a patient with psoriasis vulgaris and a heterozygous IL36RN mutation. JAMA Dermatol *151*, 311–315.

Nakayama, T., Hieshima, K., Izawa, D., Tatsumi, Y., Kanamaru, A., and Yoshie, O. (2003). Cutting edge: profile of chemokine receptor expression on human plasma cells accounts for their efficient recruitment to target tissues. J. Immunol. *170*, 1136–1140.

Neil (2010). Bench-to-bedside review: Bacterial pneumonia with influenza - pathogenesis and clinical implications. 1–8.

Nerlich, A., Ruangkiattikul, N., Laarmann, K., Janze, N., Dittrich-Breiholz, O., Kracht,

M., and Goethe, R. (2015). C/EBPβ is a transcriptional key regulator of IL-36α in murine macrophages. Biochim. Biophys. Acta *1849*, 966–978.

Ngo, V.L., Abo, H., Maxim, E., Harusato, A., Geem, D., Medina-Contreras, O., Merlin, D., Gewirtz, A.T., Nusrat, A., and Denning, T.L. (2018). A cytokine network involving IL-36γ, IL-23, and IL-22 promotes antimicrobial defense and recovery from intestinal barrier damage. Proc. Natl. Acad. Sci. U.S.a. *115*, E5076–E5085.

Pachulec, E., Abdelwahed Bagga, R.B., Chevallier, L., O'Donnell, H., Guillas, C., Jaubert, J., Montagutelli, X., Carniel, E., and Demeure, C.E. (2017). Enhanced Macrophage M1 Polarization and Resistance to Apoptosis Enable Resistance to Plague. J. Infect. Dis. *216*, 761–770.

Park, S.L., Zaid, A., Hor, J.L., Christo, S.N., Prier, J.E., Davies, B., Alexandre, Y.O., Gregory, J.L., Russell, T.A., Gebhardt, T., et al. (2018). Local proliferation maintains a stable pool of tissue-resident memory T cells after antiviral recall responses. Nat Immunol *19*, 183–191.

Parsonage, G., Machado, L.R., Hui, J.W.-Y., McLarnon, A., Schmaler, T., Balasothy, M., To, K.-F., Vlantis, A.C., van Hasselt, C.A., Lo, K.-W., et al. (2012). CXCR6 and CCR5 localize T lymphocyte subsets in nasopharyngeal carcinoma. The American Journal of Pathology *180*, 1215–1222.

Peiró, T., Patel, D.F., Akthar, S., Gregory, L.G., Pyle, C.J., Harker, J.A., Birrell, M.A., Lloyd, C.M., and Snelgrove, R.J. (2018). Neutrophils drive alveolar macrophage IL-1β release during respiratory viral infection. Thorax *73*, 546–556.

Perrone, L.A., Szretter, K.J., Katz, J.M., Mizgerd, J.P., and Tumpey, T.M. (2010). Mice lacking both TNF and IL-1 receptors exhibit reduced lung inflammation and delay in onset of death following infection with a highly virulent H5N1 virus. J. Infect. Dis. *202*, 1161–1170.

Petit, S.J., Chayen, N.E., and Pease, J.E. (2008). Site-directed mutagenesis of the chemokine receptor CXCR6 suggests a novel paradigm for interactions with the ligand CXCL16. Eur. J. Immunol. *38*, 2337–2350.

Pöhlmann, S., Krumbiegel, M., and Kirchhoff, F. (1999). Coreceptor usage of BOB/GPR15 and Bonzo/STRL33 by primary isolates of human immunodeficiency virus type 1. J. Gen. Virol. *80 (Pt 5)*, 1241–1251.

Pugin, J., Ricou, B., Steinberg, K.P., Suter, P.M., and Martin, T.R. (1996). Proinflammatory activity in bronchoalveolar lavage fluids from patients with ARDS, a prominent role for interleukin-1. Am J Respir Crit Care Med *153*, 1850–1856.

Pulendran, B., and Maddur, M.S. (2014). Innate Immune Sensing and Response to Influenza. In Current Topics in Microbiology and Immunology, (Berlin, Heidelberg: Springer Berlin Heidelberg).

Purnama, C., Ng, S.L., Tetlak, P., Setiagani, Y.A., Kandasamy, M., Baalasubramanian, S., Karjalainen, K., and Ruedl, C. (2014). Transient ablation of alveolar macrophages leads to massive pathology of influenza infection without affecting cellular adaptive immunity. Eur. J. Immunol. *44*, 2003–2012.

Quaranta, M., Knapp, B., Garzorz, N., Mattii, M., Pullabhatla, V., Pennino, D., Andres, C., Traidl-Hoffmann, C., Cavani, A., Theis, F.J., et al. (2014). Intraindividual genome expression analysis reveals a specific molecular signature of psoriasis and eczema. Science Translational Medicine *6*, 244ra90–244ra90.

Rahman, P., Sun, S., Peddle, L., Snelgrove, T., Melay, W., Greenwood, C., and Gladman, D. (2006). Association between the interleukin-1 family gene cluster and psoriatic arthritis. Arthritis Rheum. *54*, 2321–2325.

Ramadas, R.A., Ewart, S.L., Iwakura, Y., Medoff, B.D., and LeVine, A.M. (2012). IL-36α exerts pro-inflammatory effects in the lungs of mice. PLoS ONE *7*, e45784.

Ramadas, R.A., Ewart, S.L., Medoff, B.D., and LeVine, A.M. (2011). Interleukin-1 family member 9 stimulates chemokine production and neutrophil influx in mouse lungs. Am J Respir Cell Mol Biol *44*, 134–145.

Ramadas, R.A., Li, X., Shubitowski, D.M., Samineni, S., Wills-Karp, M., and Ewart, S.L. (2006). IL-1 Receptor antagonist as a positional candidate gene in a murine model of allergic asthma. Immunogenetics *58*, 851–855.

Ray, S.J., Franki, S.N., Pierce, R.H., Dimitrova, S., Koteliansky, V., Sprague, A.G., Doherty, P.C., de Fougerolles, A.R., and Topham, D.J. (2004). The collagen binding alpha1beta1 integrin VLA-1 regulates CD8 T cell-mediated immune protection against heterologous influenza infection. Immunity *20*, 167–179.

Rivera-Marrero, C.A., Stewart, J., Shafer, W.M., and Roman, J. (2004). The down-regulation of cathepsin G in THP-1 monocytes after infection with Mycobacterium tuberculosis is associated with increased intracellular survival of bacilli. Infection and Immunity *72*, 5712–5721.

Rot, A., and Andrian, Von, U.H. (2004). Chemokines in innate and adaptive host defense: basic chemokinese grammar for immune cells. Annu. Rev. Immunol. *22*, 891–928.

Rőszer, T. (2015). Understanding the Mysterious M2 Macrophage through Activation Markers and Effector Mechanisms. Mediators Inflamm. *2015*, 816460–16.

Saha, S.S., Singh, D., Raymond, E.L., Ganesan, R., Caviness, G., Grimaldi, C., Woska, J.R., Mennerich, D., Brown, S.-E., Mbow, M.L., et al. (2015). Signal transduction and intracellular trafficking by the interleukin 36 receptor. J. Biol. Chem. *290*, jbc.M115.653378–24006.

Salomon, R., Hoffmann, E., and Webster, R.G. (2007). Inhibition of the cytokine

response does not protect against lethal H5N1 influenza infection. Proc Natl Acad Sci USA *104*, 12479–12481.

Sato, T., Thorlacius, H., Johnston, B., Staton, T.L., Xiang, W., Littman, D.R., and Butcher, E.C. (2005). Role for CXCR6 in recruitment of activated CD8+ lymphocytes to inflamed liver. J. Immunol. *174*, 277–283.

Satoh-Takayama, N., Serafini, N., Verrier, T., Rekiki, A., Renauld, J.-C., Frankel, G., and Di Santo, J.P. (2014). The chemokine receptor CXCR6 controls the functional topography of interleukin-22 producing intestinal innate lymphoid cells. Immunity *41*, 776–788.

Schaerli, P., Ebert, L., Willimann, K., Blaser, A., Roos, R.S., Loetscher, P., and Moser, B. (2004). A skin-selective homing mechanism for human immune surveillance T cells. J. Exp. Med. *199*, 1265–1275.

Scheiermann, P., Bachmann, M., Härdle, L., Pleli, T., Piiper, A., Zwissler, B., Pfeilschifter, J., and Mühl, H. (2015). Application of IL-36 receptor antagonist weakens CCL20 expression and impairs recovery in the late phase of murine acetaminophen-induced liver injury. Sci. Rep. *5*, 8521–8527.

Schenkel, J.M., and Masopust, D. (2014). Tissue-resident memory T cells. Immunity *41*, 886–897.

Schmitz, N., Kurrer, M., Bachmann, M.F., and Kopf, M. (2005). Interleukin-1 is responsible for acute lung immunopathology but increases survival of respiratory influenza virus infection. J. Virol. *79*, 6441–6448.

Schneider, C., Nobs, S.P., Heer, A.K., Kurrer, M., Klinke, G., van Rooijen, N., Vogel, J., and Kopf, M. (2014). Alveolar macrophages are essential for protection from respiratory failure and associated morbidity following influenza virus infection. PLoS Pathog. *10*, e1004053.

Scholz, F., Schulte, A., Adamski, F., Hundhausen, C., Mittag, J., Schwarz, A., Kruse, M.-L., Proksch, E., and Ludwig, A. (2007). Constitutive expression and regulated release of the transmembrane chemokine CXCL16 in human and murine skin. Journal of Investigative Dermatology *127*, 1444–1455.

Schulte, A., Schulz, B., Andrzejewski, M.G., Hundhausen, C., Mletzko, S., Achilles, J., Reiss, K., Paliga, K., Weber, C., John, S.R., et al. (2007). Sequential processing of the transmembrane chemokines CX3CL1 and CXCL16 by alpha- and gamma-secretases. Biochem. Biophys. Res. Commun. *358*, 233–240.

Schultz-Cherry, S. (2015). Role of NK cells in influenza infection. Curr. Top. Microbiol. Immunol. *386*, 109–120.

Schulz, C., Gomez Perdiguero, E., Chorro, L., Szabo-Rogers, H., Cagnard, N., Kierdorf, K., Prinz, M., Wu, B., Jacobsen, S.E.W., Pollard, J.W., et al. (2012). A lineage of myeloid

cells independent of Myb and hematopoietic stem cells. Science *336*, 86–90.

Segueni, N., Vigne, S., Palmer, G., Bourigault, M.-L., Olleros, M.L., Vesin, D., Garcia, I., Ryffel, B., Quesniaux, V.F.J., and Gabay, C. (2015). Limited Contribution of IL-36 versus IL-1 and TNF Pathways in Host Response to Mycobacterial Infection. PLoS ONE *10*, e0126058.

Seidl, H., Richtig, E., Tilz, H., Stefan, M., Schmidbauer, U., Asslaber, M., Zatloukal, K., Herlyn, M., and Schaider, H. (2007). Profiles of chemokine receptors in melanocytic lesions: de novo expression of CXCR6 in melanoma. Hum. Pathol. *38*, 768–780.

Seo, S.-U., Kwon, H.-J., Ko, H.-J., Byun, Y.-H., Seong, B.L., Uematsu, S., Akira, S., and Kweon, M.-N. (2011). Type I interferon signaling regulates Ly6C(hi) monocytes and neutrophils during acute viral pneumonia in mice. PLoS Pathog. *7*, e1001304.

Sever-Chroneos, Z., Murthy, A., Davis, J., Florence, J.M., Kurdowska, A., Krupa, A., Tichelaar, J.W., White, M.R., Hartshorn, K.L., Kobzik, L., et al. (2011). GM-CSF modulates pulmonary resistance to influenza A infection. Antiviral Res. *92*, 319–328.

Sharron, M., Pöhlmann, S., Price, K., Lolis, E., Tsang, M., Kirchhoff, F., Doms, R.W., and Lee, B. (2000). Expression and coreceptor activity of STRL33/Bonzo on primary peripheral blood lymphocytes. Blood *96*, 41–49.

Shashkin, P., Simpson, D., Mishin, V., Chesnutt, B., and Ley, K. (2003). Expression of CXCL16 in human T cells. Arterioscler. Thromb. Vasc. Biol. *23*, 148–149.

Shimaoka, T., Nakayama, T., Fukumoto, N., Kume, N., Takahashi, S., Yamaguchi, J., Minami, M., Hayashida, K., Kita, T., Ohsumi, J., et al. (2004a). Cell surface-anchored SR-PSOX/CXC chemokine ligand 16 mediates firm adhesion of CXC chemokine receptor 6-expressing cells. Journal of Leukocyte Biology *75*, 267–274.

Shimaoka, T., Nakayama, T., Hieshima, K., Kume, N., Fukumoto, N., Minami, M., Hayashida, K., Kita, T., Yoshie, O., and Yonehara, S. (2004b). Chemokines generally exhibit scavenger receptor activity through their receptor-binding domain. Journal of Biological Chemistry *279*, 26807–26810.

Shimaoka, T., Nakayama, T., Kume, N., Takahashi, S., Yamaguchi, J., Minami, M., Hayashida, K., Kita, T., Ohsumi, J., Yoshie, O., et al. (2003). Cutting edge: SR-PSOX/CXC chemokine ligand 16 mediates bacterial phagocytosis by APCs through its chemokine domain. J. Immunol. *171*, 1647–1651.

Shimaoka, T., Seino, K.-I., Kume, N., Minami, M., Nishime, C., Suematsu, M., Kita, T., Taniguchi, M., Matsushima, K., and Yonehara, S. (2007). Critical role for CXC chemokine ligand 16 (SR-PSOX) in Th1 response mediated by NKT cells. J. Immunol. *179*, 8172–8179.

Short, K.R., Kroeze, E.J.B.V., Fouchier, R.A.M., and Kuiken, T. (2014). Pathogenesis of influenza-induced acute respiratory distress syndrome. Lancet Infect Dis *14*, 57–69.

Sigmundsdottir, H., Pan, J., Debes, G.F., Alt, C., Habtezion, A., Soler, D., and Butcher, E.C. (2007). DCs metabolize sunlight-induced vitamin D3 to “program” T cell attraction to the epidermal chemokine CCL27. Nat Immunol *8*, 285–293.

Slütter, B., Pewe, L.L., Kaech, S.M., and Harty, J.T. (2013). Lung Airway-Surveilling CXCR3hi Memory CD8+ T Cells Are Critical for Protection against Influenza A Virus. Immunity *39*, 939–948.

Smith, D.E., Renshaw, B.R., Ketchem, R.R., Kubin, M., Garka, K.E., and Sims, J.E. (2000). Four New Members Expand the Interleukin-1 Superfamily. Journal of Biological Chemistry *275*, 1169–1175.

Sridhar, S., Begom, S., Bermingham, A., Hoschler, K., Adamson, W., Carman, W., Bean, T., Barclay, W., Deeks, J.J., and Lalvani, A. (2013). Cellular immune correlates of protection against symptomatic pandemic influenza. Nature Medicine *19*, 1305–1312.

Stegmann, K.A., Robertson, F., Hansi, N., Gill, U., Pallant, C., Christophides, T., Pallett, L.J., Peppa, D., Dunn, C., Fusai, G., et al. (2016). CXCR6 marks a novel subset of T-bet(lo)Eomes(hi) natural killer cells residing in human liver. Sci. Rep. *6*, 26157.

Sturrock, A., Franklin, K.F., and Hoidal, J.R. (1996). Human proteinase-3 expression is regulated by PU.1 in conjunction with a cytidine-rich element. Journal of Biological Chemistry *271*, 32392–32402.

Sturrock, A., Franklin, K.F., Norman, K., and Hoidal, J.R. (2004). Human leukocyte elastase gene expression is regulated by PU.1 in conjunction with closely associated cytidine-rich and Myb binding sites. Biochim. Biophys. Acta *1676*, 104–111.

Subramaniam, R., Hillberry, Z., Chen, H., Feng, Y., Fletcher, K., Neuenschwander, P., and Shams, H. (2015). Delivery of GM-CSF to Protect against Influenza Pneumonia. PLoS ONE *10*, e0124593.

Sugiura, K., Endo, K., Akasaka, T., and Akiyama, M. (2015). Successful treatment with infliximab of sibling cases with generalized pustular psoriasis caused by deficiency of interleukin-36 receptor antagonist. J Eur Acad Dermatol Venereol *29*, 2054–2056.

Tabata, S., Kadowaki, N., Kitawaki, T., Shimaoka, T., Yonehara, S., Yoshie, O., and Uchiyama, T. (2005). Distribution and kinetics of SR-PSOX/CXCL16 and CXCR6 expression on human dendritic cell subsets and CD4+ T cells. Journal of Leukocyte Biology *77*, 777–786.

Taghizadeh, R., Noh, M., Huh, Y.H., Ciusani, E., Sigalotti, L., Maio, M., Arosio, B., Nicotra, M.R., Natali, P., Sherley, J.L., et al. (2010). CXCR6, a newly defined biomarker of tissue-specific stem cell asymmetric self-renewal, identifies more aggressive human melanoma cancer stem cells. PLoS ONE *5*, e15183.

Tate, M.D., Pickett, D.L., van Rooijen, N., Brooks, A.G., and Reading, P.C. (2010). Critical role of airway macrophages in modulating disease severity during influenza

virus infection of mice. J. Virol. *84*, 7569–7580.

Taubenberger, J.K., and Morens, D.M. (2008). The pathology of influenza virus infections. Annu Rev Pathol *3*, 499–522.

Teijaro, J.R. (2014). The Role of Cytokine Responses During Influenza Virus Pathogenesis and Potential Therapeutic Options. (Berlin, Heidelberg: Springer Berlin Heidelberg), pp. 1–20.

Terajima, M., Cruz, J., Leporati, A.M., Orphin, L., Babon, J.A.B., Co, M.D.T., Pazoles, P., Jameson, J., and Ennis, F.A. (2008). Influenza A virus matrix protein 1-specific human CD8+ T-cell response induced in trivalent inactivated vaccine recipients. J. Virol. *82*, 9283–9287.

Thomas, S.Y., Hou, R., Boyson, J.E., Means, T.K., Hess, C., Olson, D.P., Strominger, J.L., Brenner, M.B., Gumperz, J.E., Wilson, S.B., et al. (2003). CD1d-restricted NKT cells express a chemokine receptor profile indicative of Th1-type inflammatory homing cells. J. Immunol. *171*, 2571–2580.

Thompson, W.W., Shay, D.K., Weintraub, E., Brammer, L., Cox, N., Anderson, L.J., and Fukuda, K. (2003). Mortality associated with influenza and respiratory syncytial virus in the United States. Jama *289*, 179–186.

Tisoncik, J.R., Korth, M.J., Simmons, C.P., Farrar, J., Martin, T.R., and Katze, M.G. (2012). Into the eye of the cytokine storm. Microbiol. Mol. Biol. Rev. *76*, 16–32.

Tohyama, M., Sayama, K., Komatsuzawa, H., Hanakawa, Y., Shirakata, Y., Dai, X., Yang, L., Tokumaru, S., Nagai, H., Hirakawa, S., et al. (2007). CXCL16 is a novel mediator of the innate immunity of epidermal keratinocytes. International Immunology *19*, 1095–1102.

Tortola, L., Rosenwald, E., Abel, B., Blumberg, H., Schäfer, M., Coyle, A.J., Renauld, J.-C., Werner, S., Kisielow, J., and Kopf, M. (2012). Psoriasiform dermatitis is driven by IL-36-mediated DC-keratinocyte crosstalk. J. Clin. Invest. *122*, 3965–3976.

Towne, J.E., Garka, K.E., Renshaw, B.R., Virca, G.D., and Sims, J.E. (2004). Interleukin (IL)-1F6, IL-1F8, and IL-1F9 signal through IL-1Rrp2 and IL-1RAcP to activate the pathway leading to NF-kappaB and MAPKs. J. Biol. Chem. *279*, 13677–13688.

Towne, J.E., Renshaw, B.R., Douangpanya, J., Lipsky, B.P., Shen, M., Gabel, C.A., and Sims, J.E. (2011). Interleukin-36 (IL-36) ligands require processing for full agonist (IL-36α, IL-36β, and IL-36γ) or antagonist (IL-36Ra) activity. J. Biol. Chem. *286*, 42594–42602.

Tscherne, D.M., and García-Sastre, A. (2011). Virulence determinants of pandemic influenza viruses. J. Clin. Invest. *121*, 6–13.

Tse, S.-W., Cockburn, I.A., Zhang, H., Scott, A.L., and Zavala, F. (2013). Unique

transcriptional profile of liver-resident memory CD8+ T cells induced by immunization with malaria sporozoites. Genes Immun. *14*, 302–309.

Tse, S.-W., Radtke, A.J., Espinosa, D.A., Cockburn, I.A., and Zavala, F. (2014). The chemokine receptor CXCR6 is required for the maintenance of liver memory CD8$^+$ T cells specific for infectious pathogens. J. Infect. Dis. *210*, 1508–1516.

Tsurutani, N., St Rose, M.-C., Mittal, P., Adler, A., and Vella, A. (2015). IL-1 family members induce pro-inflammatory cytokine release in costimulated T cells outside of TCR stimulation (CCR3P.209). The Journal of Immunology *194*, 49.10–49.10.

Tumpey, T.M., García-Sastre, A., Taubenberger, J.K., Palese, P., Swayne, D.E., Pantin-Jackwood, M.J., Schultz-Cherry, S., Solórzano, A., van Rooijen, N., Katz, J.M., et al. (2005). Pathogenicity of influenza viruses with genes from the 1918 pandemic virus: functional roles of alveolar macrophages and neutrophils in limiting virus replication and mortality in mice. J. Virol. *79*, 14933–14944.

Turner, M.D., Nedjai, B., Hurst, T., and Pennington, D.J. (2014). Cytokines and chemokines: At the crossroads of cell signalling and inflammatory disease. Biochim. Biophys. Acta *1843*, 2563–2582.

Tyagi, S.C., and Simon, S.R. (1993). Regulation of neutrophil elastase activity by elastin-derived peptide. Journal of Biological Chemistry *268*, 16513–16518.

Tyner, J.W., Uchida, O., Kajiwara, N., Kim, E.Y., Patel, A.C., O'Sullivan, M.P., Walter, M.J., Schwendener, R.A., Cook, D.N., Danoff, T.M., et al. (2005). CCL5-CCR5 interaction provides antiapoptotic signals for macrophage survival during viral infection. Nature Medicine *11*, 1180–1187.

Unutmaz, D., Xiang, W., Sunshine, M.J., Campbell, J., Butcher, E., and Littman, D.R. (2000). The primate lentiviral receptor Bonzo/STRL33 is coordinately regulated with CCR5 and its expression pattern is conserved between human and mouse. J. Immunol. *165*, 3284–3292.

van der Voort, R., Verweij, V., de Witte, T.M., Lasonder, E., Adema, G.J., and Dolstra, H. (2010). An alternatively spliced CXCL16 isoform expressed by dendritic cells is a secreted chemoattractant for CXCR6+ cells. Journal of Leukocyte Biology *87*, 1029–1039.

van Riel, D., Leijten, L.M.E., van der Eerden, M., Hoogsteden, H.C., Boven, L.A., Lambrecht, B.N., Osterhaus, A.D.M.E., and Kuiken, T. (2011). Highly pathogenic avian influenza virus H5N1 infects alveolar macrophages without virus production or excessive TNF-alpha induction. PLoS Pathog. *7*, e1002099.

Velthuis, Te, A.J.W., and Fodor, E. (2016). Influenza virus RNA polymerase: insights into the mechanisms of viral RNA synthesis. Nat. Rev. Microbiol. *14*, 479–493.

Vos, J.B., van Sterkenburg, M.A., Rabe, K.F., Schalkwijk, J., Hiemstra, P.S., and Datson,

N.A. (2005). Transcriptional response of bronchial epithelial cells to Pseudomonas aeruginosa: identification of early mediators of host defense. Physiol. Genomics *21*, 324–336.

Wakim, L.M., Waithman, J., van Rooijen, N., Heath, W.R., and Carbone, F.R. (2008). Dendritic cell-induced memory T cell activation in nonlymphoid tissues. Science *319*, 198–202.

Wang, P., Meinhardt, B., Andre, R., Renshaw, B.R., Kimber, I., Rothwell, N.J., and Pinteaux, E. (2005). The interleukin-1-related cytokine IL-1F8 is expressed in glial cells, but fails to induce IL-1beta signalling responses. Cytokine *29*, 245–250.

Wang, X., Zhao, X., Feng, C., Weinstein, A., Xia, R., Wen, W., Lv, Q., Zuo, S., Tang, P., Yang, X., et al. (2015). IL-36γ Transforms the Tumor Microenvironment and Promotes Type 1 Lymphocyte-Mediated Antitumor Immune Responses. Cancer Cell.

Watanabe, Y., Hashimoto, Y., Shiratsuchi, A., Takizawa, T., and Nakanishi, Y. (2005). Augmentation of fatality of influenza in mice by inhibition of phagocytosis. Biochem. Biophys. Res. Commun. *337*, 881–886.

Wehr, A., Baeck, C., Heymann, F., Niemietz, P.M., Hammerich, L., Martin, C., Zimmermann, H.W., Pack, O., Gassler, N., Hittatiya, K., et al. (2013). Chemokine receptor CXCR6-dependent hepatic NK T Cell accumulation promotes inflammation and liver fibrosis. The Journal of Immunology *190*, 5226–5236.

Weiss, I.D., Wald, O., Wald, H., Beider, K., Abraham, M., Galun, E., Nagler, A., and Peled, A. (2010). IFN-gamma treatment at early stages of influenza virus infection protects mice from death in a NK cell-dependent manner. J. Interferon Cytokine Res. *30*, 439–449.

Wijburg, O.L., DiNatale, S., Vadolas, J., Van Rooijen, N., and Strugnell, R.A. (1997). Alveolar macrophages regulate the induction of primary cytotoxic T-lymphocyte responses during influenza virus infection. J. Virol. *71*, 9450–9457.

Wilbanks, A., Zondlo, S.C., Murphy, K., Mak, S., Soler, D., Langdon, P., Andrew, D.P., Wu, L., and Briskin, M. (2001). Expression cloning of the STRL33/BONZO/TYMSTRligand reveals elements of CC, CXC, and CX3C chemokines. J. Immunol. *166*, 5145–5154.

Wu, K., Byers, D.E., Jin, X., Agapov, E., Alexander-Brett, J., Patel, A.C., Cella, M., Gilfilan, S., Colonna, M., Kober, D.L., et al. (2015). TREM-2 promotes macrophage survival and lung disease after respiratory viral infection. Journal of Experimental Medicine *212*, 681–697.

Wu, T., Hu, Y., Lee, Y.-T., Bouchard, K.R., Benechet, A., Khanna, K., and Cauley, L.S. (2014). Lung-resident memory CD8 T cells (TRM) are indispensable for optimal cross-protection against pulmonary virus infection. Journal of Leukocyte Biology *95*, 215–224.

Wuttge, D.M., Zhou, X., Sheikine, Y., Wågsäter, D., Stemme, V., Hedin, U., Stemme, S., Hansson, G.K., and Sirsjö, A. (2004). CXCL16/SR-PSOX is an interferon-gamma-regulated chemokine and scavenger receptor expressed in atherosclerotic lesions. Arterioscler. Thromb. Vasc. Biol. *24*, 750–755.

Yamauchi, R., Tanaka, M., Kume, N., Minami, M., Kawamoto, T., Togi, K., Shimaoka, T., Takahashi, S., Yamaguchi, J., Nishina, T., et al. (2004). Upregulation of SR-PSOX/CXCL16 and recruitment of CD8+ T cells in cardiac valves during inflammatory valvular heart disease. Arterioscler. Thromb. Vasc. Biol. *24*, 282–287.

Zaid, A., Hor, J.L., Christo, S.N., Groom, J.R., Heath, W.R., Mackay, L.K., and Mueller, S.N. (2017). Chemokine Receptor-Dependent Control of Skin Tissue-Resident Memory T Cell Formation. The Journal of Immunology *199*, 2451–2459.

Zens, K.D., Chen, J.K., and Farber, D.L. (2016). Vaccine-generated lung tissue–resident memory T cells provide heterosubtypic protection to influenza infection. JCI Insight *1*, 1–12.

Zhao, J., Zhao, J., Mangalam, A.K., Channappanavar, R., Fett, C., Meyerholz, D.K., Agnihothram, S., Baric, R.S., David, C.S., and Perlman, S. (2016). Airway Memory CD4(+) T Cells Mediate Protective Immunity against Emerging Respiratory Coronaviruses. Immunity *44*, 1379–1391.

Zhou, L., Todorovic, V., Kakavas, S., Sielaff, B., Medina, L., Wang, L., Sadhukhan, R., Stockmann, H., Richardson, P.L., DiGiammarino, E., et al. (2017). Quantitative ligand and receptor binding studies reveal the mechanism of interleukin-36 (IL-36) pathway activation. J. Biol. Chem. jbc.M117.805739.

Zhou, X., Krueger, J.G., Kao, M.-C.J., Lee, E., Du, F., Menter, A., Wong, W.H., and Bowcock, A.M. (2003). Novel mechanisms of T-cell and dendritic cell activation revealed by profiling of psoriasis on the 63,100-element oligonucleotide array. Physiol. Genomics *13*, 69–78.